MASSACHUSETTS INSTITUTE OF TECHNOLOGY
Department of Naval Architecture and Marine Engineering

Report No. 66-7

EFFECTS OF SHALLOW WATER ON SHIP MOTION PARAMETERS IN PITCH AND HEAVE

by

W. Freakes
and
K. L. Keay

Publication and Distribution Sponsored by

Maritime Administration
United States Department of Commerce

Contract No. MA-2710

M.I.T. Contract DSR 6026

Cambridge, Massachusetts 02139 August, 1966

DUDLEY KNOX LIBRARY
NAVAL POSTGRADUATE SCHOOL
MONTEREY CA 93943-5101

MASSACHUSETTS INSTITUTE OF TECHNOLOGY

Department of Naval Architecture and Marine Engineering

Report No. 66-7

EFFECTS OF SHALLOW WATER ON SHIP MOTION PARAMETERS IN PITCH AND HEAVE

by

W. Freakes

and

K. L. Keay

Publication and Distribution Sponsored by

Maritime Administration
Unites States Department of Commerce

Contract No. MA-2710

M.I.T. Contract DSR 6026

Cambridge, Massachusetts 02139 August, 1966

EFFECTS OF SHALLOW WATER ON SHIP MOTION PARAMETERS IN PITCH AND HEAVE

by

William Freakes

and

Karl L. Keay

Submitted to the Department of Naval Architecture and Marine Engineering on May 20, 1966, in partial fulfillment of the requirements for the degree of Naval Engineer and the degree of Master of Science in Naval Architecture and Marine Engineering.

ABSTRACT

A Mariner class ship model was tested at various shallow water depths and Froude Numbers constrained to motion in one degree of freedom, either pitch-no heave or heave-no pitch. Under these constraints, using a step response technique, the response of the model to a step disturbance in pitch or heave was recorded. This response was then analyzed to obtain virtual mass or virtual inertia and damping coefficients in heave and pitch. These results are presented to show the effects of shallow water on these ship motion parameters at various Froude Numbers as a function of frequency of oscillation.

THESIS SUPERVISOR: M. A. Abkowitz

TITLE: Professor of Naval Architecture

ACKNOWLEDGEMENTS

The authors wish to thank Professor M. A. Abkowitz for his continuous advice during this project.

The authors wish to thank Mr. Frank Sellars for his support, especially in obtaining the analog to digital conversion of the data.

The encouragement of Commander W. R. Porter was appreciated.

The assistance of Professor J. E. Kerwin was highly beneficial in altering the computer program.

The assistance of Mr. H. der Kinderen in performing the experimental work was greatly appreciated.

This work was done in part by the Computation Center at the Massachusetts Institute of Technology, Cambridge, Massachusetts.

TABLE OF CONTENTS

INDEX OF TABLES

INDEX OF FIGURES

CHAPTER I

INTRODUCTION

The effects of shallow water on the virtual mass, virtual inertia, and damping coefficients in pitch and heave are of interest to designers of ships which must operate in restricted waters. There are several methods outlined in the literature for theoretically determining these coefficients. Wendel (11)* and Koch (6) have done theoretical work on shallow water effects. Saunders (9) outlines some of the results obtained by Prohaska (8) in determining added mass and heave damping for elongated bodies of various cross sections.

Pauling and Porter (7) developed a method of using the conformal transformation of a unit circle into ship sections to determine added mass and damping in heave for a ship section in deep water. This method was used by Gies and Hines (4) who determined the coefficients at each section for the Mariner hullform in deep water and then integrated these coefficients over the ship length using strip theory. This method has not been applied to shallow water.

Kerwin and Narita (5) developed a step response technique for experimentally determining these coefficients and Gies and Hines (4) used this technique in determining these coefficients for the Mariner hullform in deep water.. The step response technique has been used in pitch and heave on models in shallow water in this current research project. By restricting the motion of the model to pitch-no heave or heave-no pitch, the independent equations of motion in pitch and heave

- - - - - -

* Numbers in parenthesis refer to references listed in the bibliography.

can be solved separately for the desired coefficients.

The linearized equations of motion for a surface ship have been arranged and decoupled by Abkowitz (1). The results are a set of linearized second order differential equations in pitch and heave as follows:

$$(m-Z_{\dot{w}})\ddot{z} - Z_w\dot{z} - Z_z z - Z_{\dot{\theta}}\ddot{\theta} - (Z_{\dot{\theta}}+u_o Z_{\dot{w}})\dot{\theta} - (Z_\theta + u_o Z_w)\theta = Z_{ex} \qquad (1)$$

$$(I_y - M_{\dot{\theta}})\ddot{\theta} - (M_{\dot{\theta}}+u_o M_{\dot{w}})\dot{\theta} - (M_\theta + u_o M_w)\theta - M_{\dot{w}}\ddot{z} - M_w\dot{z} - M_z z = M_{ex} \qquad (2)$$

The symbols in the equations (1) and (2) are defined as follows:

m = mass of ship

I_y = moment of inertia about the y axis

z = heave displacement in the vertical plane

$\dot{z}$ = heave velocity in the vertical plane

$\ddot{z}$ = heave acceleration in the vertical plane

θ = angular displacement in pitch

$\dot{\theta}$ = angular velocity in pitch

$\ddot{\theta}$ = angular acceleration in pitch

w = velocity of the ship parallel to the ship's z axis

u_o = forward velocity of the ship

$Z_{\dot{w}}$ = added mass coefficient

Z_w = heave damping coefficient

Z_z = static restoring force coefficient

$Z_{\dot{\theta}}$ = heave force coefficient due to angular velocity

Z_θ = heave force coefficient due to angular displacement

Z_{ex} = heave excitation force

$M_{\dot{\theta}}$ = added moment of inertia coefficient

$M_{\dot{\theta}}$ = pitch damping coefficient

M_{θ} = static restoring moment coefficient

$M_{\ddot{w}}$ = heave coupled virtual moment of inertia coefficient

M_{w} = heave coupled pitch damping coefficient

M_{z} = heave coupled pitch restoring moment coefficient

Mex = pitch exciting moment

Equations (1) and (2) have several terms which are coupled. If these coupled terms are removed by restricting the motion to one degree of freedom in the step response experiment, the resulting equations become:

$$(m - Z_{\dot{w}})\ddot{z} - Z_{w}\dot{z} - Z_{z}z = Zex \tag{3}$$

$$(Iy - M_{\ddot{\theta}})\ddot{\theta} - M_{\dot{\theta}}\dot{\theta} - M_{\theta}\theta = Mex \tag{4}$$

We now have two independent second order differential equations which can be solved provided we know the value of the constants.

The coefficient of the $\ddot{z}$ term in equation (3) is the virtual mass of the ship in heave. The virtual mass of a body is the sum of the mass of the body and the added mass of the body. The added mass is a hydrodynamic force acting on the body which is caused by accelerating the fluid around the body. Similarly, the coefficient of the $\ddot{\theta}$ term in equation (4) is the virtual inertia of the ship. It consists of the actual moment of inertia of the ship and the added inertia. Like added mass, added inertia is a hydrodynamic moment acting on a body caused by the body accelerating the fluid around it.

The coefficients of the $\dot{z}$ and $\dot{\theta}$ terms in equations (3) and (4) are the damping coefficients in heave and pitch respectively. These

terms are the energy dissipation terms in the equations. For ships operating on the surface, the energy dissipation occurs principally as surface waves which radiate from the ship.

The step response technique evaluates the coefficients of the differential equations by performing a convolution integral on the response of the model. The response of any linear system to a step input function yields the response to any other input other than a step by the proper evaluation of the convolution integral. This property of linear systems can be applied to a ship to determine the response to a sinusoidal input and this approach is used in this work to determine virtual mass and damping coefficients in heave and the virtual inertia and damping coefficients in pitch, at shallow depths for various model speeds.

CHAPTER II

PROCEDURE

2.1 Model Characteristics

The dimensions and principal characteristics of the Mariner type ship model are listed in Table I.

Table I

CHARACTERISTICS OF THE MODEL

Length between perpendiculars	5.28 feet
Displacement	47.0 pounds
Draft (in fresh water)	0.283 feet
Beam	0.76 feet
Block coefficient	0.6125
Radius of gyration	1.26 feet
Model material	Fiberglass, reinforced plastic
Scale ratio	100:1

2.2 General Discussion

The model testing was conducted in the ship model towing tank at the Massachusetts Institute of Technology. The tests were conducted at Froude Numbers of 0.0, 0.1, 0.2, and 0.3 and water depths of 1.5, 2.5, 4.0, and 12.6 times the model draft. Froude Number is defined as the ratio of ship speed to the square root of ship length times the gravitational acceleration, g. Under each of these combinations, tests were run in both pitch with no heave and heave with no pitch.

In pitch with no heave, at depths of 1.5 and 2.5 times model draft, tests were conducted with a bow up step and then again with a stern up step.

The shallow depths were attained by pumping the tank down to the desired depths. Due to the shallow depths, it was necessary to build an extension from the towing carriage to lower the heave rod and the model towing mechanism down to the model. For this purpose, a one-half inch plywood sheet was used. The plywood was braced perpendicular to the direction of motion of the towing carriage and was very sturdy. A similar extension was used to hold the magnet at the bow and at the stern during the pitch excitation runs.

The effect of the towing carriage vibration on the model was of concern, particularly at the shallow tank depths. At the shallow tank depths, the moment arm for the model induced large forces acting on the towing carriage causing excessive vibration of the carriage. To reduce this effect and give a smoother carriage run, one hundred pounds of lead was placed on the carriage. As a result, carriage vibration was reduced to an acceptable level.

2.3 Application of the Step Input

2.3.1 General

The method of applying the step disturbance was that developed by Kerwin and Narita (5) and used previously by Gies and Hines (4). The step response was induced by using a small electromagnet which lifted the model by a certain amount. After the run had started and the model was up to speed, the current to the electromagnet was interrupted causing the magnet to drop the model. The response to this step impulse was then recorded on electromagnetic tape along with a

magnet parting signal to indicate the instant at which the model was dropped.

The magnet was powered by a low voltage direct current power supply and the circuit could be remotely controlled from the towing tank control room. The magnet parting circuit consisted of a dry cell battery powered circuit which was attached to the magnet and the model. When the model dropped, the circuit was opened giving an instantaneous indication of when the model was dropped.

Two steel holding plates were attached to the model. One was placed on the top of the heave rod for lifting the model for the heave-no pitch runs. The other was attached either at the bow or stern when lifting the bow or stern during the pitch-no heave runs.

2.3.2 Pitch-No Heave Configuration

In the pitch-no heave configuration, the model was first allowed to assume its calm water draft. Then, the heave rod was locked to prevent any motion by the model in heave and permitting only pitching motion as shown in Figure II.

The magnet was placed in position over either the bow or the stern and locked in place. The magnet was attached to a millimeter measuring bar and when locked in the proper position would not slip. Before each run, the ship's bow or stern was lifted manually until the magnet made contact. The magnet circuit is shown in Figure I. Whenever the magnet was in contact with the plate on the ship, the magnet parting signal circuit was automatically completed as shown in Figure I.

Before each run it was necessary to wait for the water to settle to a flat calm. When the run started, the model was towed with the

FIGURE II

PITCH-NO HEAVE CONFIGURATION

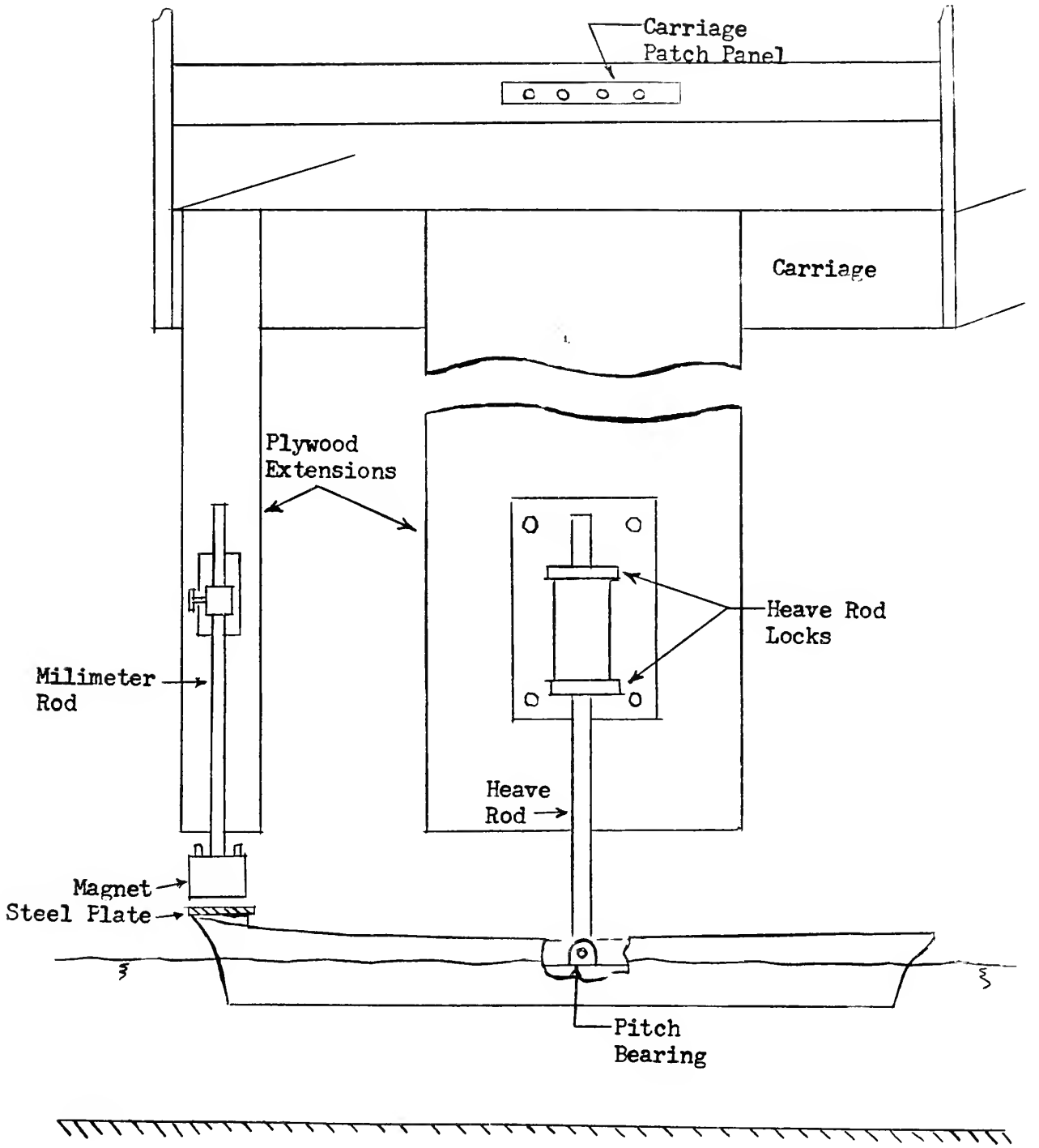

bow or stern being held up by the magnet. After the model was up to speed and the recording equipment was running, the magnet circuit was opened by throwing the switch in the control room. This released the model and at the same instant opened the magnet parting circuit.

When the magnet parted, the model reacted to the step-like displacement and came to rest at its open water flat calm pitch angle under a sinusoidal decaying motion. The magnet parting circuit provided the exact instant at which the motion started, the exact time being necessary for computational purposes.

2.3.3 Heave-No Pitch Configuration

In the heave-no pitch configuration, the model was attached to the heave rod with a rigid attachment as shown in Figure III. This prevented the model from pitching and permitted only motion in heave. The heave rod was attached approximately at the model's center of floatation thus eliminating any pitch moments from the heave rod.

The magnet was placed directly over the heave rod, and a steel plate was attached to the top of the heave rod. The magnet was attached to a millimeter bar which was used to accurately place the magnet above the heave rod and lock it in place. The magnet power circuit and magnet parting circuit were the same as in the pitch-no heave configuration and are shown in Figure I.

Before each run, the model was lifted bodily until the magnet made contact. The model was then held in this position. When the water had settled to a flat calm, the model was towed in this raised position until the desired moment and then dropped in the manner described for the pitch-no heave configuration.

2.4 Response Measurement

2.4.1 Pitch Response Measurement

The response of the model in pitch was measured by using a pitch bearing linear transformer. This pitch bearing was located approximately at the model's center of floatation and was attached to the heave rod. The heave rod was locked as shown in Figure II to prevent any motion in heave. The pitch bearing includes a small differential transformer capable of accurate angular measurements at small angles. As the maximum pitch angle used was 1.5 degrees, this proved to be satisfactory. The pitch bearing was repeatedly checked for calibration and linearity. The signal from the pitch bearing was recorded on a Sanborn paper recorder and simultaneously on magnetic tape.

At the same time as the pitch bearing signal was being recorded, the magnet parting circuit signal was also being recorded. This signal was used to indicate the instant that the model began to receive the step-response input. It was recorded on an adjacent channel of the tape and also on paper. After each run the results on paper were checked to ensure that the response was smooth and that a good sharp magnet parting signal had been obtained. On several runs, the magnet parting signal was not as sharp as desired and the runs were repeated.

2.4.2 Heave Response Measurement

The response of the model in heave was measured by using a linearsyn connected directly to the heave rod as shown in Figure III. A linearsyn is a linear motion measuring device of the differential transformer type consisting of a coil and a moveable magnetic core. The motions between the coil and core are measured and movements as small as 0.000001 inches can be detected.

FIGURE III

HEAVE-NO PITCH CONFIGURATION

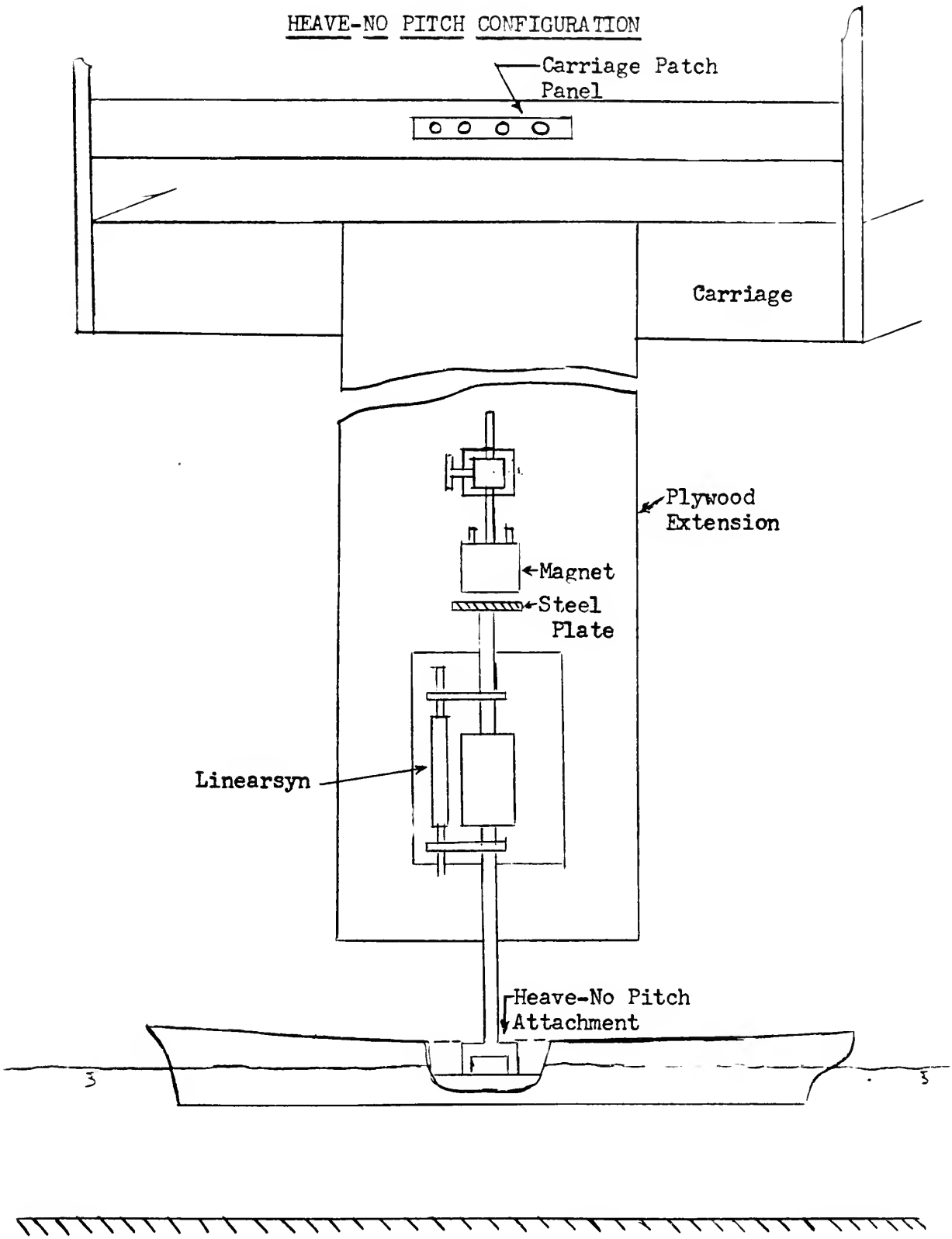

The model was given an initial displacement of 0.4 inches. This figure was arrived at from a combination of linearsyn calibration marks which could be used and the scales available on the Sanborn recorder. A one-inch deflection of the linearsyn was calibrated on the Sanborn at an attenuation scale of X50. Then the scale was changed to X20, giving 0.4 inches as the maximum value on the recorder. The 0.4 inches proved sufficient to give several cycles of oscillation.

2.5 Test Procedure

Before running the tests in shallow water, the model was tested with the tank at full depth. This was primarily to make sure a good signal was being received on the recorder from the model and the magnet parting circuit. These proving satisfactory, the tank was then pumped down to the shallowest depth desired, 1.5H (5.1 inches). The shallowest depth was used first because it was faster to fill the tank for subsequent runs than to pump it down.

At this depth, static restoring force and moment measurements were made at speeds corresponding to Froude Numbers of 0.00, 0.10, 0.20, and 0.30. This gave the static restoring force in heave or the static restoring moment in pitch at each speed. These were only recorded on paper and not on tape. Next, the model was run in the pitch-no heave configuration and then the heave-no pitch configuration at speeds corresponding to Froude Numbers of 0.00, 0.10, 0.20, and 0.30 and the responses were recorded.

After all runs were completed at the depth of 1.5H, the tank was filled to a depth of 2.5H (8.5 inches). The complete series of runs was repeated at this depth as described above. Then the tank was

filled to a depth of 4.0H (13.6 inches) and again a complete set of runs were made except that at this depth, no runs were made in pitch-no heave with the stern up.

The zero speed runs were made at the center of the tank. After each of the other runs, the model was positioned at the end of the tank and the magnet engaged. Then is was necessary to wait for the tank to settle to a flat calm before starting the next run. When the tank had settled, the carriage was started and when the carriage was up to speed, the magnetic tape recorder and the Sanborn paper recorder were started. Next, the switch was thrown cutting the current to the magnet and dropping the model. The Sanborn paper recorder was observed to see when the motion had settled out and then the tape recorder was stopped. The model was then run out for the next run.

CHAPTER III

DATA ANALYSIS

3.1 Response Analysis

The procedure for analyzing the model response was similar to that used previously by Kerwin and Narita (5) and Gies and Hines (4). The mathematical procedure of analysis is discussed in the references named above and will be briefly covered below.

The response of a ship to a step input can be represented by

$$P(t) = 1/C\ (1 + R(t)) \tag{5}$$

C is the static restoring force or moment and R(t) is the transient portion of the response. As R(t) goes to zero, P(t) approaches 1/C.

If a regular sinusoidal input is represented by

$$X(t) = X_0 \sin \omega t \tag{6}$$

the response to this sinusoidal input can be represented by

$$Y(t) = \int_{-\infty}^{t} X(\tau)\ H(t - \tau)\ d\tau \tag{7}$$

where $H(t - \tau)$ is the impulse response of the system. In this case, however, the step displacement response S(t) is known and not the impulse response. In this form, the convolution integral becomes

$$Y(t) = \int_{-\infty}^{t} \frac{dX(\tau)}{d\tau}\ S(t - \tau)\ d\tau \tag{8}$$

giving the same results.

In the steady state, the response to a one degree sinusoidal excitation of a system such as a ship can be represented by a linear second order differential equation such as

$$A \frac{d^2x}{dt^2} + B \frac{dx}{dt} + Cx = F_o \sin wt \qquad (9)$$

where x can represent Θ in pitch or z in heave. A represents the virtual mass in heave or virtual inertia in pitch, B represents the damping coefficient and C represents the static restoring force in heave or the static restoring moment in pitch. Each of these coefficients will be a function of the frequency, w.

The solution to equation (9) can be shown to be of the form

$$x(t) = a \sin wt + b \cos wt \qquad (10)$$

where a and b are constants. The substitution of (9) into (10) and solving will yield

$$A = \frac{C - \frac{F_o a}{a^2+b^2}}{w^2} \qquad (11)$$

and

$$B = - \frac{F_o b}{w(a^2+b^2)} \qquad (12)$$

where F_o is the amplitude of the external excitation.

By inserting the correct values into (11) and (12), the value of the coefficients A and B can be obtained for both pitch and heave.

3.2 Convolution Interval

The response of the model was recorded on tape and digitized at one-thousandth of a second intervals for input to the convolution integral computer program. To save computer time, it was advantageous to use intervals of more than one-thousandth of a second in the computer program. Gies and Hines (4) investigated the effects on a known value second order system of varying the convolution interval in the frequency range of their interest. The results of their analysis was used for determining the convolution interval to be used in processing this data. In addition, it was found that the results obtained in this work were interesting at lower frequencies. Accordingly, the response of a known second order system was tested at low frequency to supplement the data of Gies and Hines (4). The results are shown in Table II.

The actual value of the virtual inertia is 2.50 (slug feet^2) and the value of the damping coefficient is 7.50 (foot-pound/second). The values obtained from Table II show that the results are not as accurate at low frequencies as at frequencies close to the undamped natural frequency. However, the percent error using a convolution interval of 0.010 seconds is only 2.75 percent in virtual inertia and 1.2 percent in damping coefficient. In analyzing the response at radian frequencies below 4.0 radians/second a convolution interval of 0.010 seconds was used. In the radian frequency range of 4.0 to 10.0 radians/second a convolution interval of 0.020 seconds was used and above 10.0 radians/second an interval of 0.010 seconds was used.

Table II

EFFECT OF CONVOLUTION INTERVAL ON COEFFICIENTS

Period (Seconds)	Convolution Interval (Seconds)	Added Inertia (Slug Feet^2)	Damping (foot-pound) Second
4.200	0.100	1.991	8.014
4.200	0.060	2.108	7.842
4.200	0.040	2.215	7.643
4.200	0.020	2.217	7.674
4.200	0.010	2.269	7.591

3.3 Static Coefficients

In performing the model tests, it was necessary to determine the static restoring force in heave and static restoring moment in pitch for input to the computer program. Gies and Hines (4) had used the same model previously and found the static restoring moment in pitch to be independent of speed and the static restoring force in heave to have a slight speed dependence.

The coefficients obtained in this work show the coefficients to be speed dependent at shallow depths. The pitch restoring moment coefficients are listed in Table IV and the heave restoring force coefficients are listed in Table III.

Gerritsma (2) discusses the variations of static coefficients with speed and block coefficient from tests conducted on Series 60 models. Figures IV and V show the effects of speed and depth on the static coefficients as found in this work compared with results obtained by Gerritsma (2) for a Series 60 model with a block

coefficient of 0.60. The ratio C/C_{st} is the ratio of the restoring force coefficient to the zero speed restoring force coefficient.

The pitch runs at the shallower depths were run with the bow up and again with the stern up. The variations in the coefficients between bow up initially and stern up initially are shown in Table V. While the static coefficient in pitch is greater with the stern up initially, the ratios to the static coefficient at zero speed are the same for bow up initially and stern up initially.

Table III

HEAVE STATIC RESTORING FORCE COEFFICIENTS

(pounds/foot)

	Froude Number			
Depth	0.00	0.10	0.20	0.30
12.6H	187.4	176.4	189.0	187.4
4.0H	187.4	177.0	188.0	200.0
2.5H	187.4	187.4	198.0	209.0
1.5H	187.4	169.0	545.0	-----

Table IV

PITCH STATIC RESTORING MOMENT COEFFICIENTS

(pound-feet/radian)

	Froude Number			
	0.00	0.10	0.20	0.30
Depth				
12.6H	262.0	262.0	262.0	262.0
4.0H	262.0	262.0	250.0	198.0
2.5H	262.0	242.0	228.0	-----
1.5H	262.0	242.0	182.0	-----

Table V

PITCH STATIC RESTORING MOMENT COEFFICIENTS

(pound-feet/radian)

	Froude Number			
	0.00	0.10	0.20	0.30
Depth				
1.5H - bow up	262.0	242.0	182.0	-----
1.5H - stern up	288.0	268.0	215.0	-----
2.5H - bow up	262.0	242.0	228.0	-----
2.5H - stern up	288.0	268.0	250.0	215.0

FIGURE IV

HEAVE RESTORING FORCE COEFFICIENT

AS A FUNCTION OF DEPTH

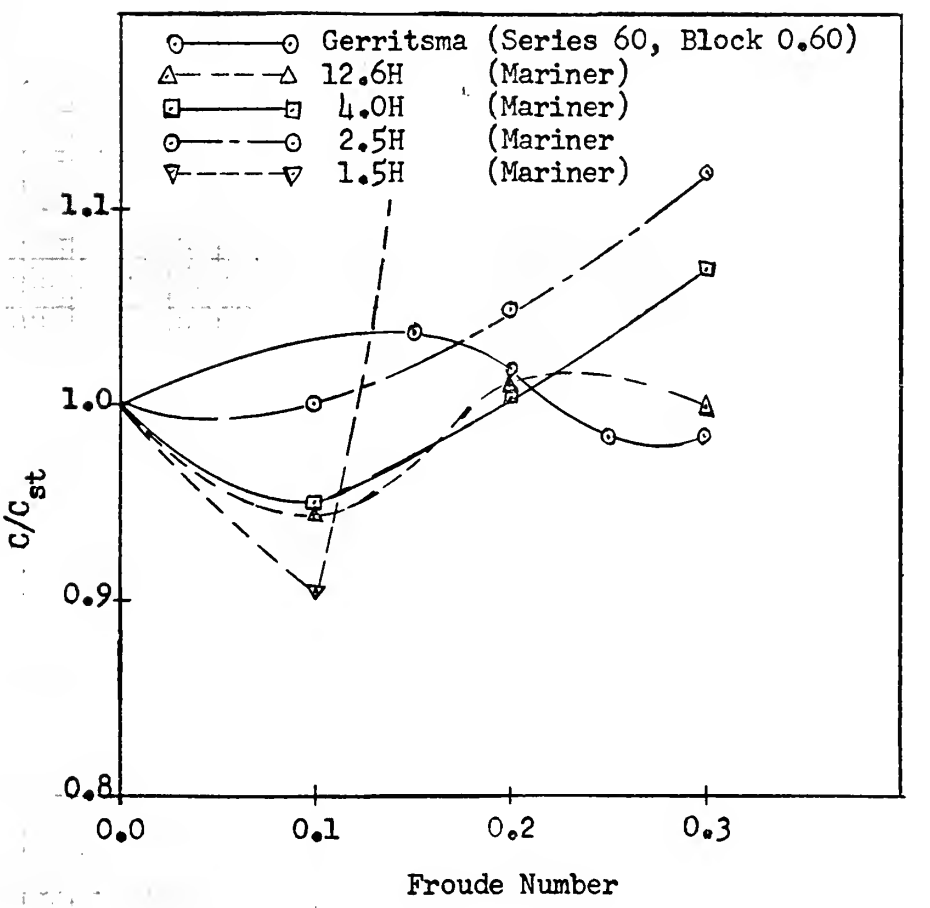

FIGURE V

PITCH STATIC RESTORING MOMENT COEFFICIENT

AS A FUNCTION OF DEPTH

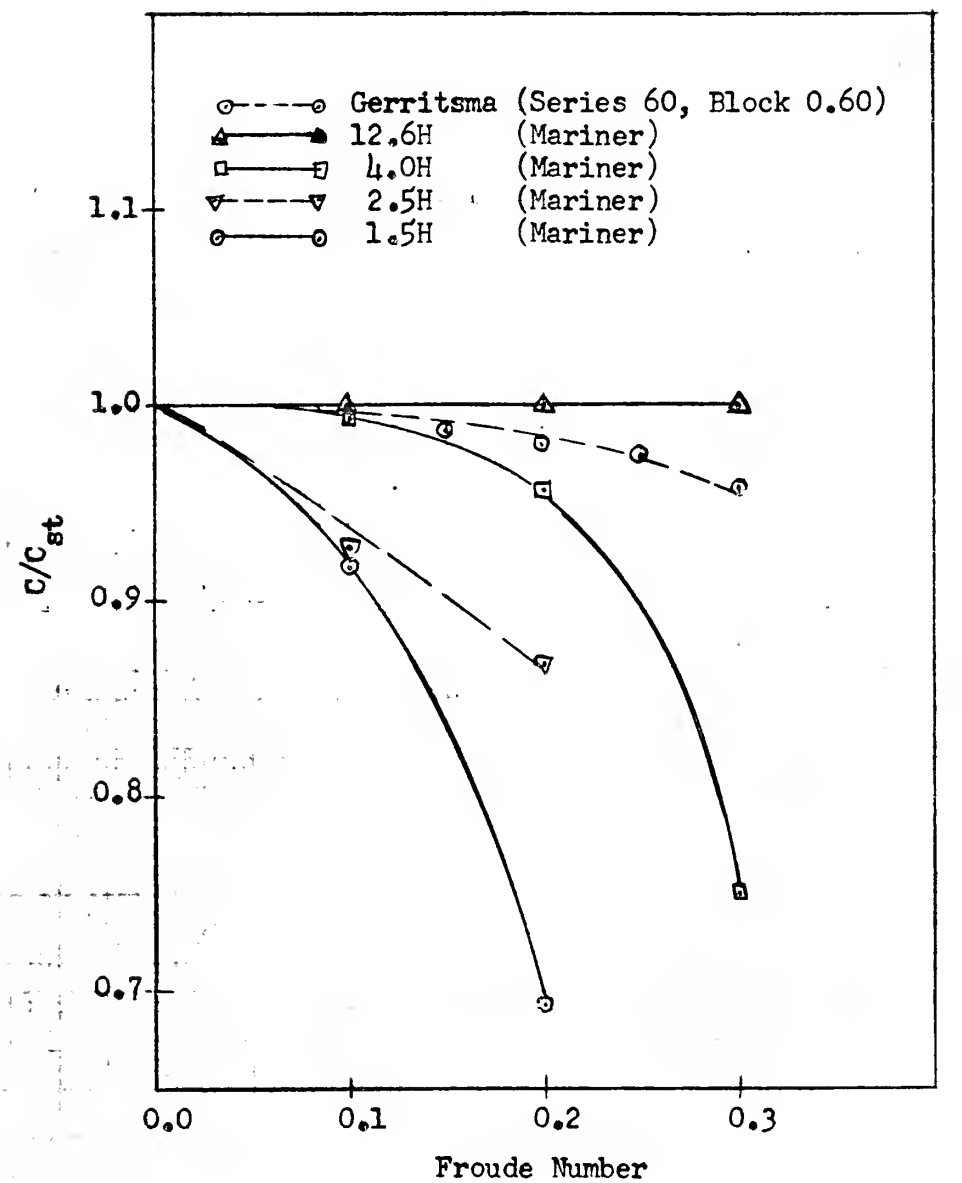

CHAPTER IV

RESULTS

4.1 Pitch-No Heave Condition

The values of virtual inertia and damping coefficients in pitch were obtained by conducting a total of twenty-four tests. A test was conducted at each Froude number and at each water depth with the bow up initially. Then a test was conducted at each Froude number and at the two shallow depths with the stern up initially.

The response curves were decaying sinusoids in all cases. At the higher speeds there was a large amount of vibration in the response curves due principally to oscillation of the towing carriage. The test data at a Froude number of 0.30 and a water depth of 1.5 times the draft was erratic due to the large amount of squat causing the model to touch bottom and therefore was not recorded.

4.1.1 Virtual Inertia and Damping

The values of virtual inertia and damping are listed in Tables VIII and X of Appendix D. Table VIII shows the values of virtual inertia and damping in pitch as a function of radian frequency for the bow up initially. Table X shows these same values for the stern up initially.

The values of virtual inertia and damping as a function of depth are plotted in Figures VI - IX and Figures X - XIII, respectively, at each of the four Froude numbers. Figures VI, X, XIV, and XVIII show a comparison with zero speed, deep water theoretical results from Gies and Hines (4). Figures XIV - XVII and XVIII - XXI are plots of the values of virtual inertia and damping, respectively, as a function

of Froude number at each of the four water depths.

Figures XXII - XXIII and XXIV - XXV are plots of the values of virtual inertia and damping, respectively, for the stern up tests as a function of Froude number at the two shallow depths.

A comparison of the values of virtual inertia and damping for the bow up tests against the same values for the stern up tests are given in Appendix A.

The symbols used in Appendix D and the figures are as follows:

w	radian frequency of excitation
A	virtual inertia coefficient
B	pitch damping coefficient
W	non-dimensional frequency
A'	non-dimensional virtual inertia coefficient
B'	non-dimensional pitch damping coefficient

4.2 Heave-No Pitch Condition

A total of sixteen tests were conducted to obtain the values of virtual mass and damping in heave. Tests were conducted at each Froude number and at each water depth.

The response curves were decaying sinusoids. The amount of vibration in the response curves was less in the heave-no pitch condition. The test run at high speed and shallowest depth was too erratic to record.

4.2.1 Virtual Mass and Damping

The values of virtual mass and damping in heave are shown in Table IX of Appendix D as a function of radian frequency. Figures XXVI - XXIX and XXX - XXXIII are plots of the values of virtual mass

and damping, respectively, as a function of depth at each of the Froude numbers. Figures XXVI, XXX, XXXIV, and XXXVIII show a comparison with theoretical results in deep water at zero Froude number from Gies and Hines (4). The values of virtual mass and damping are plotted in Figures XXXIV - XXXVII and XXXVIII - XLI as a function of Froude number at each of the water depths.

The symbols used in Appendix D and the figures are defined as follows:

w radian frequency of excitation

D virtual mass coefficient

E heave damping coefficient

W non-dimensional frequency

D' non-dimensional virtual mass coefficient

E' non-dimensional heave damping coefficient

4.3 Frequency Range

The values of virtual mass/inertia and damping are plotted in Figures VI - XLI against the radian frequency of excitation. This frequency is non-dimensionalized by multiplying by the square root of model length divided by the value of gravity.

The range of frequencies investigated was 1.5 to 13.0 radians per second or non-dimensionalized, 0.6 to 5.3. Only the deep water tests and the tests at a Froude number of 0.10 were investigated at very low frequencies because of the large amount of computer time required to compute low frequency results.

4.4 Definition of Terms

Terms used in the figures of this thesis are defined as follows:

H = Ship's draft

g = Gravitational acceleration

$\frac{U_o}{\sqrt{Lg}}$ = Froude Number

$W = w\sqrt{L/g}$ = Non-dimensional frequency

$A' = \frac{Ag}{\Delta L^2}$ = Non-dimensional virtual Inertia

$D' = \frac{Dg}{\Delta}$ = Non-dimensional virtual mass

$B' = \frac{B\sqrt{Lg}}{\Delta L^2}$ = Non-dimensional pitch damping

$E' = \frac{E\sqrt{Lg}}{\Delta}$ = Non-dimensional heave damping

Δ = Displacement

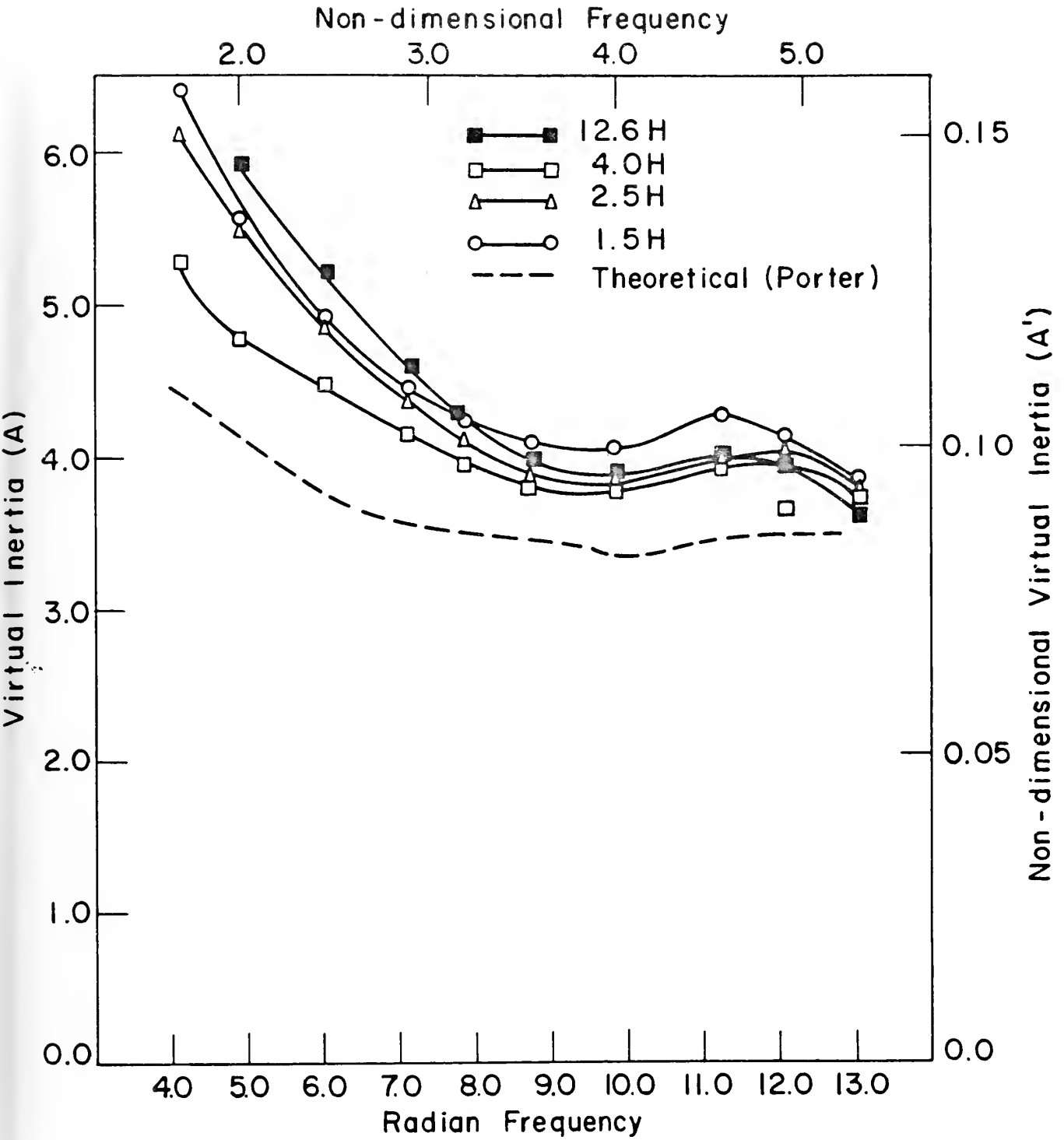

FIGURE VI VIRTUAL INERTIA AT ZERO FROUDE NUMBER AS A FUNCTION OF DEPTH

FIGURE VII

VIRTUAL INERTIA AT A FROUDE NUMBER OF 0.10

AS A FUNCTION OF DEPTH

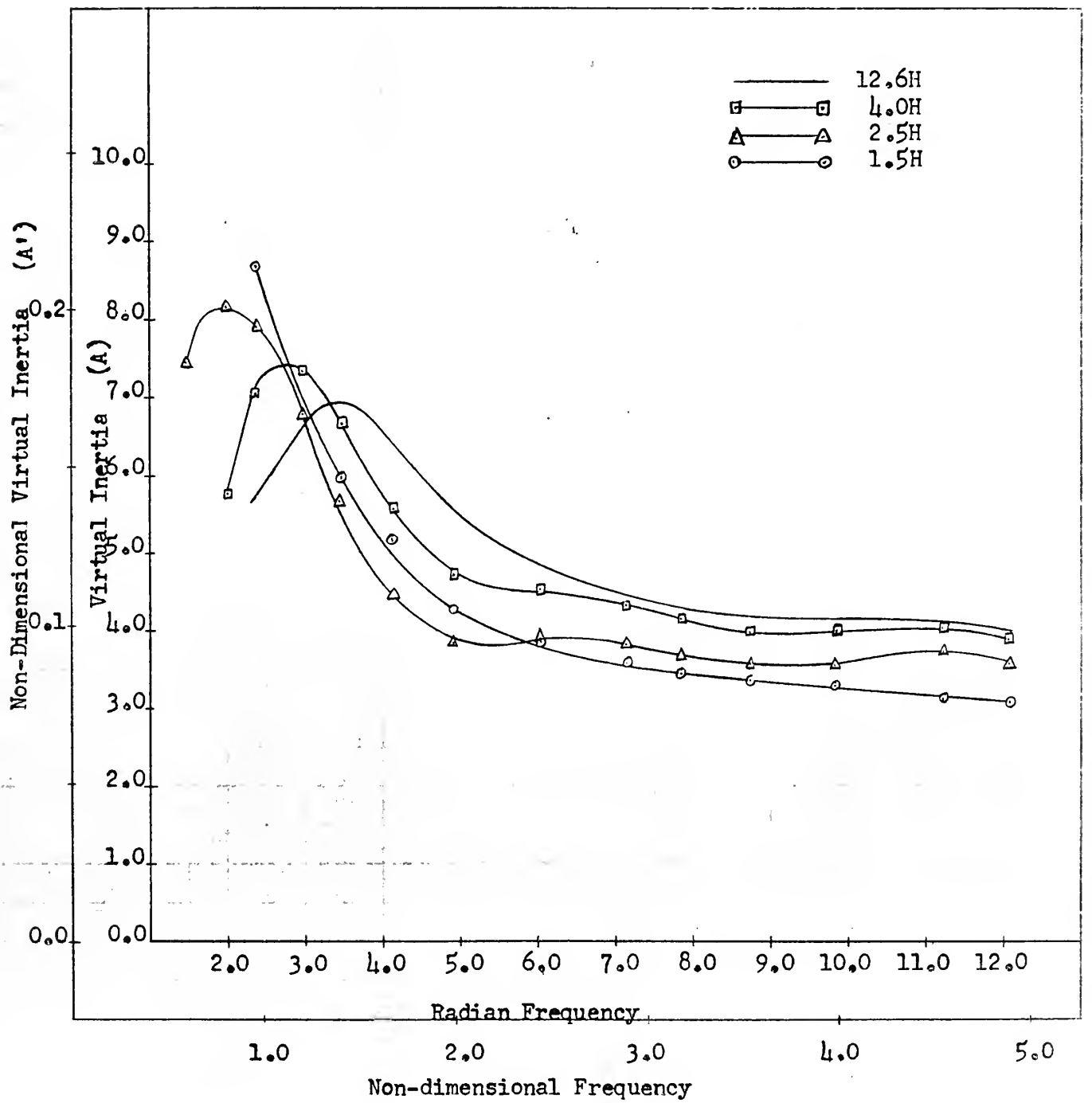

FIGURE VIII

VIRTUAL INERTIA AT A FROUDE NO. OF 0.20

AS A FUNCTION OF DEPTH

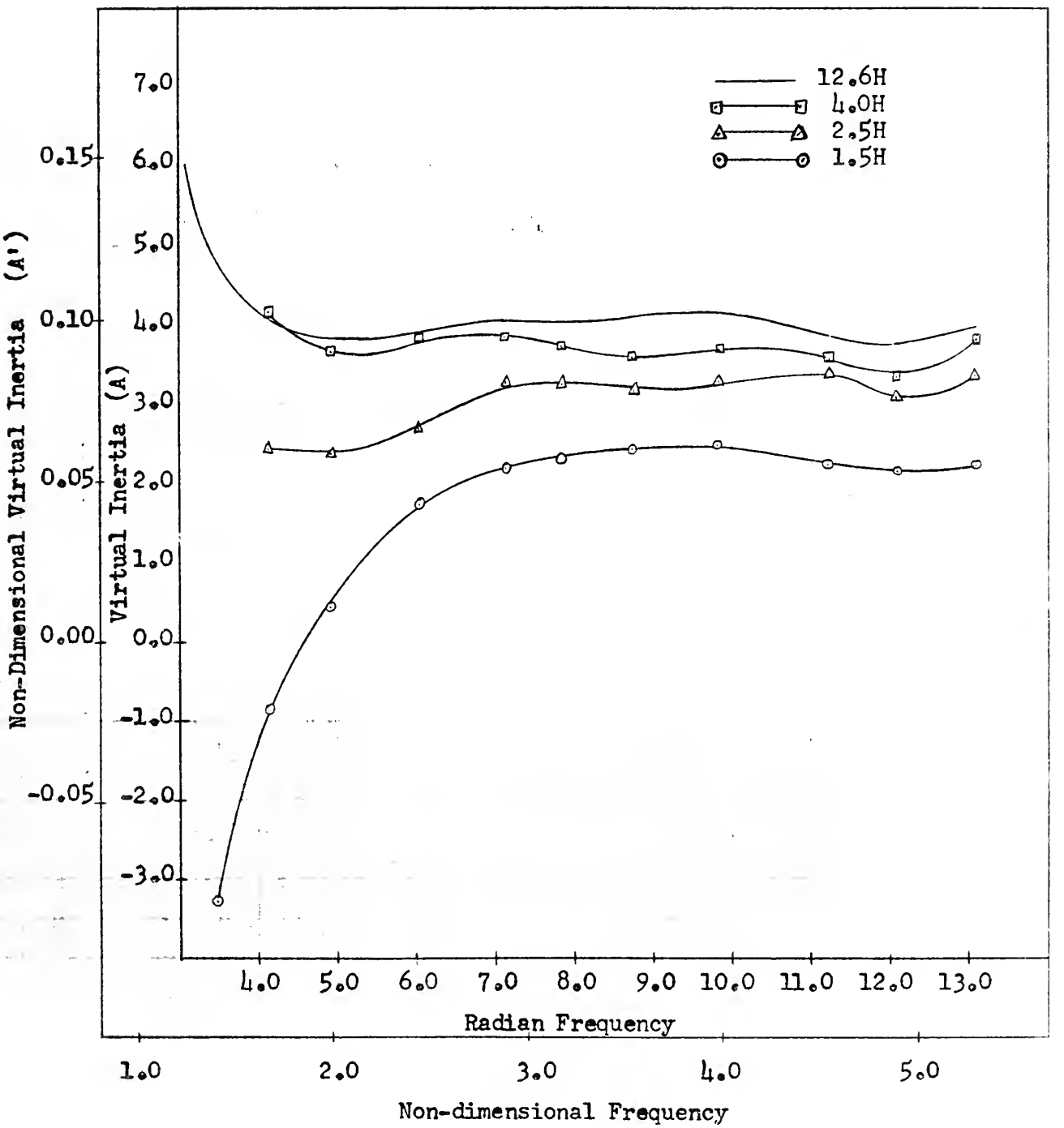

FIGURE IX

VIRTUAI INERTIA AT A FROUDE NUMBER OF 0.30

AS A FUNCTION OF DEPTH

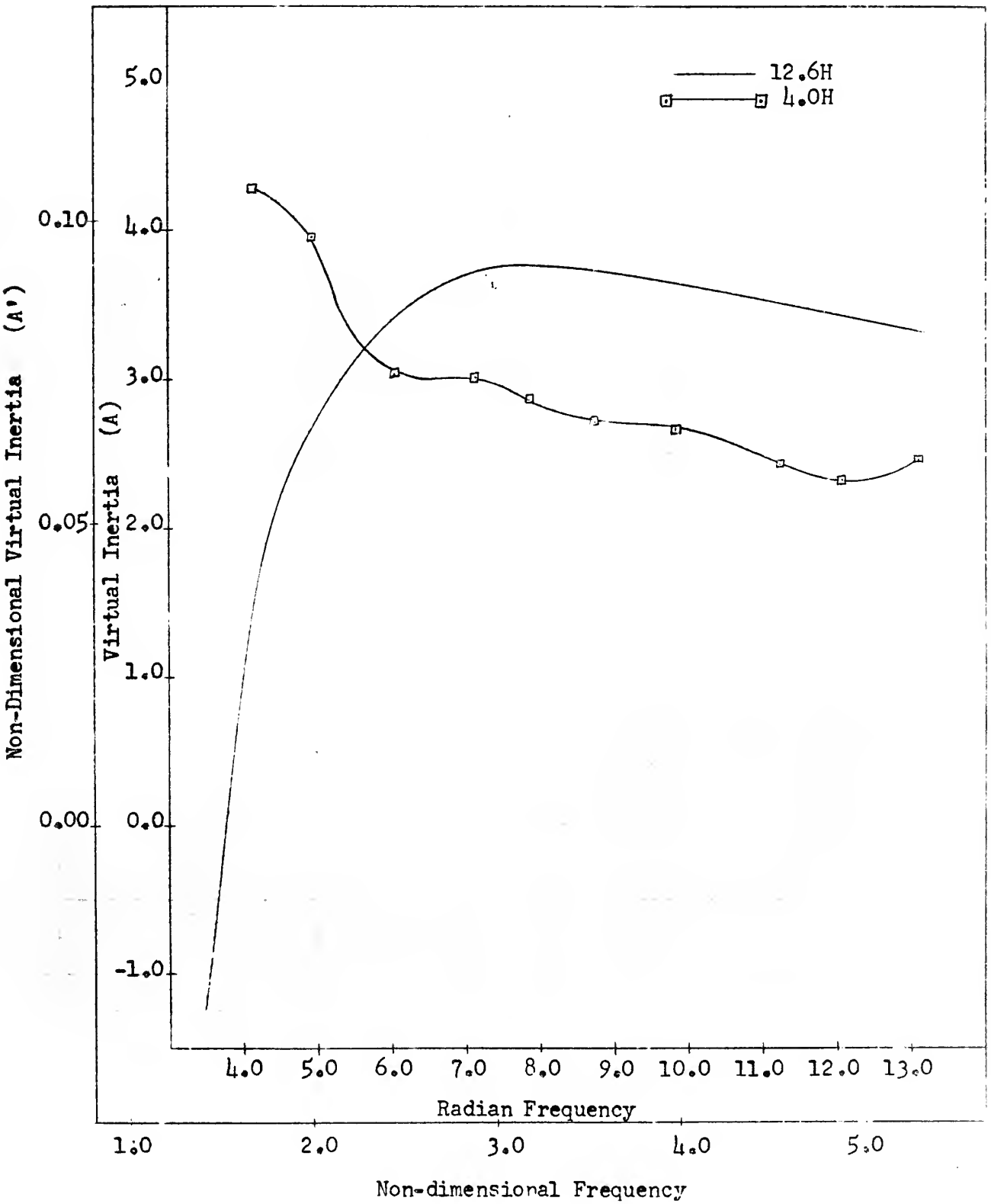

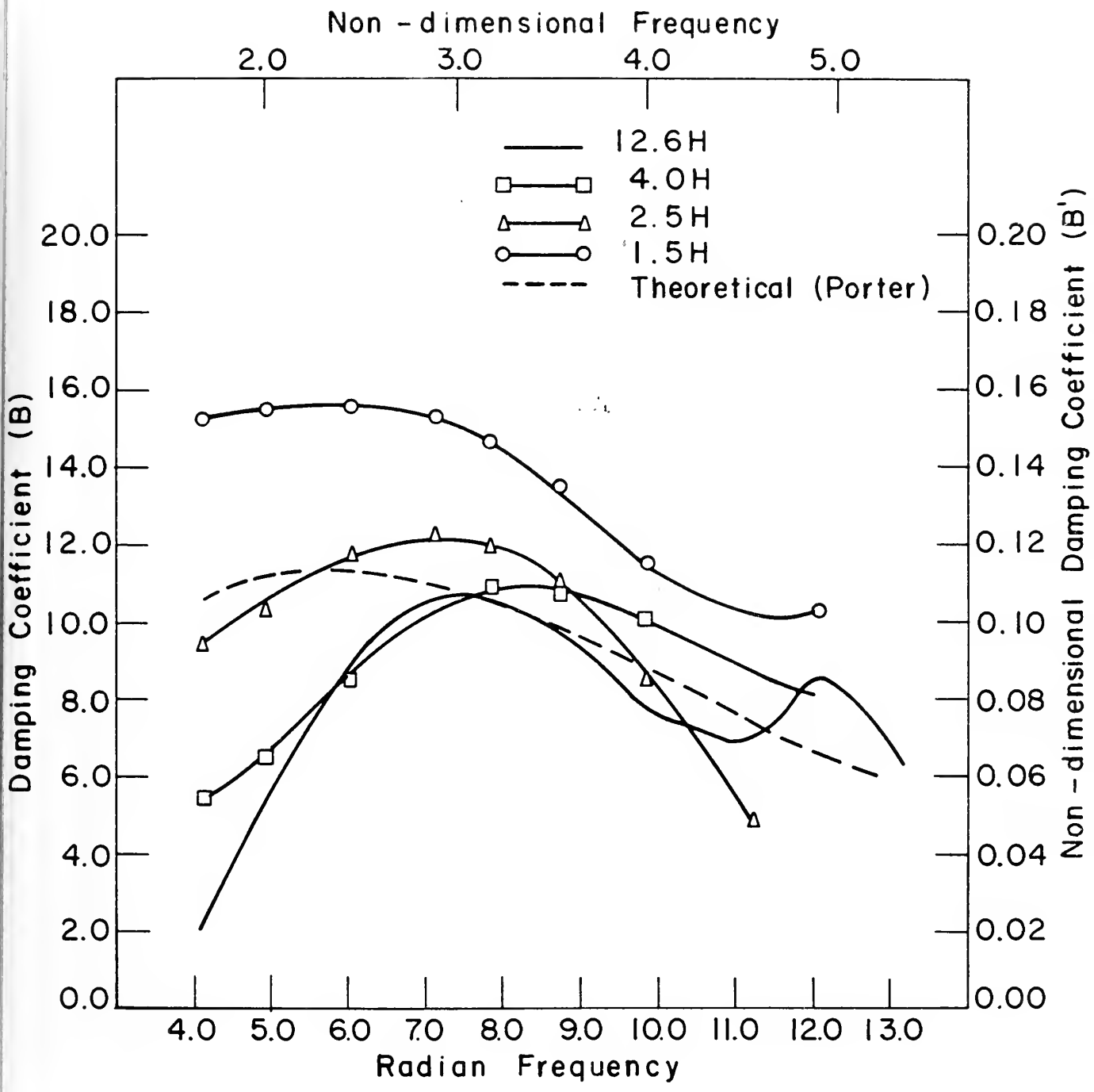

FIGURE X PITCH DAMPING AT ZERO FROUDE NUMBER AS A FUNCTION OF DEPTH

FIGURE XI

PITCH DAMPING AT A FROUDE NUMBER OF 0.10

AS A FUNCTION OF DEPTH

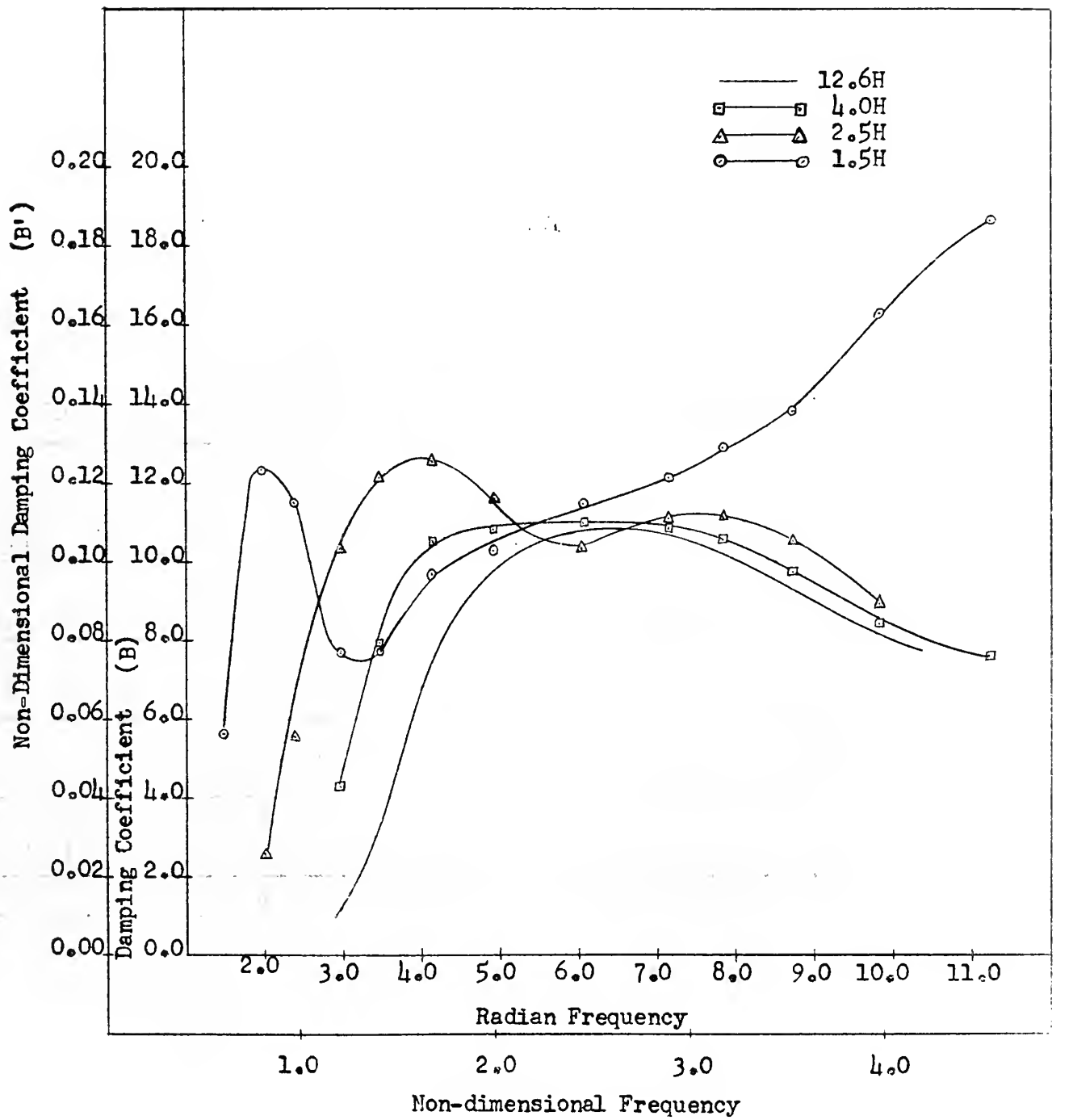

FIGURE XII

PITCH DAMPING COEFFICIENT AT FROUDE NUMBER OF 0.20

AS A FUNCTION OF DEPTH

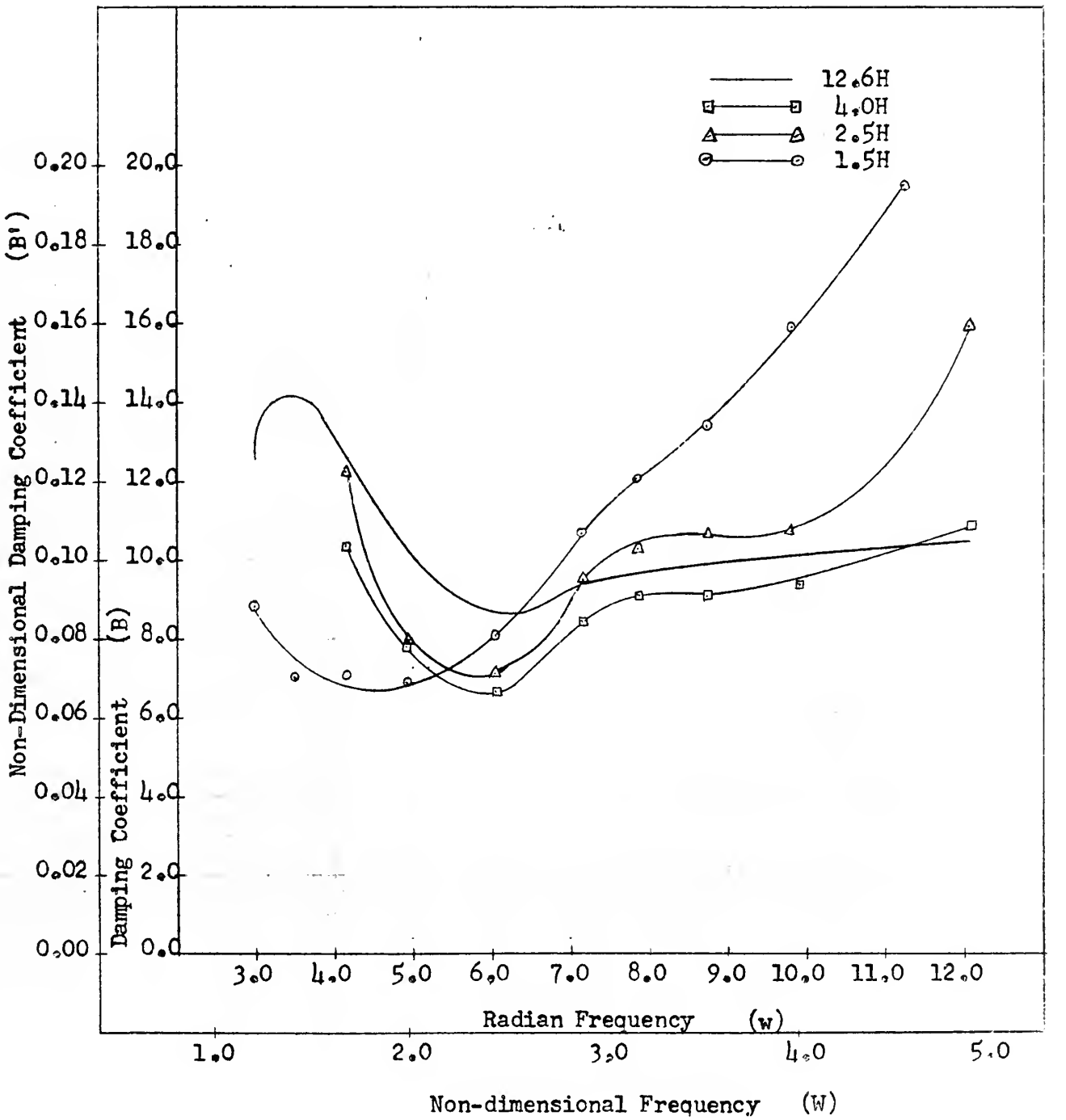

FIGURE XIII

PITCH DAMPING AT A FROUDE NUMBER OF 0.30

AS A FUNCTION OF DEPTH

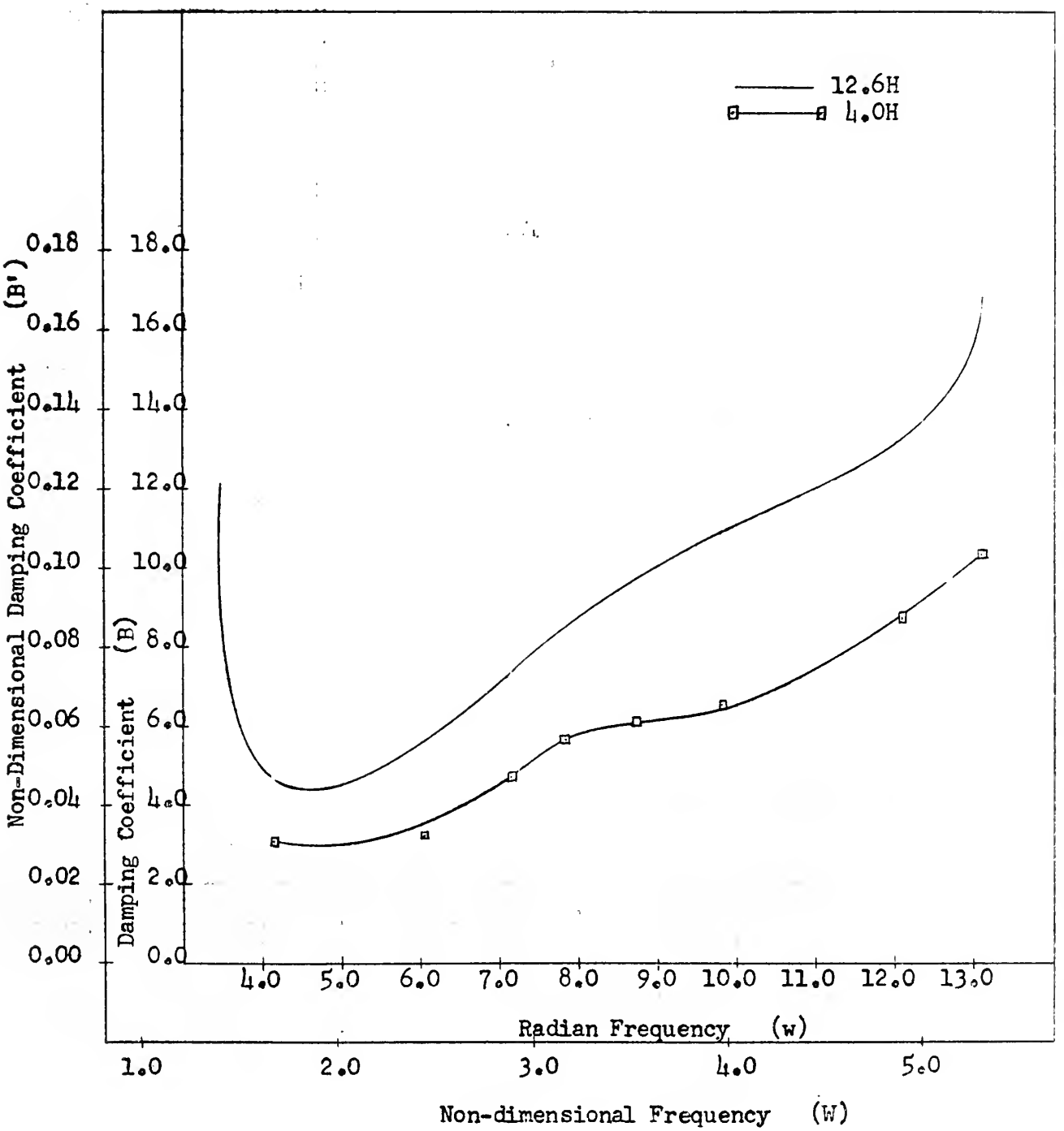

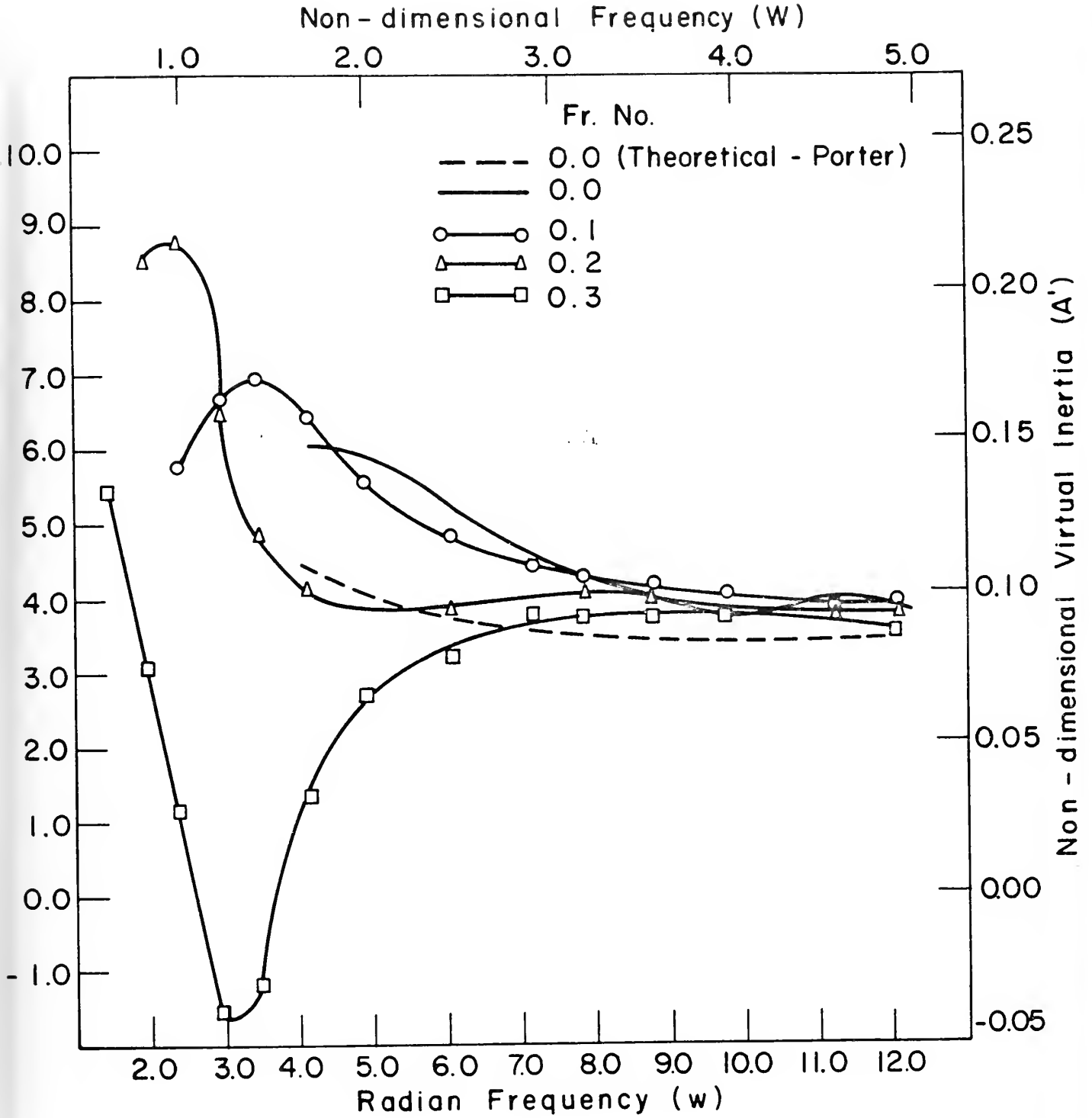

GURE XIV VIRTUAL INERTIA AT A DEPTH OF 12.6H AS A FUNCTION OF FROUDE NUMBER

FIGURE XV

VIRTUAL INERTIA AT A DEPTH OF 4.0H

AS A FUNCTION OF FROUDE NUMBER

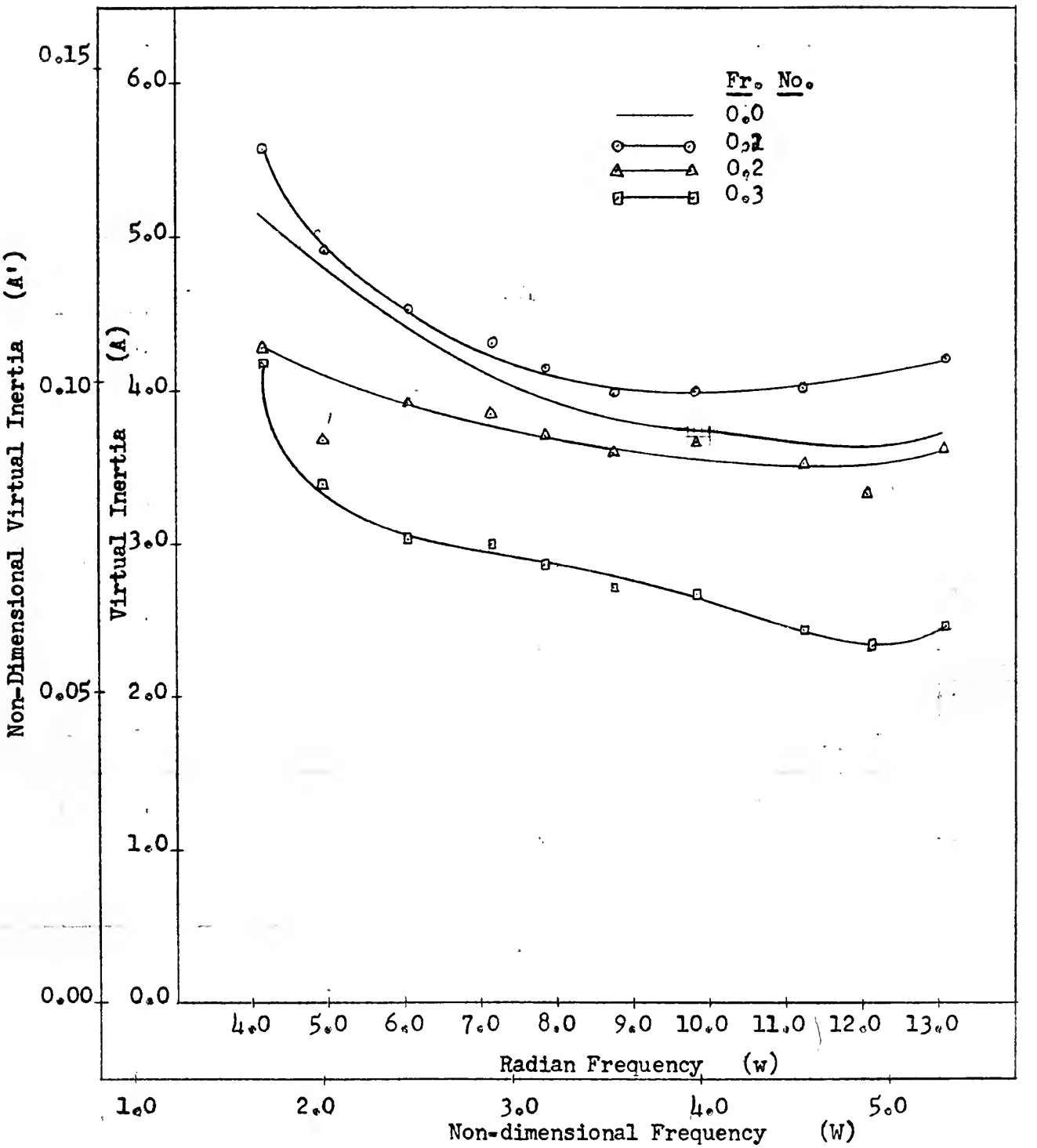

FIGURE XVI

VIRTUAL INERTIA AT A DEPTH OF 2.5H

AS A FUNCTION OF FROUDE NUMBER

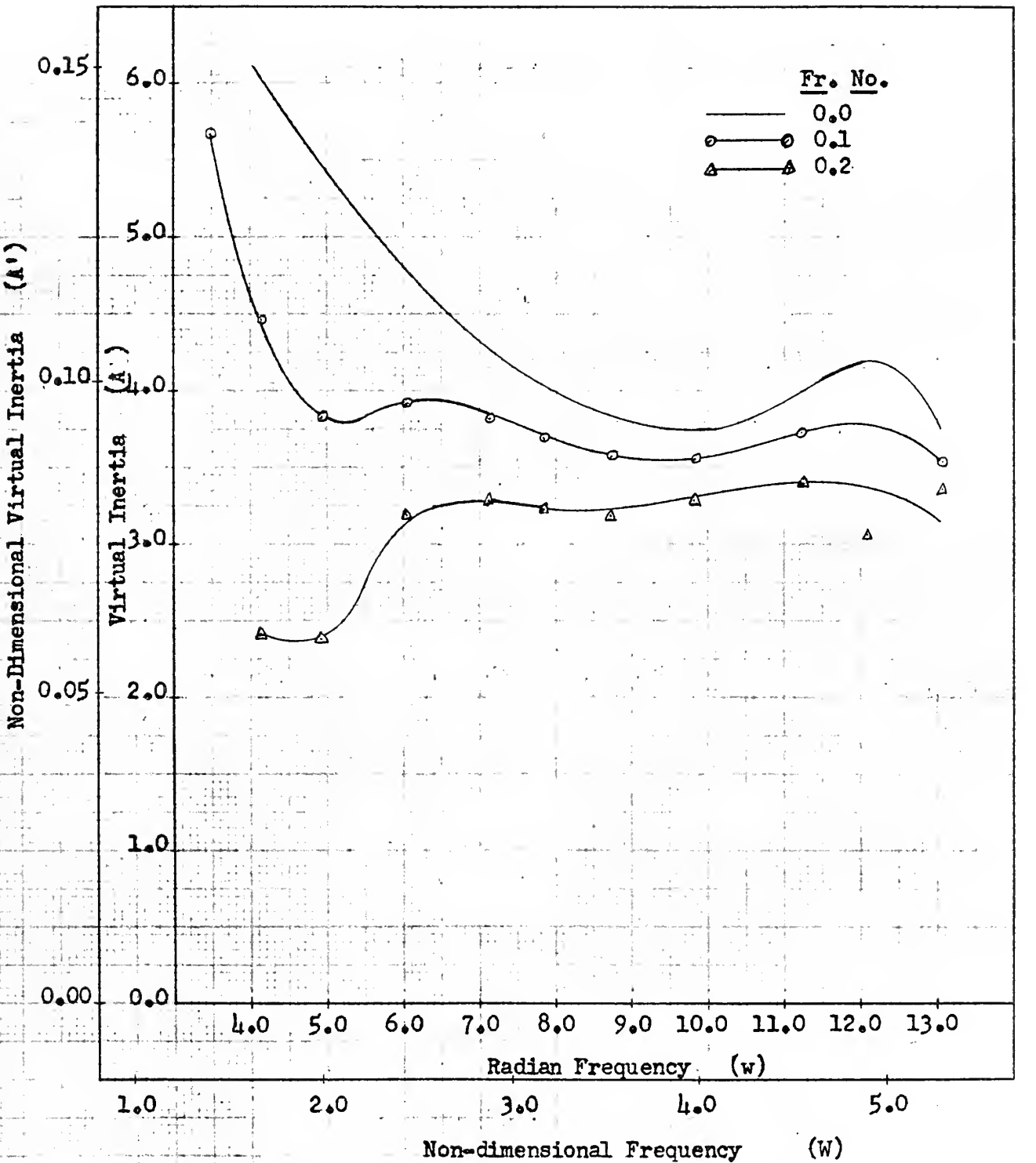

FIGURE XVII

VIRTUAL INERTIA AT A DEPTH OF 1.5H

AS A FUNCTION OF FROUDE NUMBER

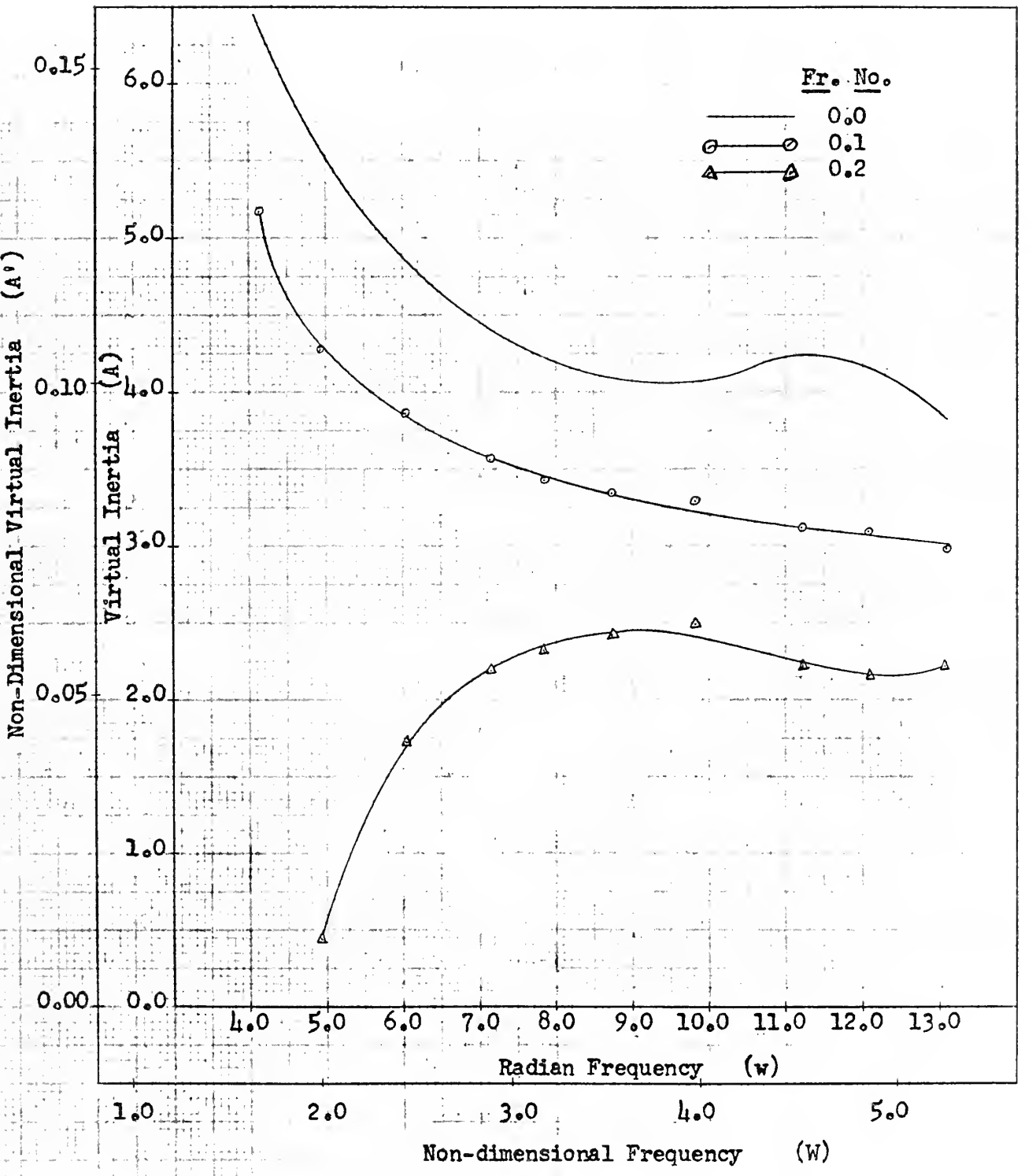

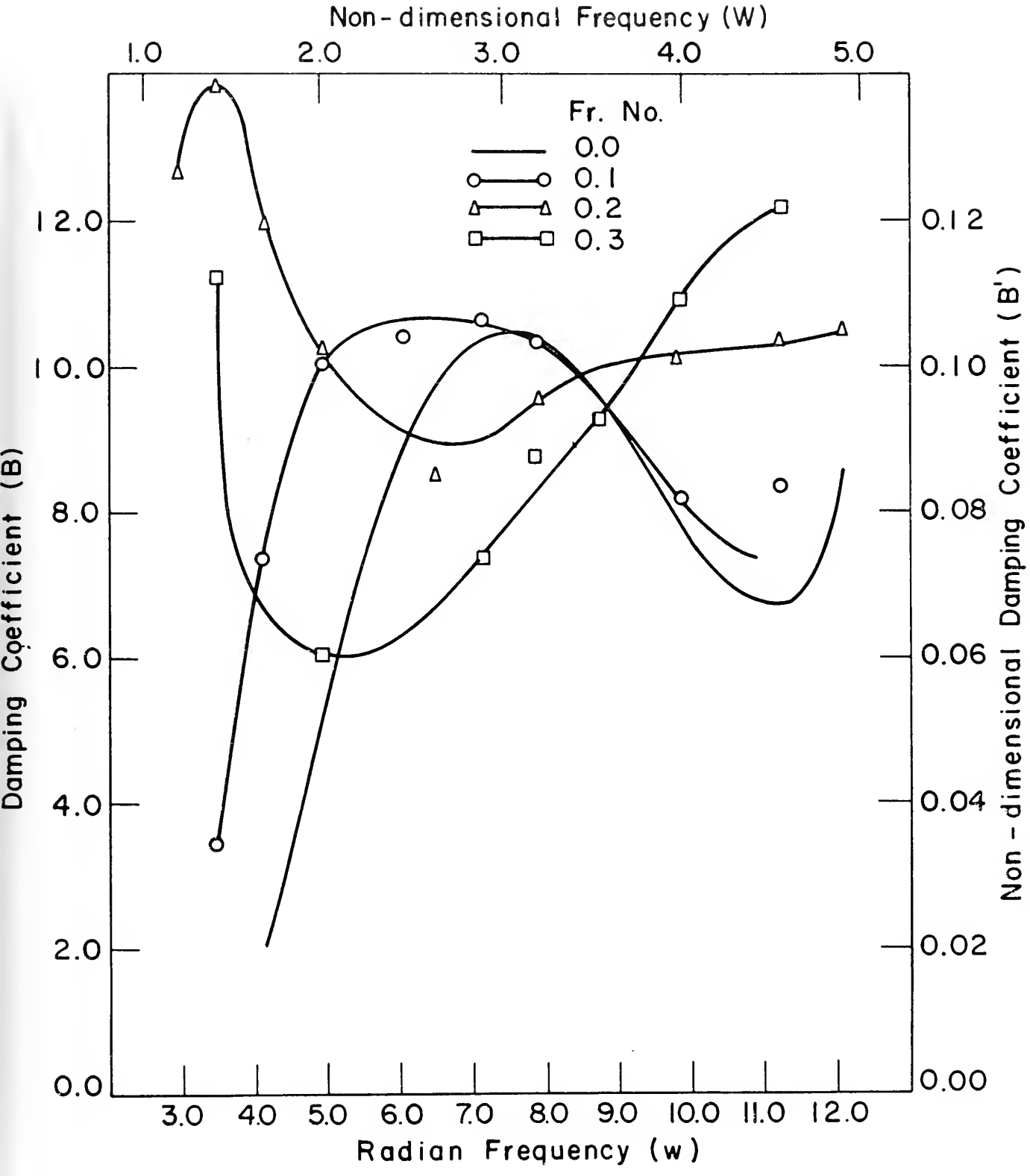

FIGURE XVIII PITCH DAMPING AT A DEPTH OF 12.6H AS A FUNCTION OF FROUDE NUMBER

FIGURE XIX

PITCH DAMPING AT A DEPTH OF 4.0H

AS A FUNCTION OF FROUDE NUMBER

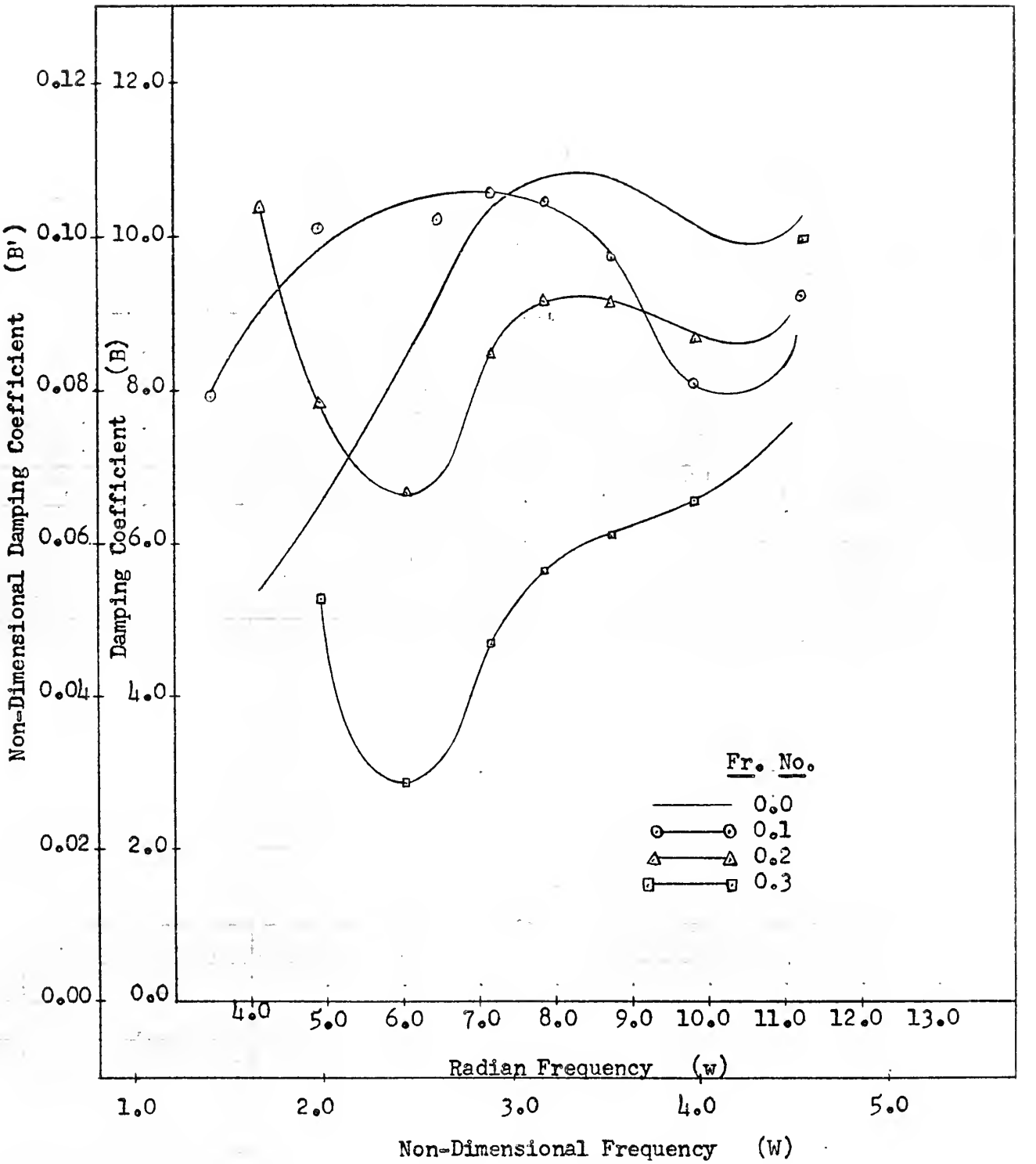

FIGURE XX

PITCH DAMPING AT A DEPTH OF 2.5H

AS A FUNCTION OF FROUDE NUMBER

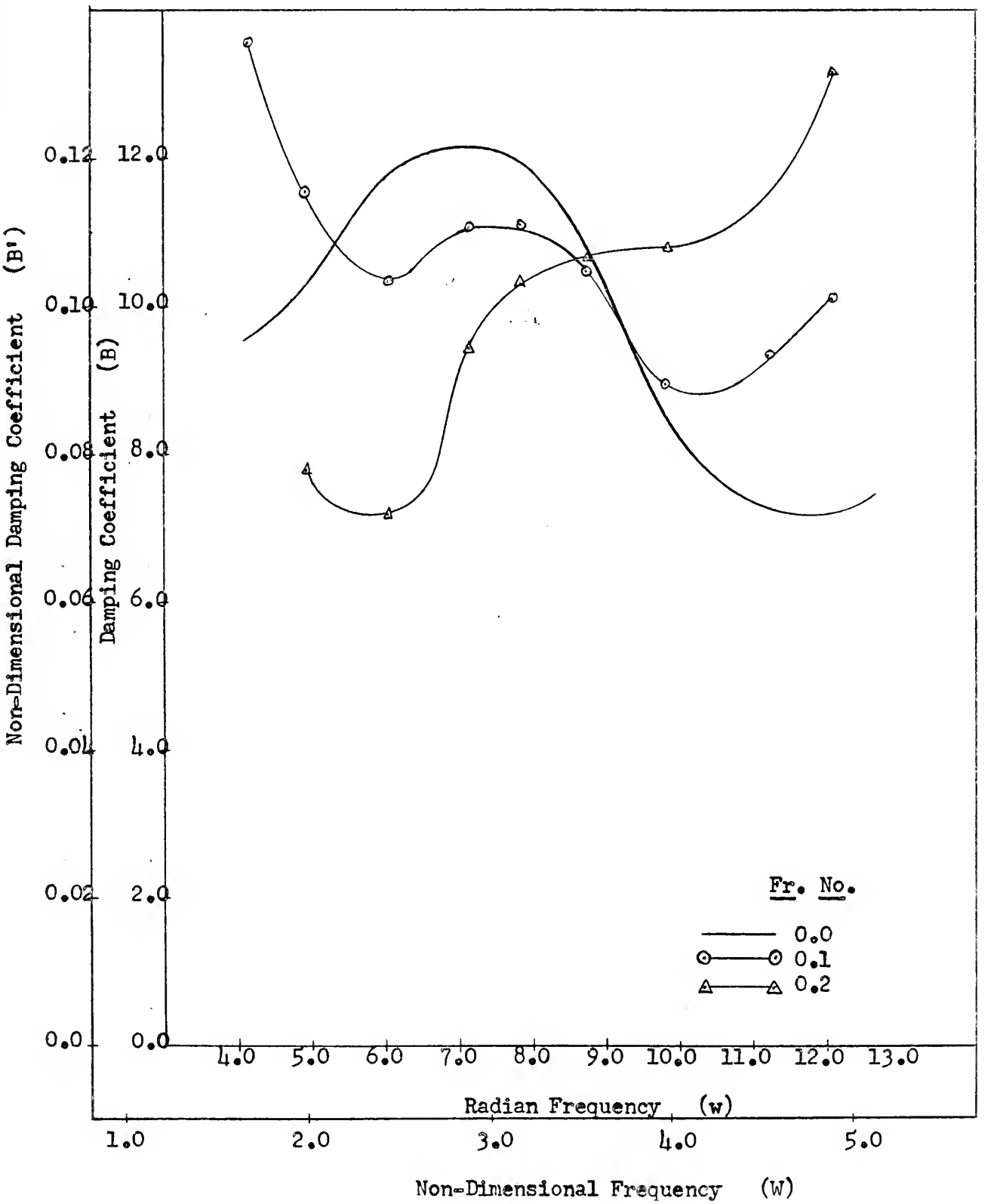

FIGURE XXI

PITCH DAMPING AT A DEPTH OF 1.5H

AS A FUNCTION OF FROUDE NUMBER

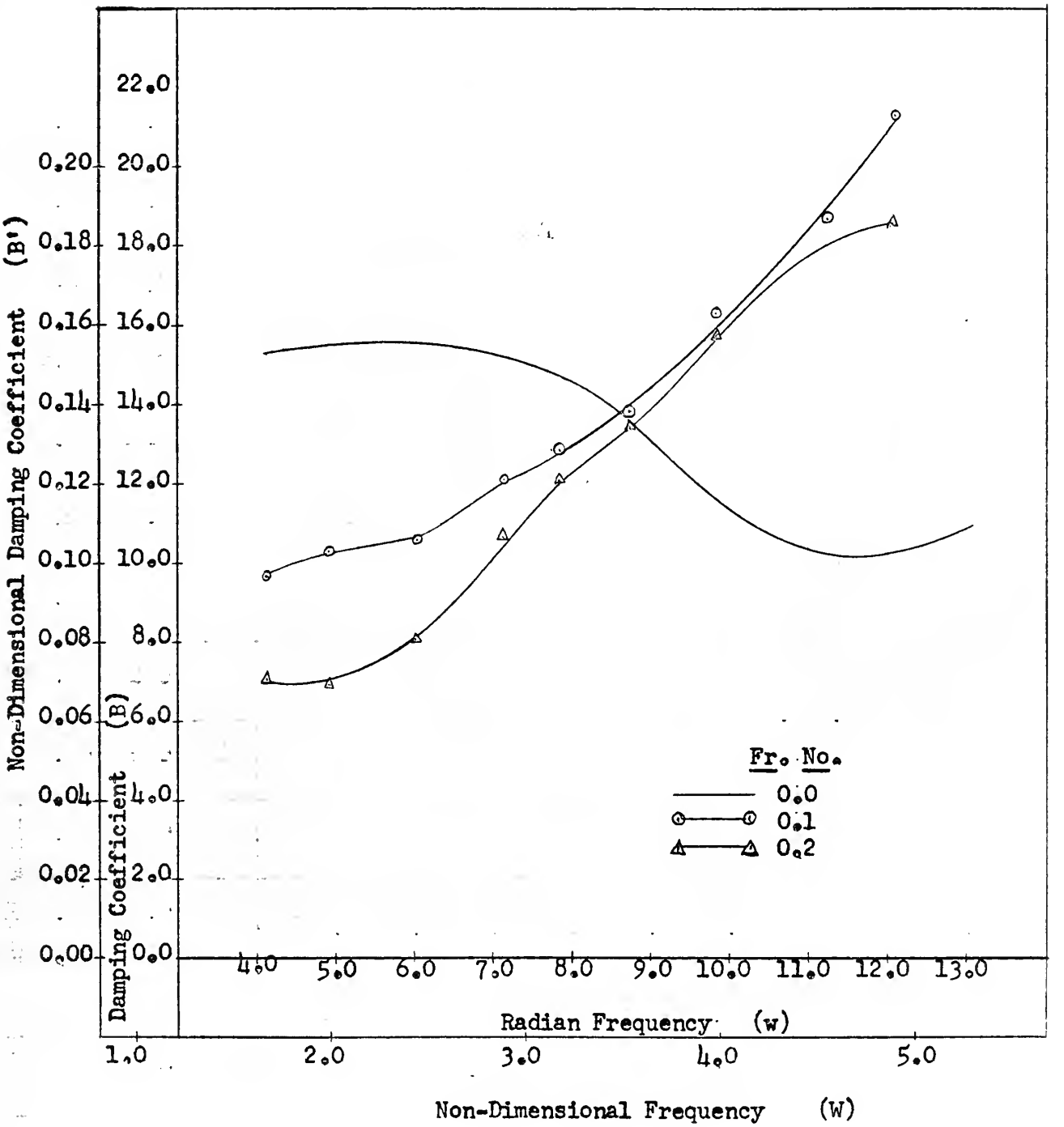

FIGURE XXII

VIRTUAL INERTIA (STERN-UP INITIALLY) AT A DEPTH OF 2.5H

AS A FUNCTION OF FROUDE NUMBER

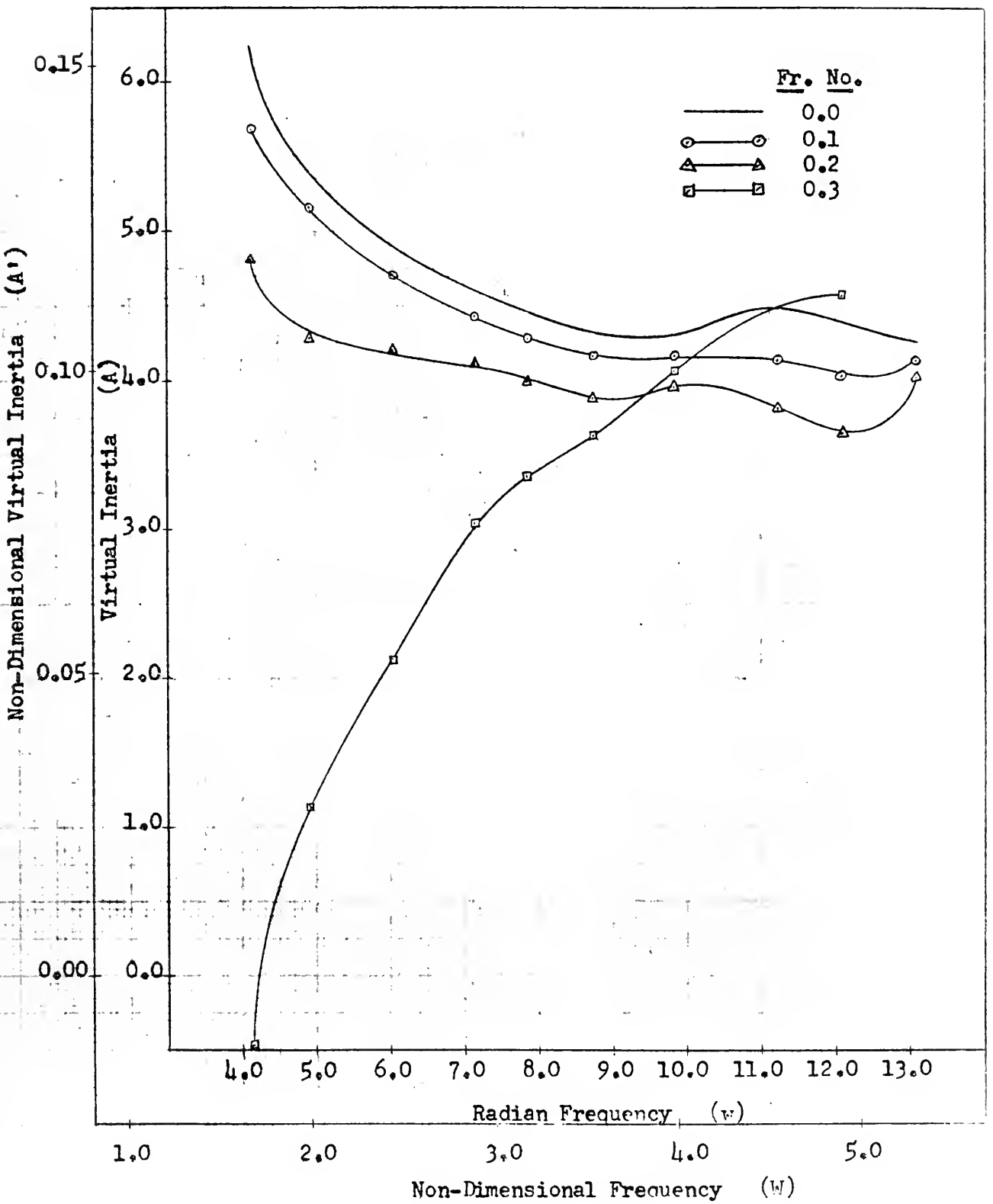

FIGURE XXIII

VIRTUAL INERTIA (STERN-UP INITIALLY) AT A DEPTH OF 1.5H

AS A FUNCTION OF FROUDE NUMBER

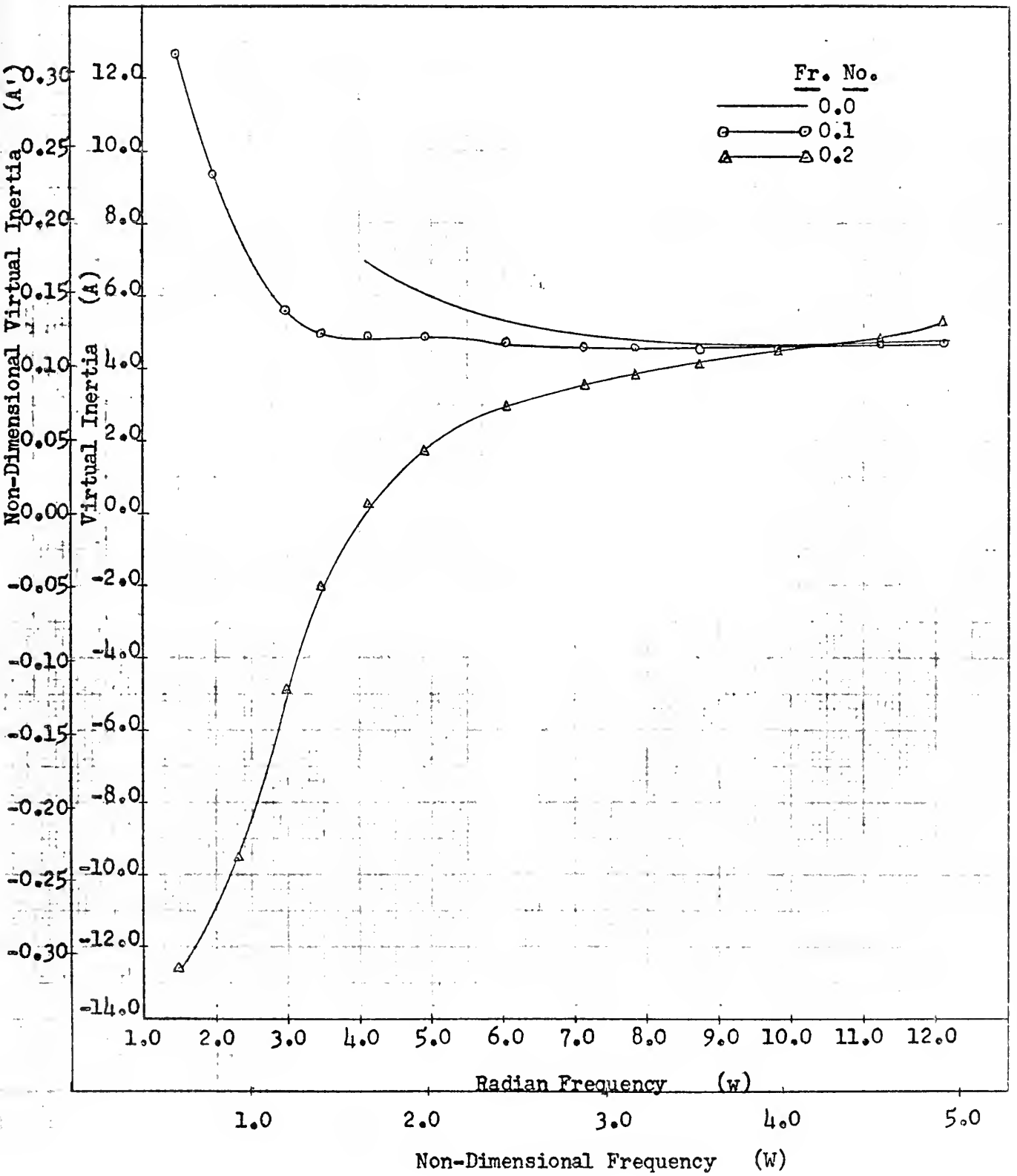

FIGURE XXIV

DAMPING IN PITCH (STERN-UP INITIALLY) AT A DEPTH OF 2.5H

AS A FUNCTION OF FROUDE NUMBER

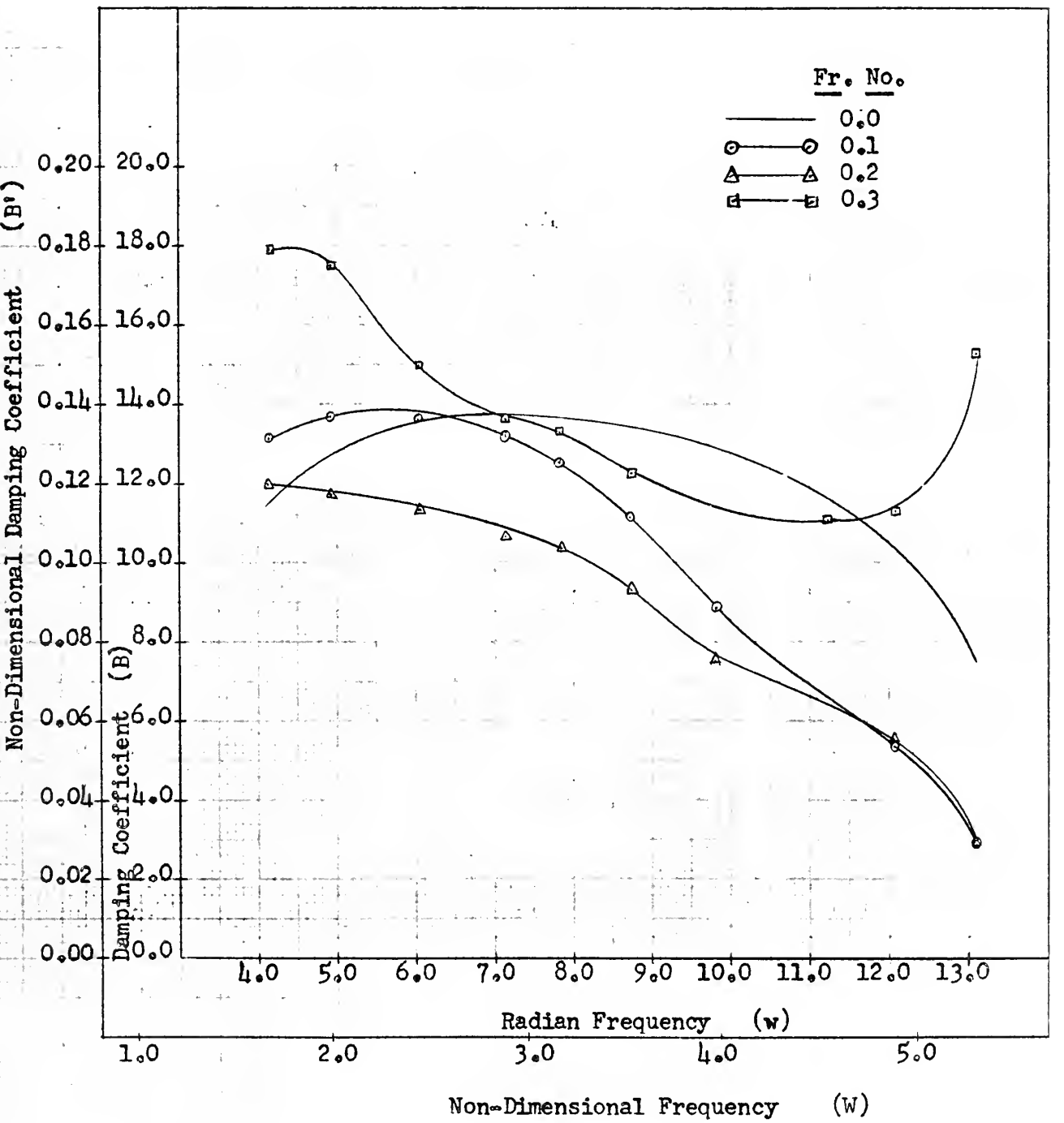

FIGURE XXV

DAMPING IN PITCH (STERN-UP INITIALLY) AT A DEPTH OF 1.5H

AS A FUNCTION OF FROUDE NUMBER

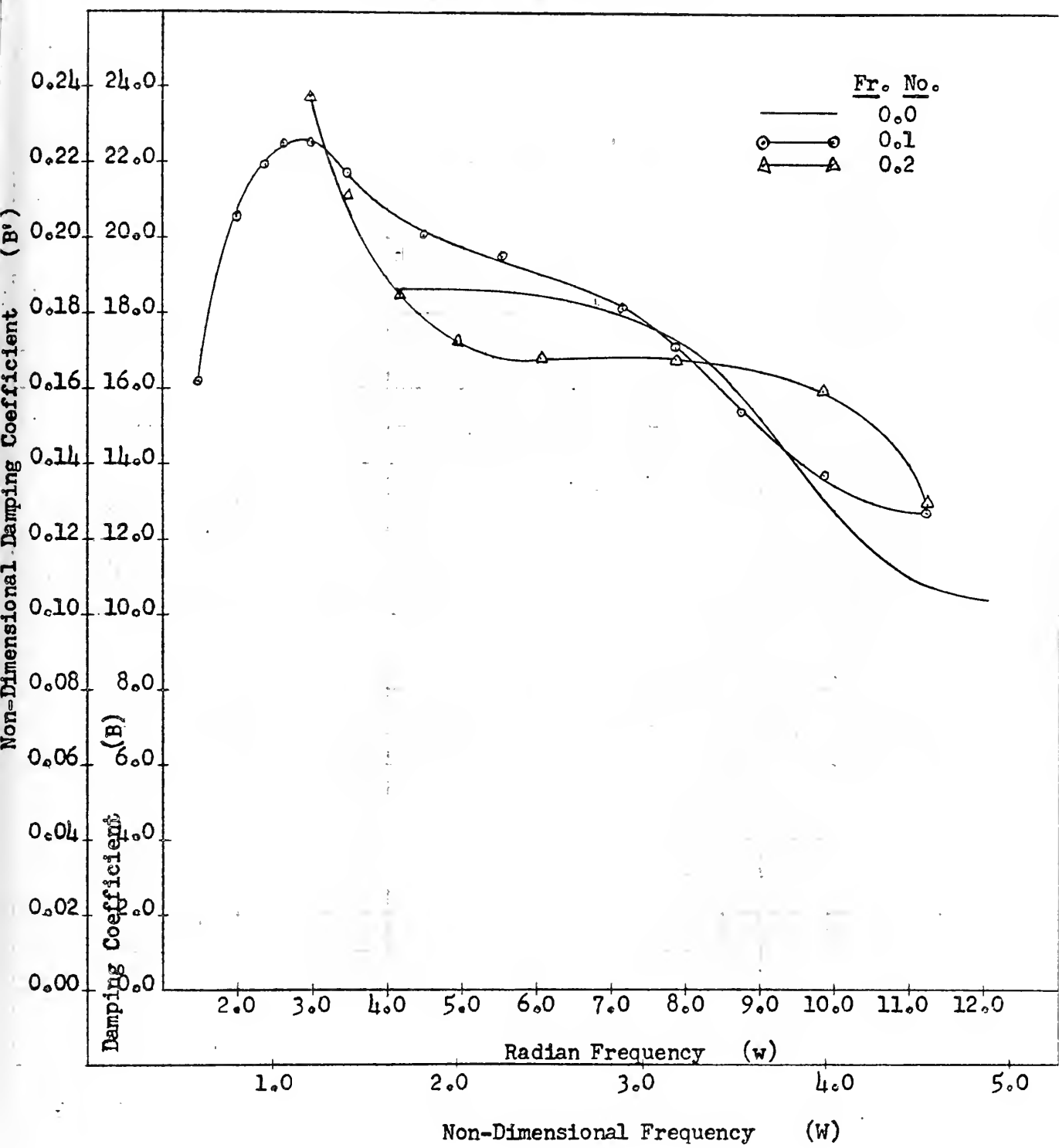

FIGURE XXVI

VIRTUAL MASS AT ZERO FROUDE NUMBER

AS A FUNCTION OF DEPTH

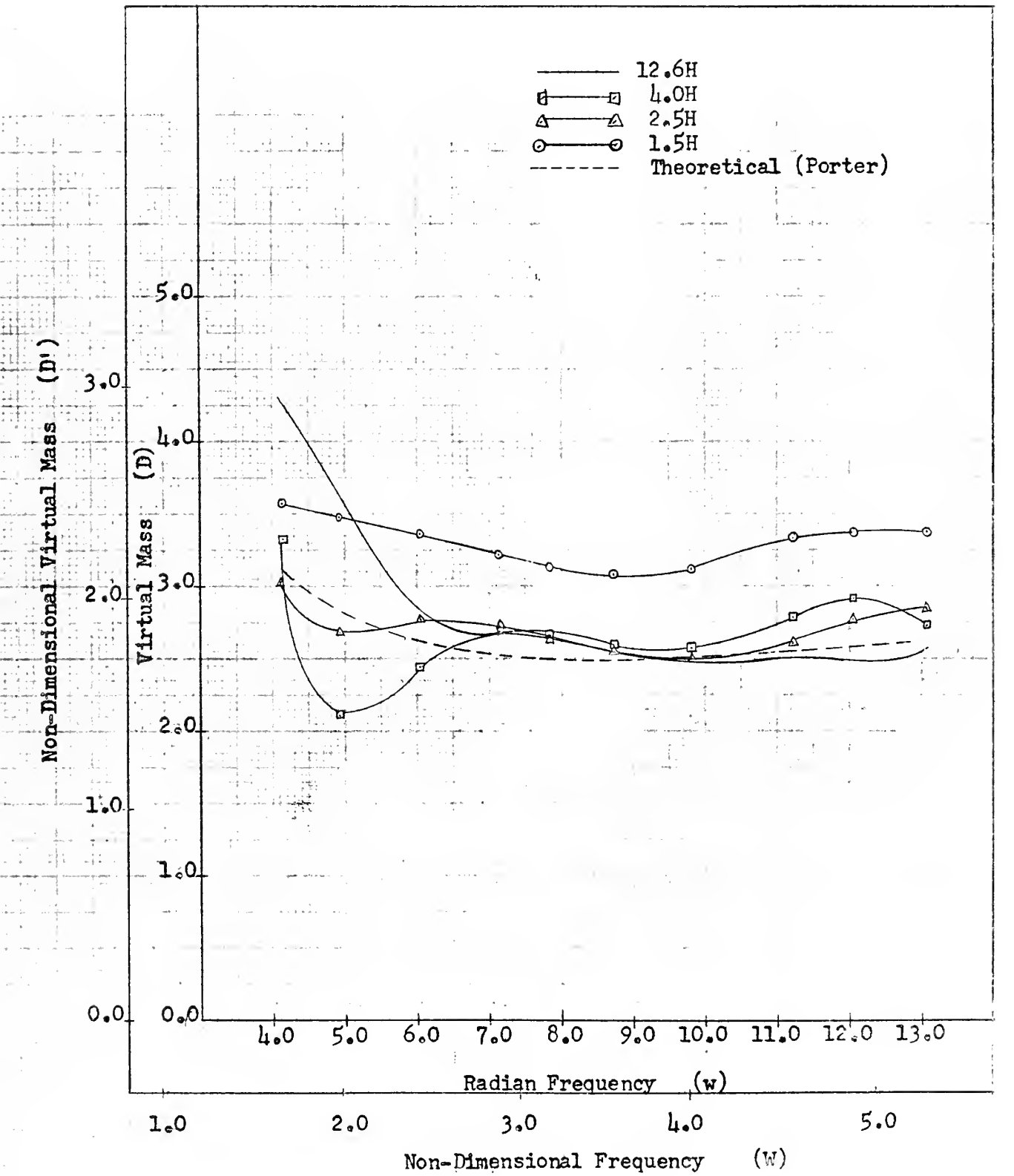

FIGURE XXVII

VIRTUAL MASS AT A FROUDE NUMBER OF 0.10

AS A FUNCTION OF DEPTH

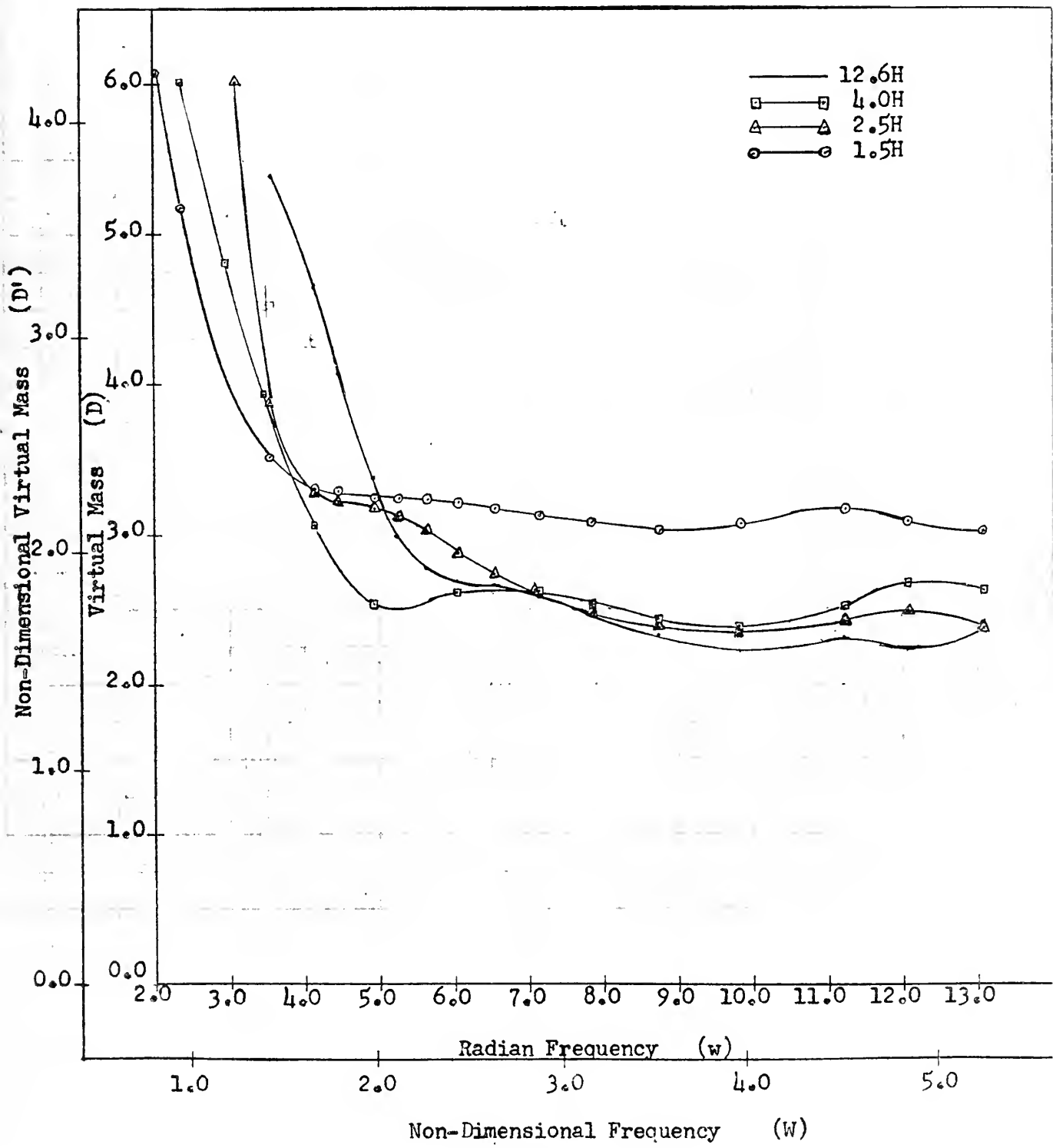

FIGURE XXVIII

VIRTUAL MASS AT A FROUDE NUMBER OF 0.20

AS A FUNCTION OF DEPTH

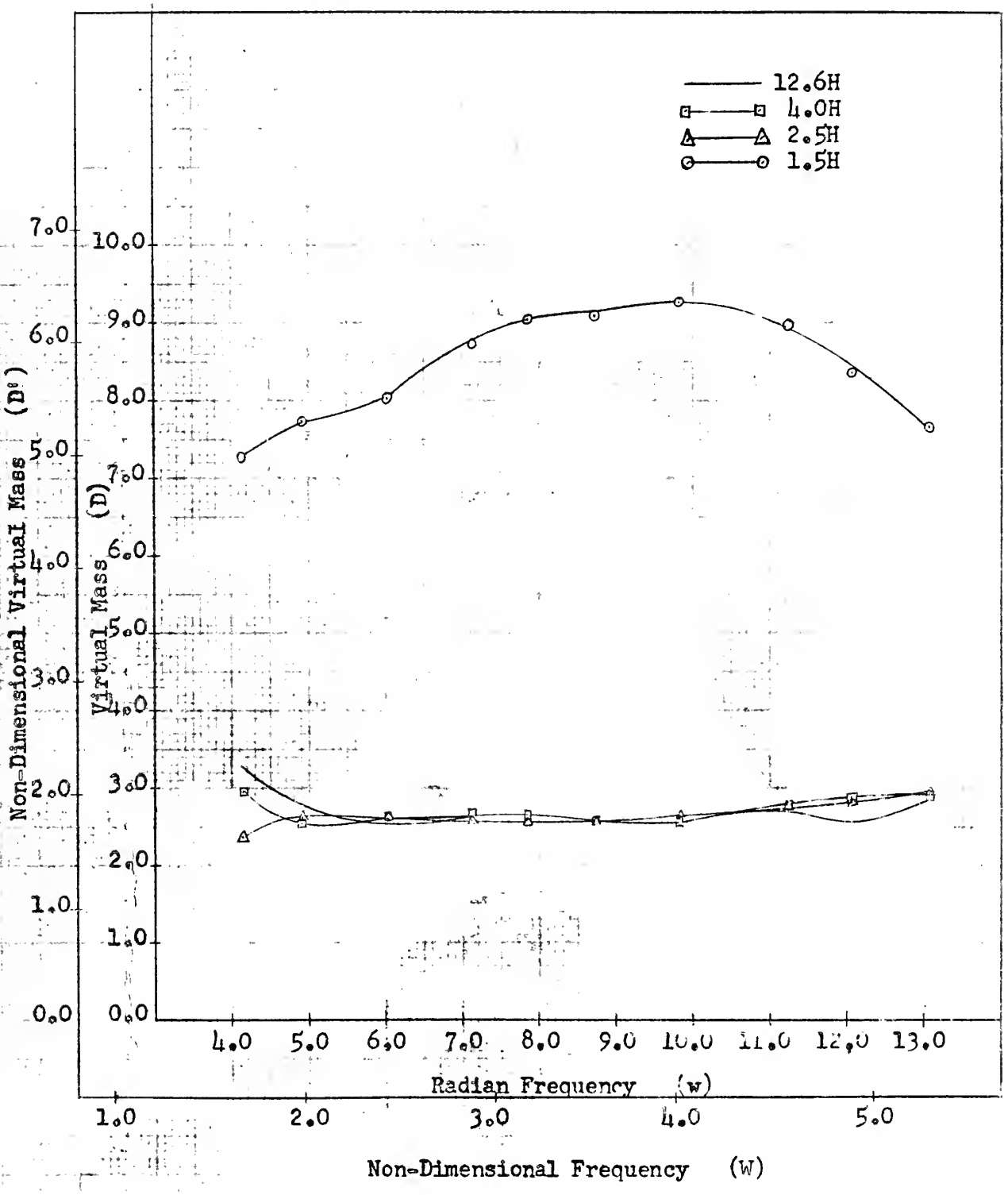

FIGURE XXIX

VIRTUAL MASS AT A FROUDE NUMBER OF 0.30

AS A FUNCTION OF DEPTH

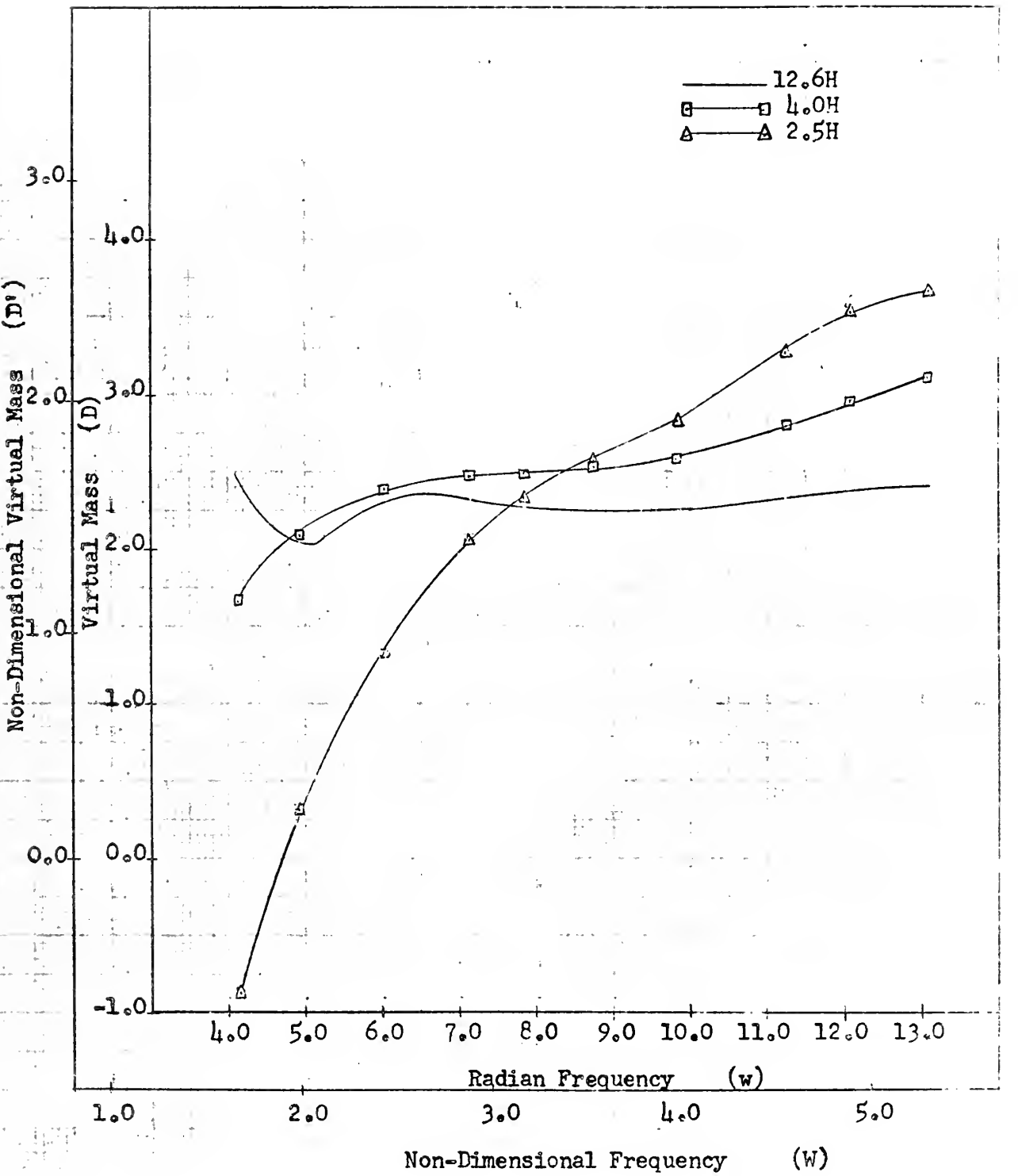

FIGURE XXX

HEAVE DAMPING COEFFICIENT AT A FROUDE NUMBER OF 0.0

AS A FUNCTION OF DEPTH

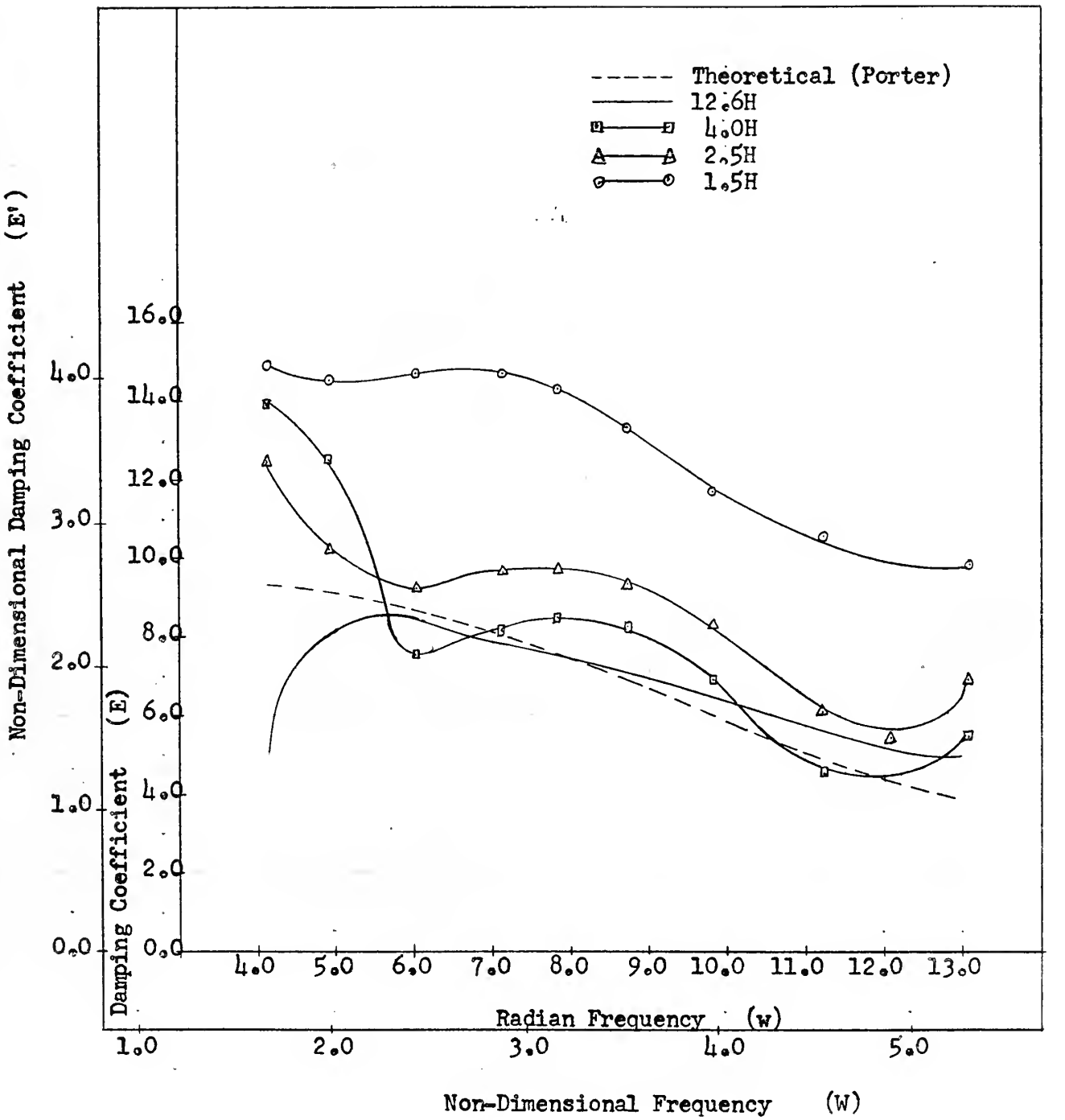

FIGURE XXXI

HEAVE DAMPING COEFFICIENT AT A FROUDE NUMBER OF 0.10

AS A FUNCTION OF DEPTH

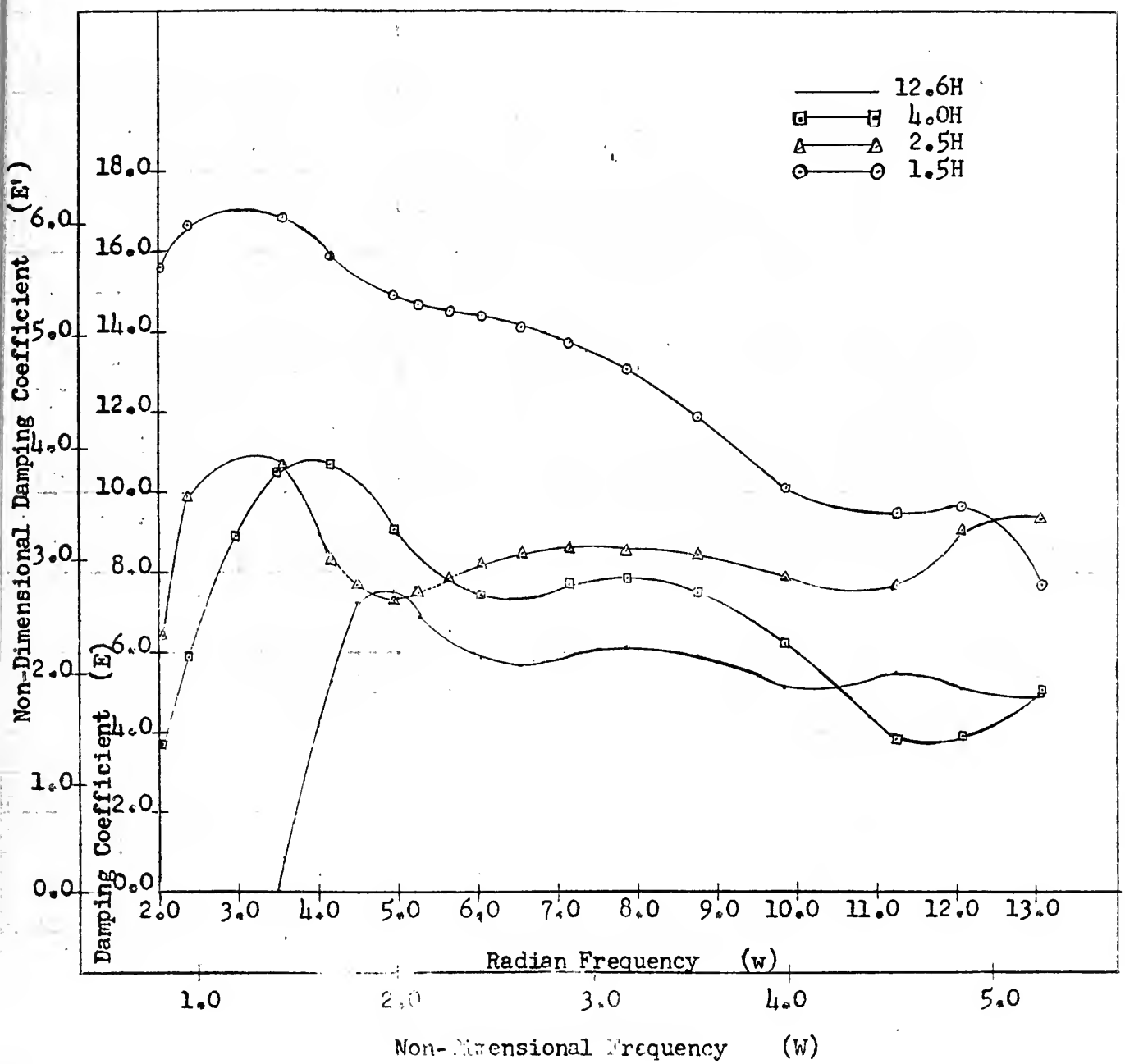

FIGURE XXXII

HEAVE DAMPING COEFFICIENT AT A FROUDE NUMBER OF 0.20
AS A FUNCTION OF DEPTH

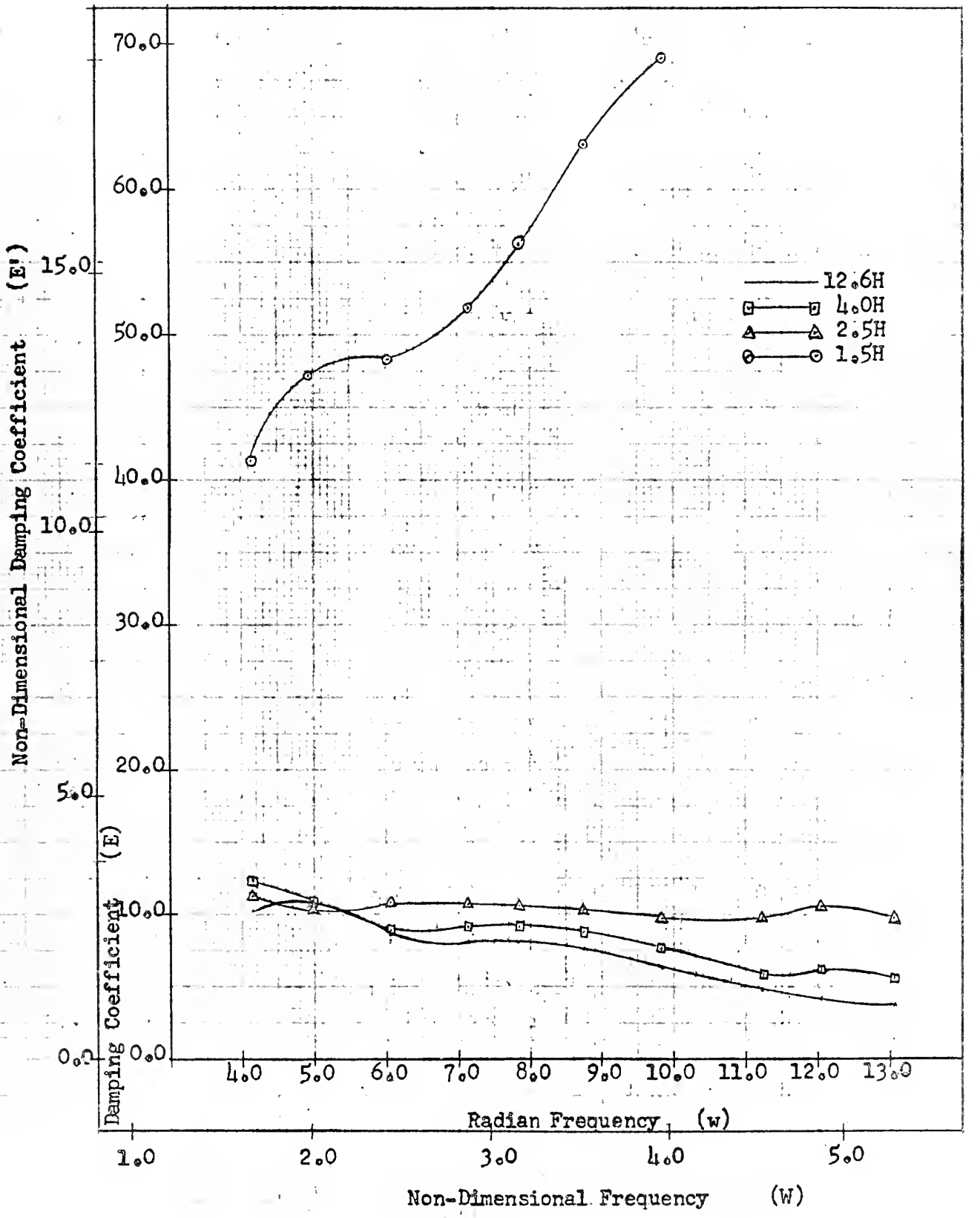

FIGURE XXXIII

HEAVE DAMPING COEFFICIENT AT A FROUDE NUMBER OF 0.30

AS A FUNCTION OF DEPTH

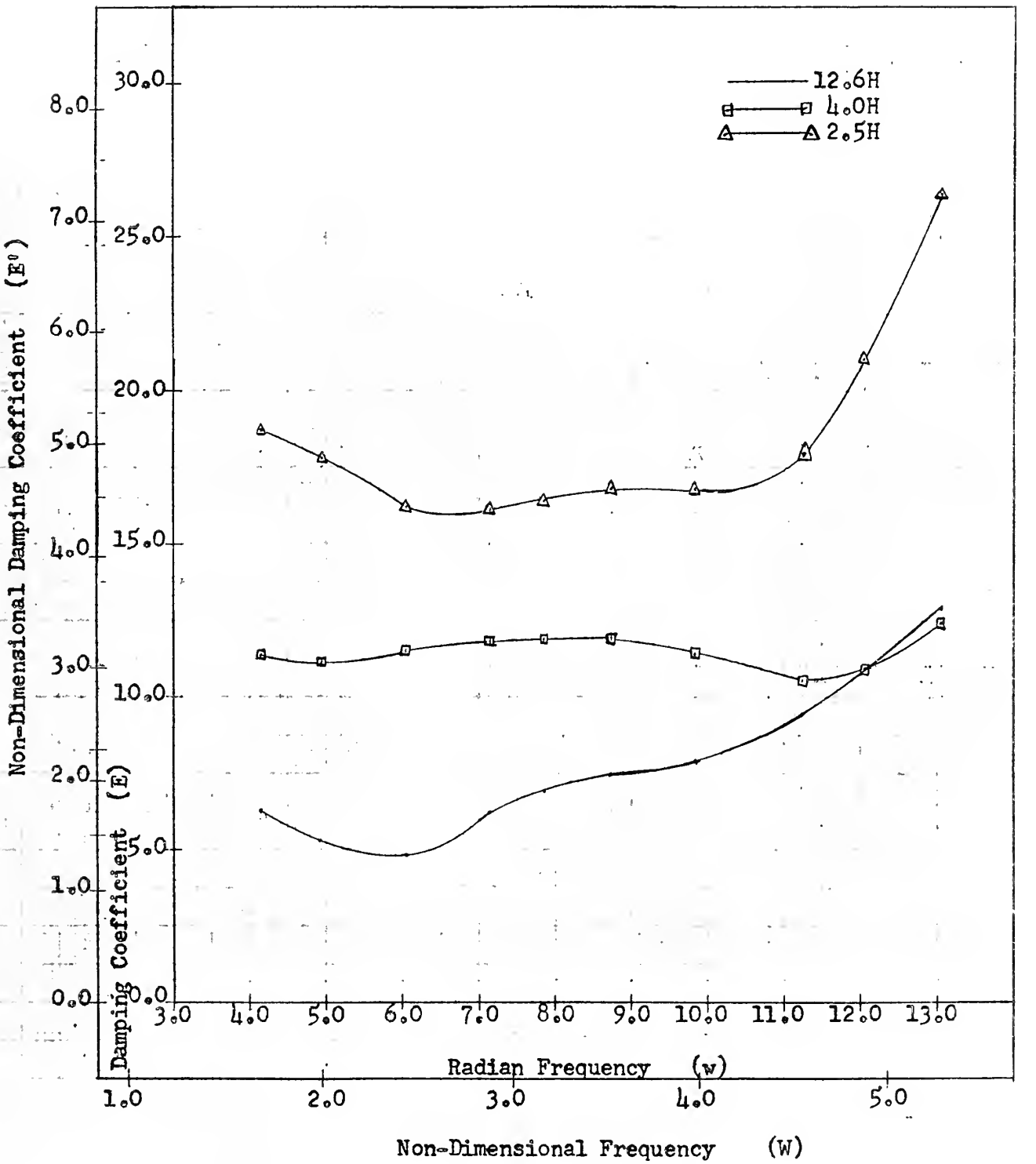

FIGURE XXXIV

VIRTUAL MASS AT A DEPTH OF 12.6H

AS A FUNCTION OF FROUDE NUMBER

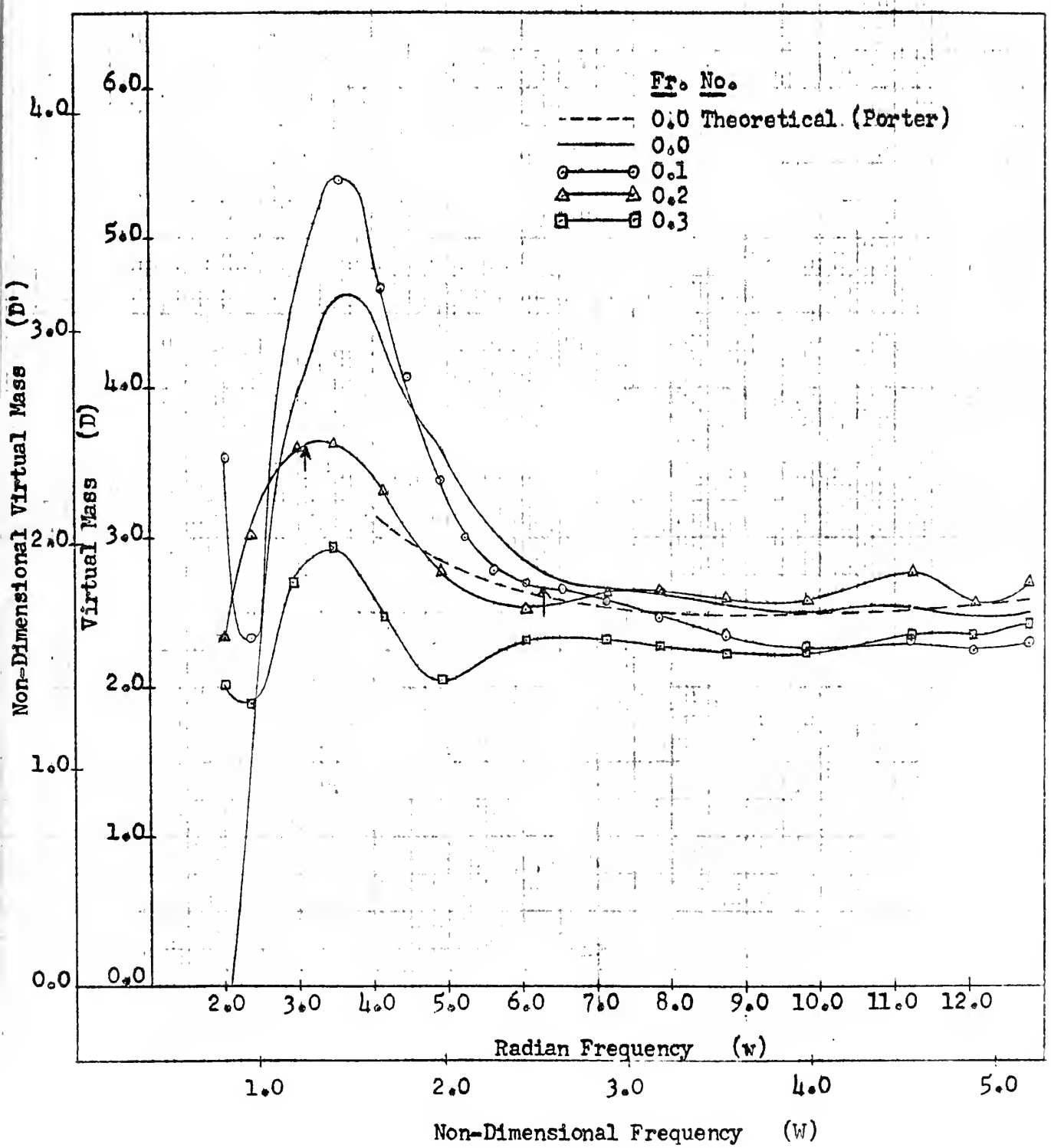

FIGURE XXXV

VIRTUAL MASS AT A DEPTH OF 4.0H

AS A FUNCTION OF FROUDE NUMBER

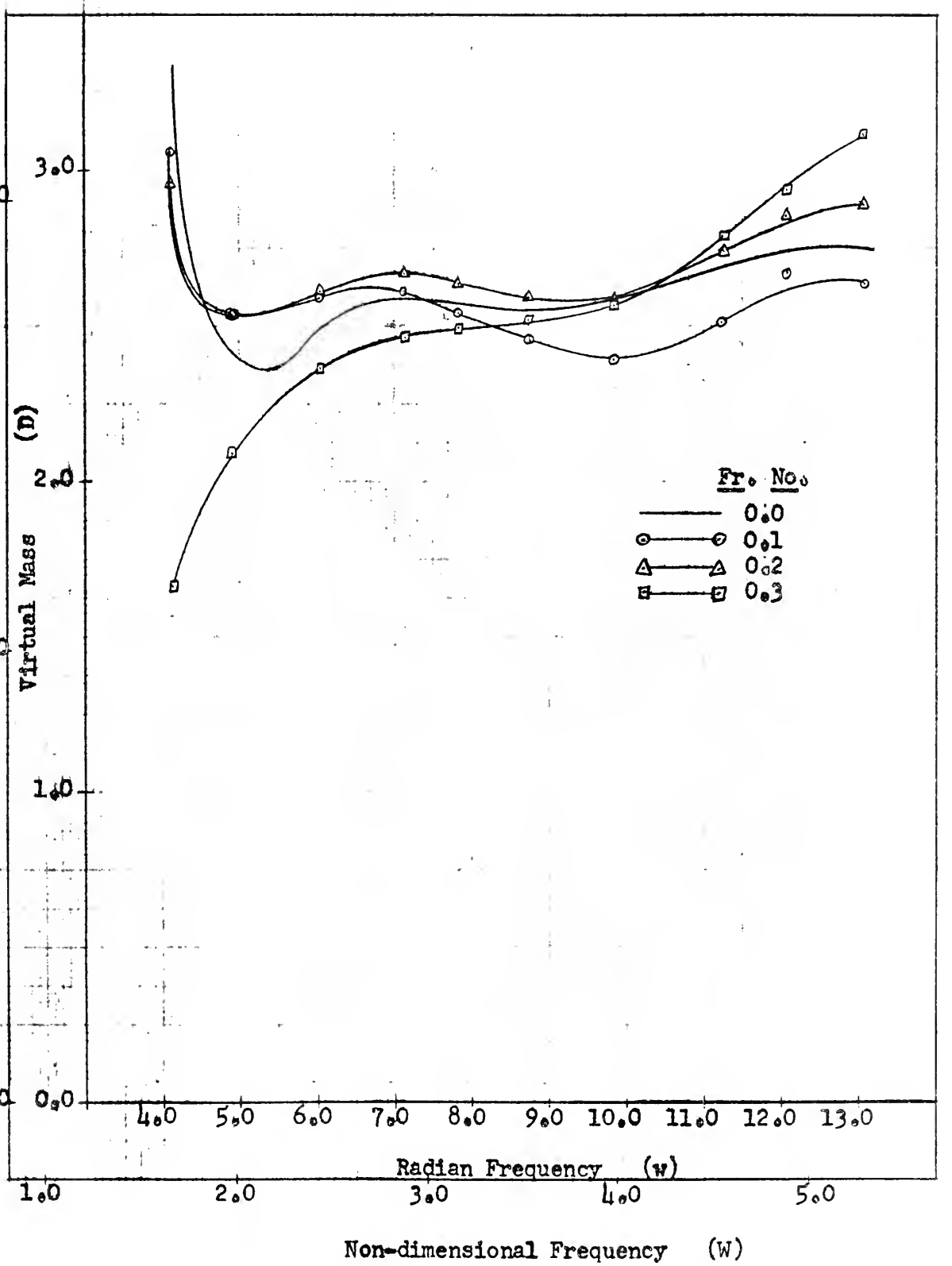

FIGURE XXXVI

VIRTUAL MASS AT A DEPTH OF 2.5H

AS A FUNCTION OF FROUDE NUMBER

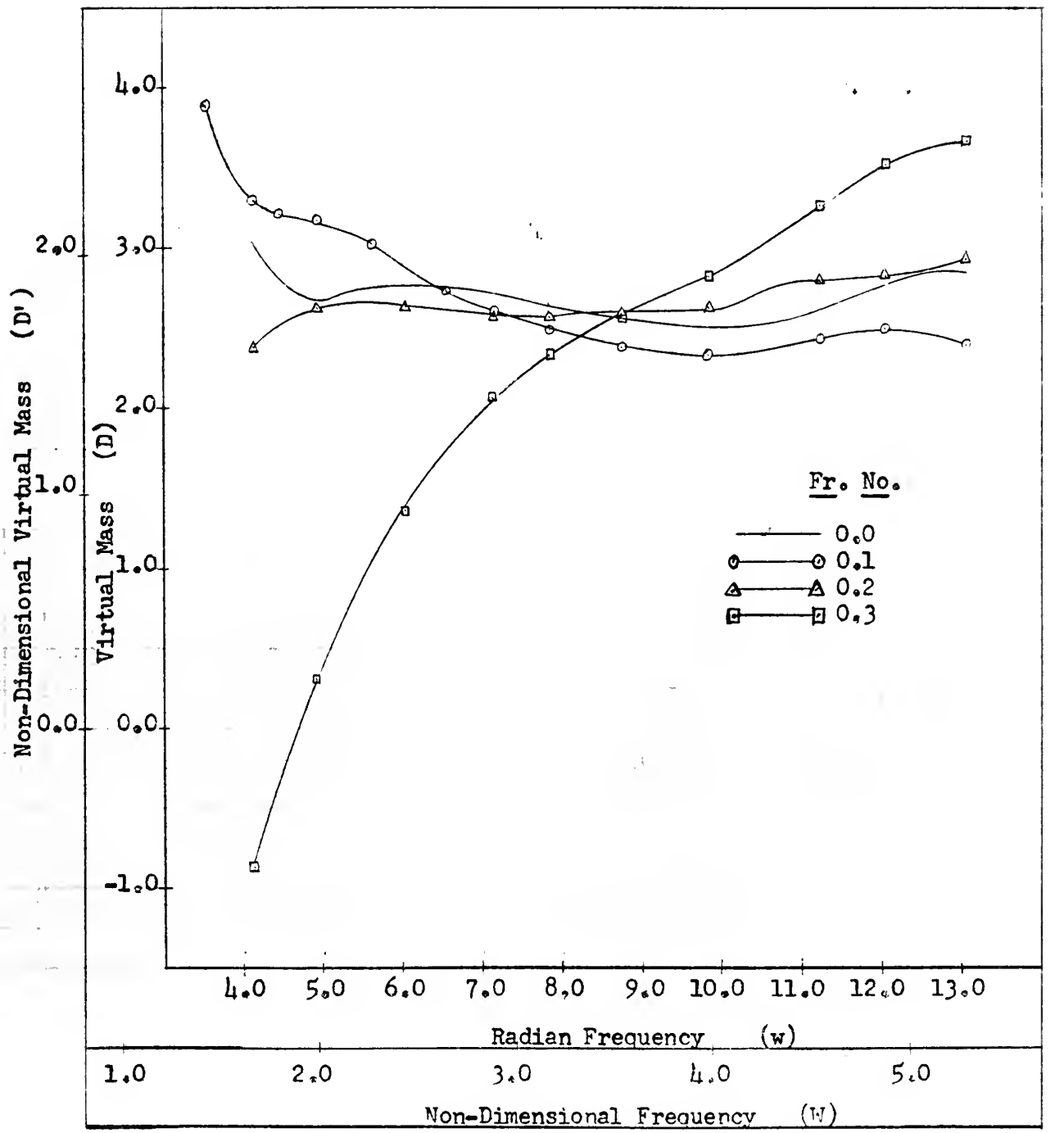

FIGURE XXXVII

VIRTUAL MASS AT A DEPTH OF 1.5H

AS A FUNCTION OF FROUDE NUMBER

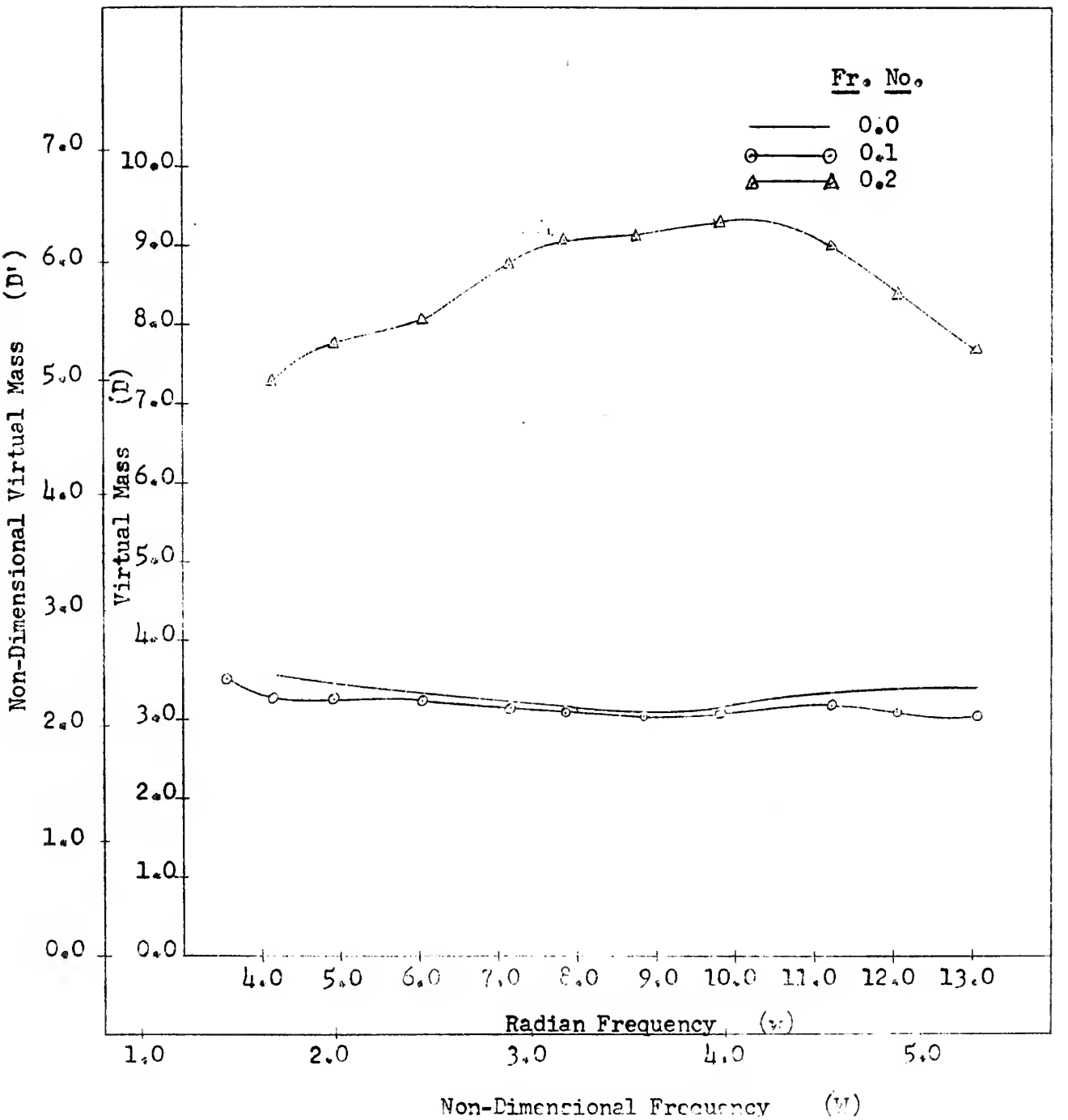

FIGURE XXXVIII

HEAVE DAMPING AT A DEPTH OF 12.6H

AS A FUNCTION OF FROUDE NUMBER

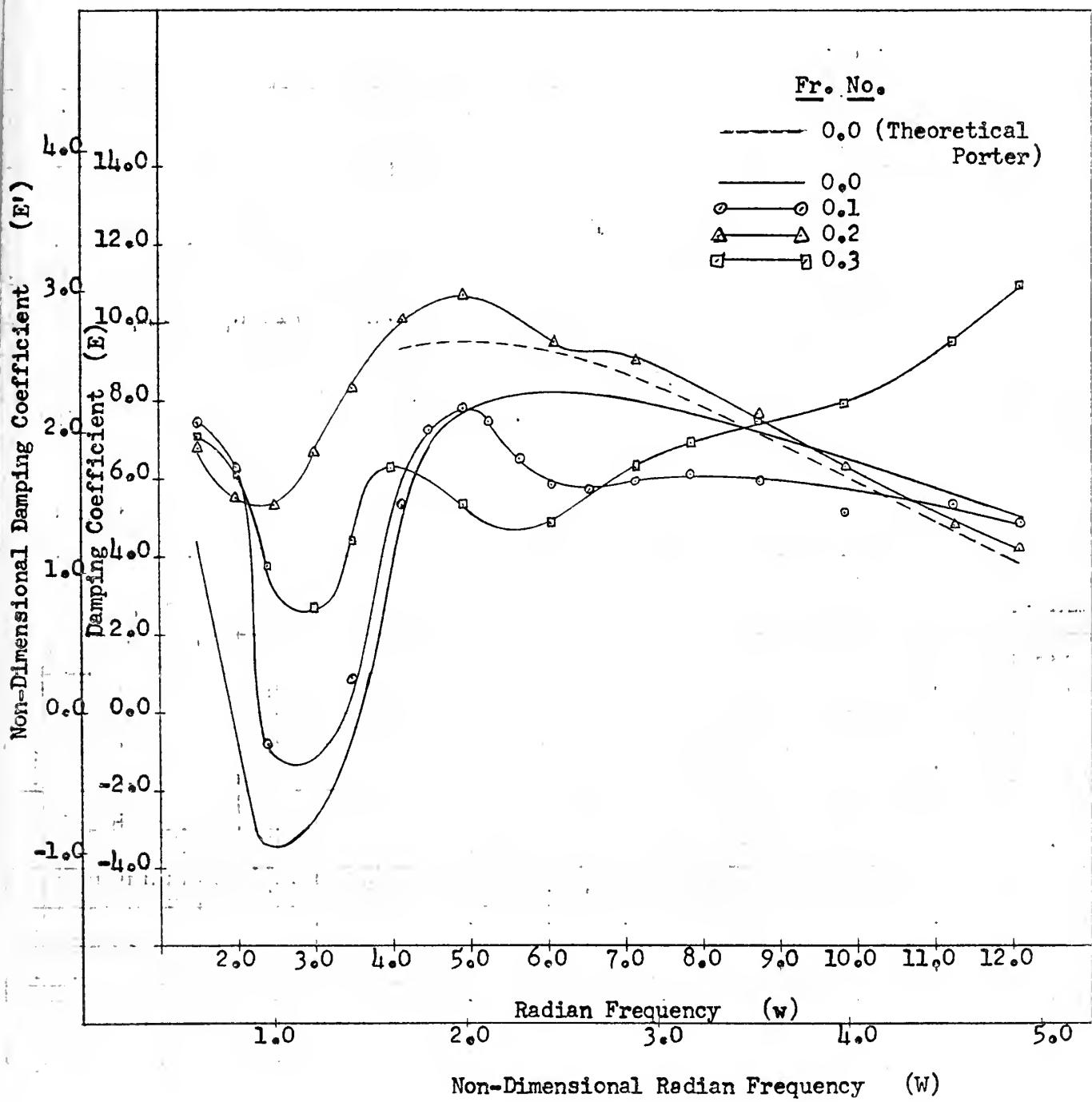

FIGURE XXXIX

HEAVE DAMPING COEFFICIENT AT A DEPTH OF 4.0H

AS A FUNCTION OF FROUDE NUMBER

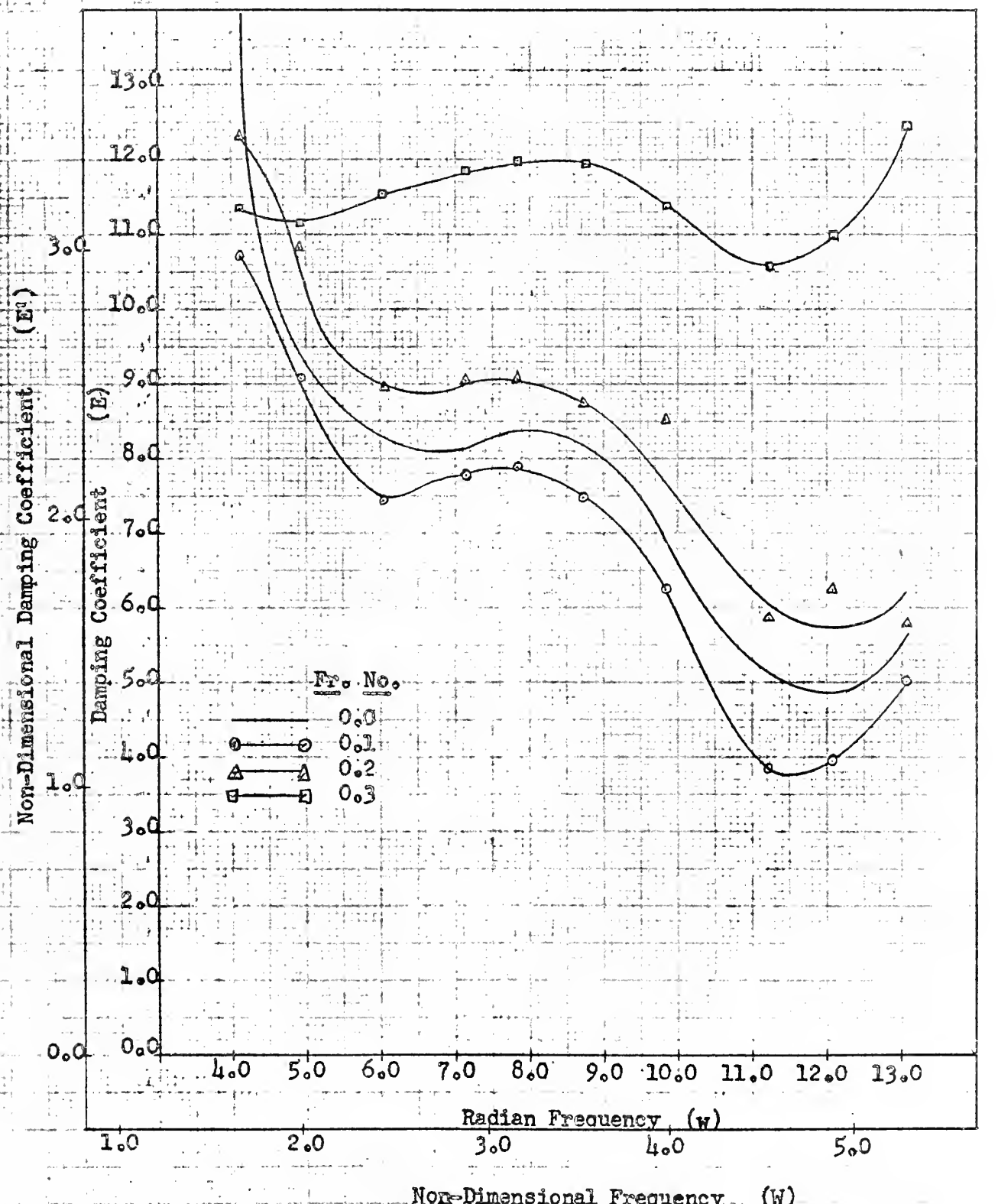

FIGURE XL

HEAVE DAMPING COEFFICIENT AT A DEPTH OF 2.5H

AS A FUNCTION OF FROUDE NUMBER

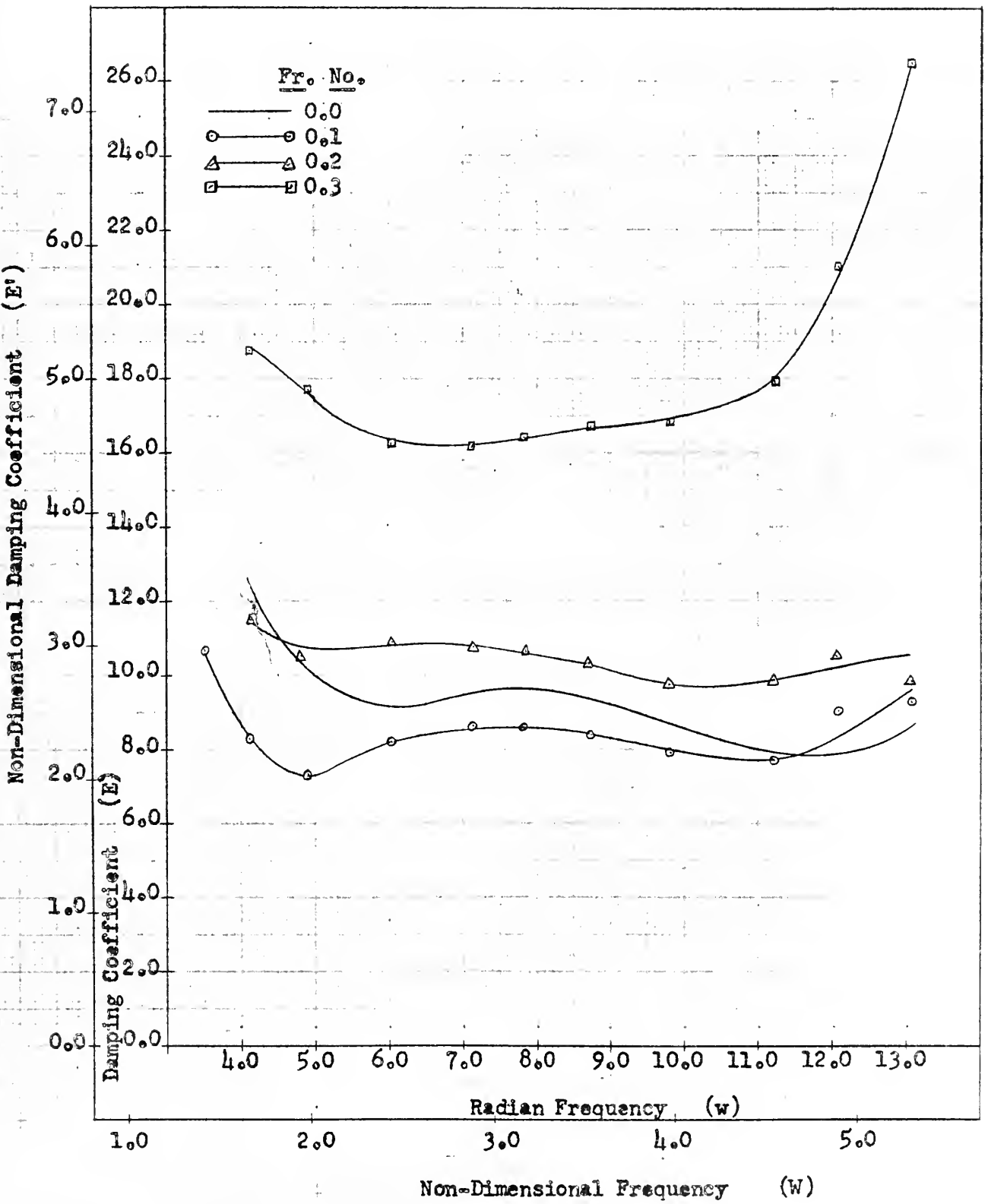

FIGURE XLI

HEAVE DAMPING COEFFICIENT AT A DEPTH OF 1.5H

AS A FUNCTION OF FROUDE NUMBER

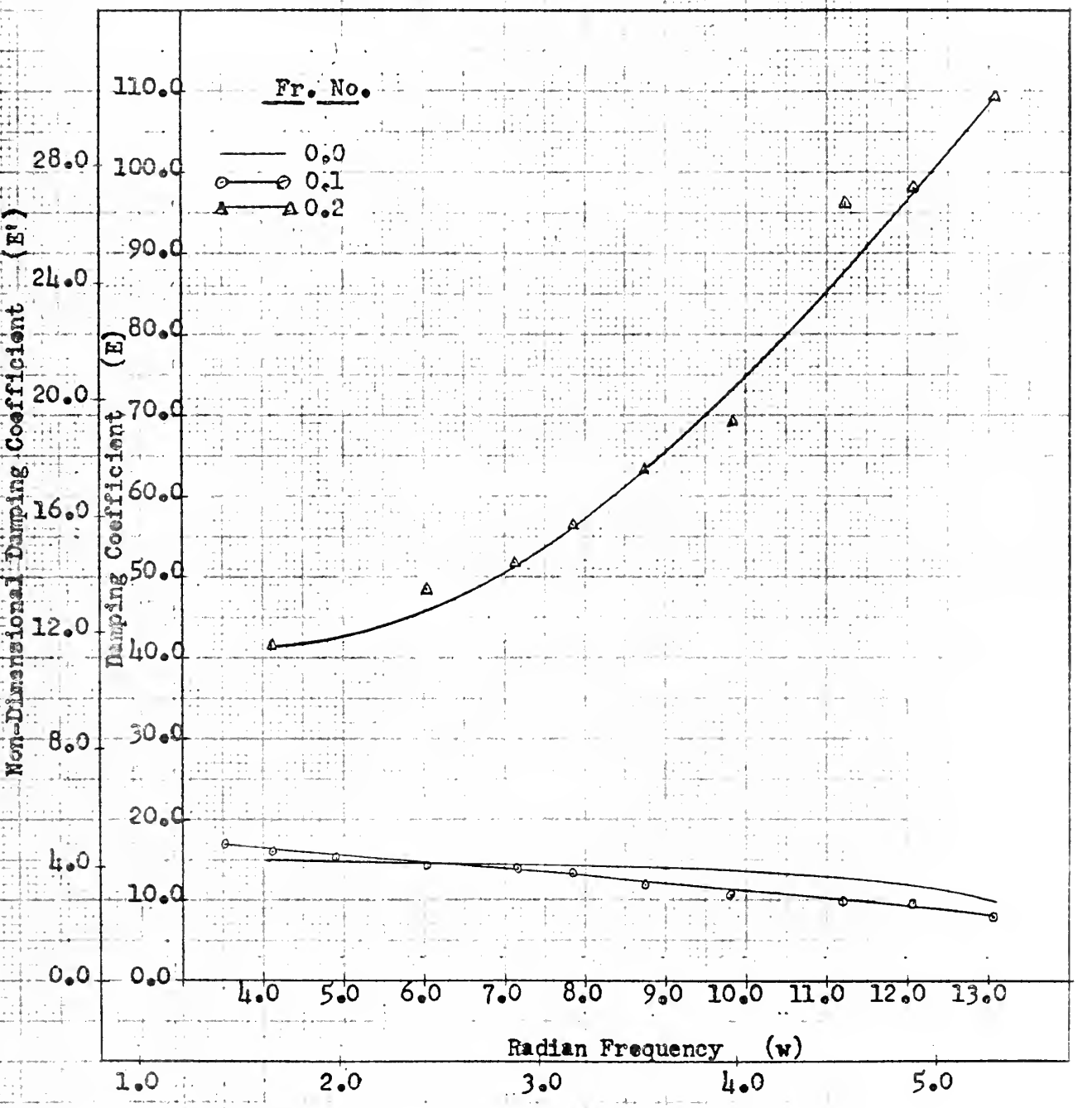

CHAPTER V

DISCUSSION OF RESULTS

5.1 Experimental Errors

The resulting curves of virtual mass/inertia and damping as shown in Figures VI - XLI are representative values for the Mariner Class hullform. The trend of these curves compares favorably with other results in the literature. However, there are limitations in the computation technique and experimental errors which may limit their accuracy.

The most noteworthy of the experimental errors was the amount of carriage vibration at the higher Froude numbers. One hundred pounds of lead was placed on the carriage to reduce the vibration. In general, the vibrations were random and although they appeared to be high frequency their random nature would have some effect on the results.

Another source of possible error was the possibility of the magnet hanging after the circuit was opened. This would happen if the magnet was out of alignment with the plate. This source of error was corrected by making sure the magnet was seated squarely on the plate.

The computational technique limits the accuracy of results, especially at frequencies away from the natural frequency of the model. This effect is shown in Table 3 of Kerwin and Narita (5), Table III of Gies and Hines (4), and Table II of this work.

5.2 Heave - No Pitch

5.2.1 Virtual Mass

The virtual mass in the heave-no pitch condition shows definite effects of the shallow depths. The deep water values correspond in value and general form to those shown in Figure 8 of Golvato (3). The expected effect below $\tau = wv/g = 1/4$ for the deep water speeds is shown in Figure XXXIV. $\tau = 1/4$ is indicated for each Froude number by an arrow on the plot.

Figures XXVI through XXIX show the effects of depth on virtual mass at different Froude numbers. In general, the results show that shallow water does not have a great effect on virtual mass until the depth is below 2.5H. In all of these plots the virtual mass at 12.6H, 4.0H and 2.5H show little depth effect and little speed effect. The virtual mass at 1.5H is considerably higher and increases with speed. At a Froude number of 0.30 and a depth 1.5H the model touched bottom and results were not recorded.

The low frequency results are shown in Figure XXVII for all depths at Froude number = 0.10. These results show a low frequency effect similar to that expected below $\tau = 1/4$ even for the shallow depths.

5.2.2 Heave Damping Coefficient

The heave damping coefficients show shallow water effects similar to those found in virtual mass. However, heave damping appears to be more speed dependent than was virtual mass. The deep water (12.6H) results compare favorably with results obtained by Golvato (3). Heave damping increases in value as depth decreases. Like virtual

mass, the value of the damping coefficient does not increase sharply until the depth gets less than 2.5H. The curves at a Froude number of 0.30 at the various depths show a marked increase in heave damping coefficient at speeds above Froude number = 0.20.

At the higher frequencies, the heave damping coefficients do not go to zero as the theoretical results would indicate. This result corresponds to results obtained by Golvato (3). At the higher speeds, the heave damping coefficients tend to increase with increasing frequency, which may be due to increasing viscous effects.

5.3 Pitch - No Heave

5.3.1 Virtual Inertia

Figures VI through IX show the effects of depth on virtual inertia at the various Froude numbers. At a Froude number of 0.00 (Figure VI) the effect of decreasing depth is to increase the value of virtual inertia. At Froude numbers greater than zero, however, the effect of decreasing depth is to decrease the value of virtual inertia. Figures XIV through XVII show the effects of speed on virtual inertia at various depths. These plots show clearly that increasing speed at deep depths increases the value of virtual inertia. They also show that as depth decreases, this trend reverses and increasing speed decreases the value of virtual inertia. The results at a depth of 12.6H compare favorably with results obtained by Kerwin and Narita (5) in tests conducted on a Series 60 model.

5.3.2 Pitch Damping Coefficient

The results obtained for pitch damping coefficient are not as smooth as those obtained for virtual inertia nor those obtained in

the heave no-pitch condition. The results are shown in Figures X through XIII and Figures XVIII through XXI.

In general, the pitch damping coefficient does not depart appreciably from the deep water values for Froude numbers greater than zero, except at the shallowest depth (1.5H). At a Froude number of zero, the effect of depth is to increase the pitch damping coefficient with decreasing depth (Figure X). At the lower frequencies, decreasing depth also causes a phase shift in the peak values of damping coefficient. At the higher frequencies, the damping coefficient for the shallowest depth (1.5H) are markedly higher (Figures X through XII).

The data obtained in the pitch-no heave condition show more effects of carriage vibration than did that obtained in the heave-no pitch condition. This may account for the scatter in the pitch damping results, especially at the higher frequencies. The results obtained in the pitch-no heave condition compare reasonably well with the results obtained by Kerwin and Narita (5) from tests on a Series 60 model.

5.3.3 Pitch With Stern Up Initially

Gies and Hines (4) and Kerwin and Narita (5) found that the direction of the initial disturbance in pitch on a model in deep water did not affect the results. This was not the case in shallow water. Tests show that at shallow depths, the values of virtual inertia in pitch and pitch damping coefficient are dependent on whether the step was induced with the bow up initially or the stern up initially. These results are shown in Appendix A.

CHAPTER VI

CONCLUSIONS

6.1 Experimental Results

The results of these model tests show that shallow water has a definite effect on virtual mass and damping in heave and virtual inertia and damping in pitch. The results obtained in the heave-no pitch condition appear to be more accurate than those in the pitch-no heave condition. From paper traces of the response signals, the pitch-no heave runs showed more effect of carriage vibration than those in the heave-no pitch condition.

As discussed in Chapter V, virtual mass in heave increases sharply with shallow depth and also with increasing speed. Heave damping shows the same depth dependence as virtual mass but shows a greater speed dependence.

Virtual inertia in pitch shows a tendency to decrease with decreasing depth in the frequency range near the ship's natural frequency. At zero speed, however, the trend is exactly opposite as virtual inertia increases with decreasing depth. Virtual inertia is also speed dependent and while it increases with increasing speed at deep depths, it reverses that trend as depth decreases and decreases with increasing speed.

Pitch damping, while the results are not as smooth, show the same depth dependence as virtual inertia. Pitch damping also appears to peak at lower frequencies as depth decreases.

6.2 Step Response Technique

The step response technique provides a good means for determining virtual mass and damping coefficients where the motion can be decoupled as in pitch-no heave or heave-no pitch. The computer program accuracy is dependent on the convolution interval as shown in Gies and Hines (4) and in Table II of this paper. The results of the computer program are more consistent at frequencies near the undamped natural frequency of the model and show more scatter as frequency increases or decreases.

The response of the model shows some effect of the vibration of the carriage. The response in the heave-no pitch condition showed less effect of carriage vibration than did the response in the pitch-no heave condition. Attempts were made to make the vibration of the carriage as small as possible but some vibration was still noticeable in the response.

CHAPTER VII

RECOMMENDATIONS

7.1 Experimental Technique

In recording the one kilocycle signal on the magnetic tape, it is recommended that the signal be run continuously even where no data is recorded. This will ensure that the signal is recorded where needed and eliminate the possibility of missing the starting point of a run. It is also recommended that in recording the data on magnetic tape, the run spacings be as close to fifty feet as possible. It was found when doing analog-digital conversion that if the spacing were much greater than fifty feet, computer time was lost as the computer waited for the tape to catch up. If the spacing was much less than fifty feet, the reverse occurred and the tape had to be stopped while the computer finished the last run. A spacing of fifty feet between runs permitted the tape to run continuously and a smooth analog-digital conversion resulted.

When conducting the model tests it is important to ensure that the magnet breaks cleanly from the steel plate when the model is released. This problem occurred several times in these tests, especially in the pitch-no heave condition. If the magnet is not aligned truly perpendicular to the steel plate, it will tend to pivot as the magnet releases. This prevents the magnet parting circuit from giving a clear indication of the instant that the model is dropped.

7.2 Future Work

Some areas for future investigation in shallow water effects presented themselves during this project. At the shallowest depths it was noted that sediment on the tank bottom moved away from the model path and at deeper depths the sediment tended to collect under the model path. Some investigation into flow around a ship at shallow depths might prove useful in examining such things as sediment transport into a channel caused by ships transiting the channel. Another possible area of investigation is the pressure distribution over a hull in shallow water. The dependence of virtual inertia and pitch damping in shallow water on whether the step response was introduced with the bow up initially or the stern up initially also could be investigated to determine the effect of hullform on these coefficients at shallow depths.

In this project sinkage and squat were arrived at independently as discussed in Appendix B. Further investigation into the combined effects of sinkage and squat at shallow depths would be warranted to show the actual draft and trim of a ship as compared to the water depth at different speeds.

BIBLIOGRAPHY

1. Abkowitz, M. A., "The Linearized Equations of Motion for the Pitching and Heaving of Ships," Proceedings, Symposium on the Behavior of Ships in a Seaway, Netherlands Ship Model Basin, Wageningen, 1957, pp.178-189.

2. Gerritsma, J., "Shipmotions in Longitudinal Waves," International Shipbuilding Progress, Vol. 7, No. 66, February 1960, pp. 49-71.

3. Golovato, P., "A Study of the Forces and Moments on a Heaving Surface Ship," David Taylor Model Basin Report 1074, September, 1957.

4. Gies, L. C., and Hines, D. H., "The Experimental Determination of Ship Motion Parameters by a Step Response Technique for a Mariner Class Hullform in Pitch and Heave," M.I.T., Department of Naval Architecture and Marine Engineering Report, No. 65-4, 1965.

5. Kerwin, J. E. and Narita, H., "Determination of Ship Motion Parameters by a Step Response Technique," Journal of Ship Research, Vol. 9, No. 3, December, 1965, pp. 183-189.

6. Koch, J. J., "Experimental Method for Determining the Virtual Mass for Oscillations of Ships," David Taylor Model Basin Report T-225, May 1949.

7. Paulling, J. R. and Porter, W. R., "Analysis and Measurement of Pressure and Forces on Heaving Cylinders in a Free Surface," Proceedings of the Fourth U.S. National Congress of Applied Mechanics, 1962.

8. Prohaska, C. W., "Vibration Verticales du Navire (Vertical Vibrations of the Ship)," Association Technique Maritime et Aeronautique, 1947, Vol. 46, pp. 171-219; abstracted in English in Shipbuilder and Marine Engine Builder, October 1947, pp. 542-546 and November 1947, pp. 593-599.

9. Saunders, H. E., Hydrodynamics in Ship Design, New York: Society of Naval Architects and Marine Engineers, 1957.

10. Taylor, D. W., The Speed and Power of Ships, Washington: United States Government Printing Office, 1943.

11. Wendel, Kurt, "Hydrodynamic Masses and Hydrodynamic Moments of Inertia," David Taylor Model Basin Report T-260, 1956.

APPENDIX

APPENDIX A

COMPARISON OF BOW UP AND STERN UP TESTS

The direction of the initial disturbance for the pitch tests in shallow water had a determining factor on the value of the virtual inertia and damping coefficients. The value of these coefficients was higher for the stern up tests than for the bow up tests. The results of these tests are shown in Figures XLII and XLIII. Figure XLII compares the virtual inertia coefficients for the different initial condition at a depth of 1.5H at Froude numbers of 0.00 and 0.20. Figure XLIII compares the pitch damping coefficients at the same depth at Froude numbers of 0.00 and 0.10.

This result could be predicted by considering the increase in pressures caused by the water being constrained to motions approaching a two-dimensional character. With the model at a given speed in shallow water, these extra pressures cause waves that are larger and longer than for the same speed in deep water. Another factor that should be considered is the change in stream velocities past the model in shallow water.

These factors would cause a change in the virtual inertia and damping coefficients depending on the direction of the initial pitch disturbance.

FIGURE XLII

VIRTUAL INERTIA AT A DEPTH OF 1.5H

A FUNCTION OF FROUDE NUMBER

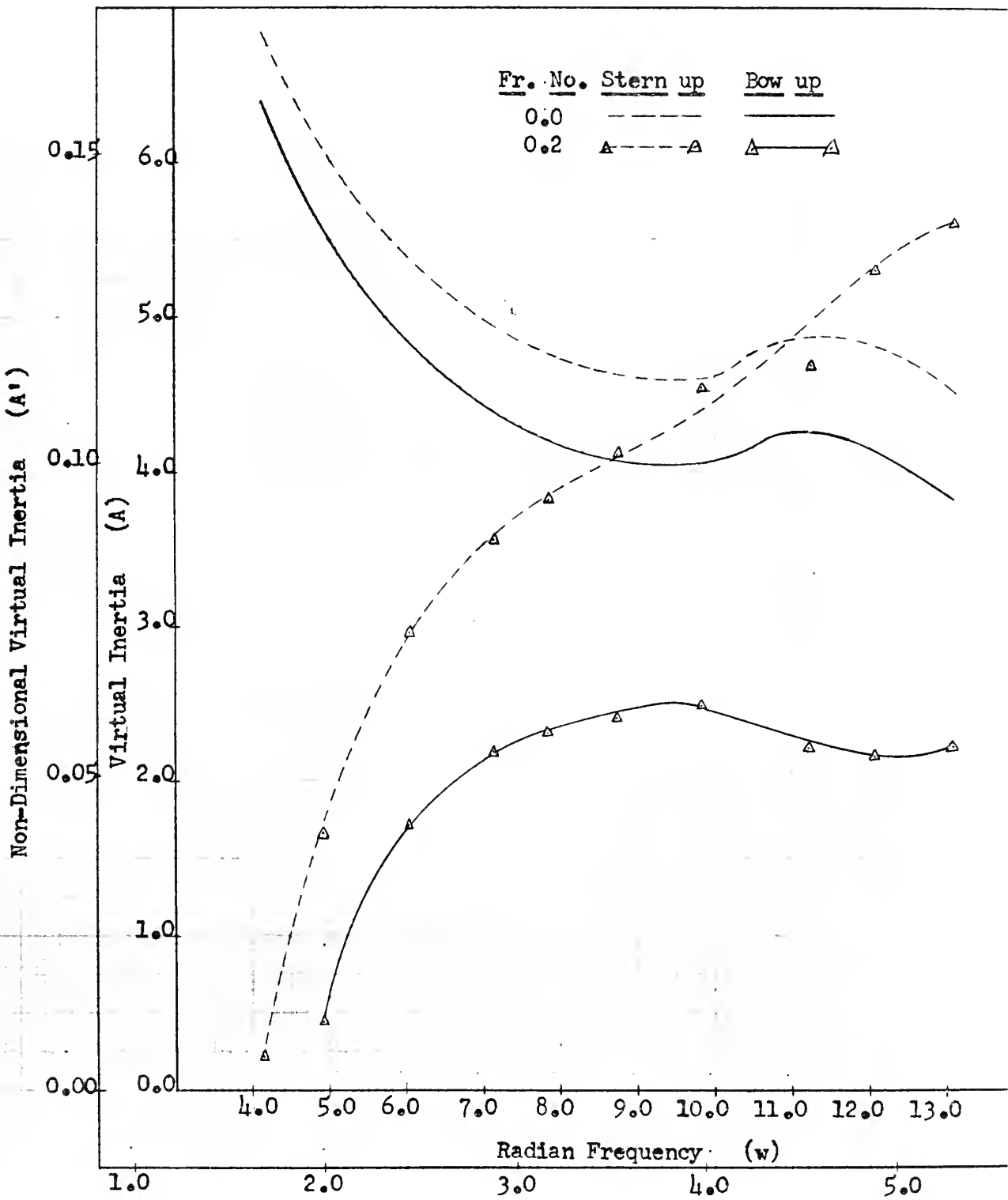

FIGURE XLIII

PITCH DAMPING AT A DEPTH OF 1.5H

AS A FUNCTION OF FROUDE NUMBER

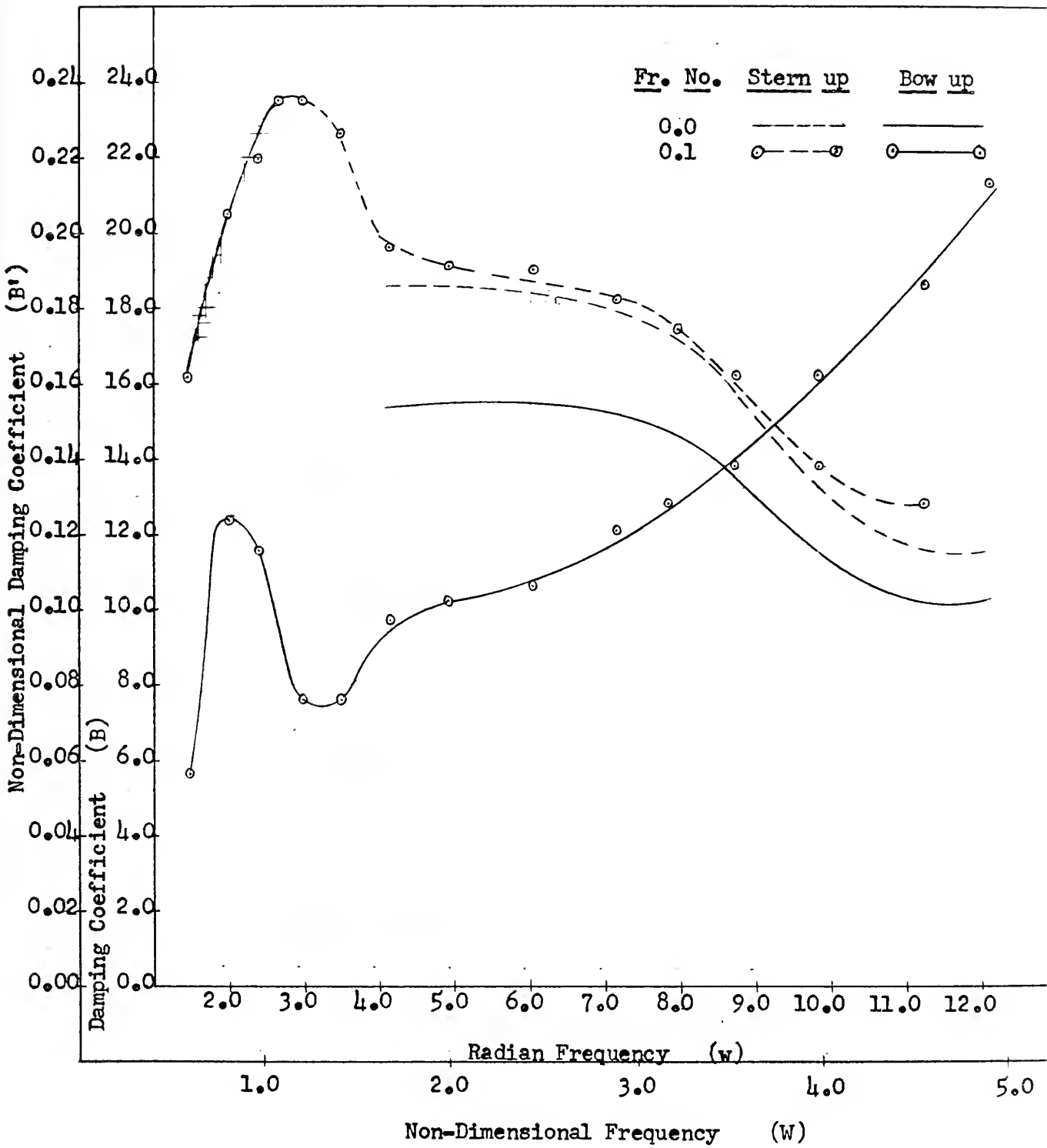

APPENDIX B

SINKAGE AND SQUAT

This appendix shows the comparison between sinkage data obtained from tests conducted with a model of the Mariner class hullform and experimental sinkage data in the literature.

Sinkage can be defined as the parallel departure from a reference level with the ship at rest of the bow and stern as speed is increased. At a critical speed the bow begins to settle more slowly than the stern. This change in trim is called squat. Experimental data showing changes in level of the bow and stern with speed and depth of water of many different models has been plotted in The Speed And Power Of Ships, by Admiral D. W. Taylor, USN (10).

Figure XLIV shows the variation of stern sinkage and squat as a fraction of ship's draft as a function of speed at four water depths. The dashed line is a plot of stern sinkage and squat at infinite depth of a model of comparative dimensions taken from Figure 85 of Taylor (10). The experiments on the Mariner model were conducted at three speeds.

The modes of oscillation of the model in pitch and heave were isolated so that the model could oscillate in only one degree of freedom for a given run. Table VI shows the variation of trim angle with increasing speed at four different water depths. Table VII shows the variation of parallel sinkage with speed at these same depths.

Tables VI and VII were combined linearly to obtain the stern sinkage shown in Figure XLIV. The error incorporated by this linearization is small in the speed range where a small amount of trim angle is

experienced. When the trim angle is two or three degrees the error involved could be as much as 30 per cent.

TABLE VI

Trim Angle (degrees)

$V/\sqrt{L}$	12.6H	4H	2.5H	1.5H
.353	0	0	0	.04
.706	0	0	.08	.24
1.09	.04	.32	2.64	---

TABLE VII

Parallel Sinkage (ft.)

$V/\sqrt{L}$	12.6H	4H	2.5H	1.5H
.353	.0027	.0027	.0040	.0070
.706	.0090	.0120	.0213	.0286
1.09	.0250	.0320	.0640	-----

FIGURE XLIV

STERN SINKAGE AS A FUNCTION OF DEPTH

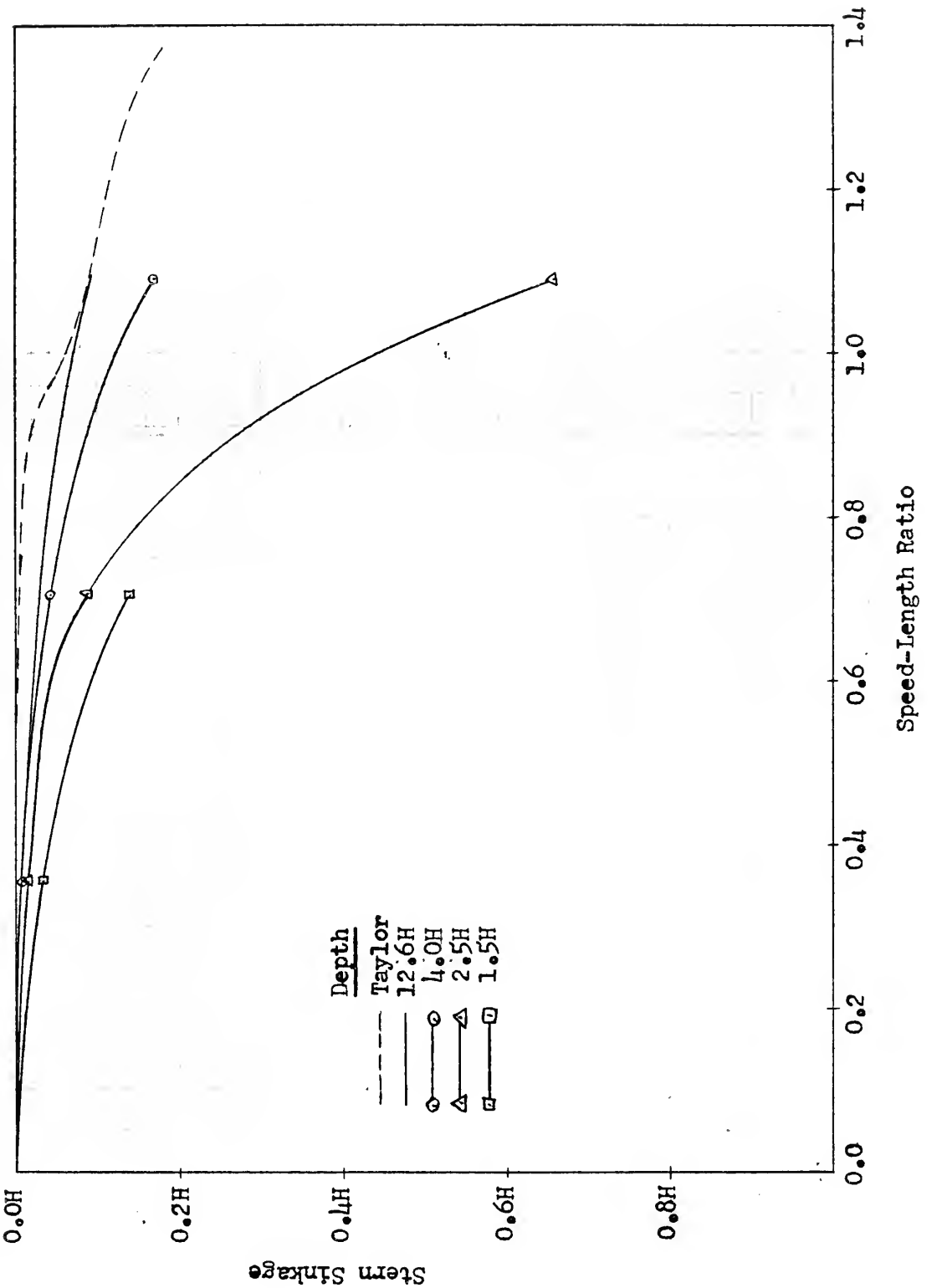

APPENDIX C

DISCUSSION OF COMPUTER PROGRAM

Abstract

The computer program was originated by Kerwin and Narita (5). It takes the digitized step response data and computes the normalized step response. From this response, the response to regular sinusoidal excitations can be computed. The response to the sinusoidal input is used to determine the coefficients of virtual inertia and damping in pitch or heave. These coefficients and the frequencies are then non-dimensionalized.

Method

Experimental data is recorded in analog form on magnetic tape. The data is then converted to digital form by a seperate analog-digital conversion program.

Normalizing the step response is a linear transformation of the input data. It is approximated by averaging the last MA points in the record and requiring that this value be zero. The integer MA is an input to the program.

From the normalized response, one cycle of regular sinusoidal excitation is computed by the convolution integral method. This operation is simple in principle, but actual computation can be very time consuming. A detailed discussion of this computational technique is given in Kerwin and Narita (5).

The coefficients of virtual inertia and damping are determined from the amplitudes of the first sine and cosine harmonics of the total

response. The final step is the computation of the non-dimensional damping, virtual inertia and frequency.

Input

The input consists of one general information card and any number of frequency information cards.

Card I Format (4I5,4F10.6, I5)

Columns 1- 5: Run number (NRUN)

Columns 6-10: Number of points of good input data (MT)

Columns 11-15: Number of points to be averaged in the normalizing process (MA)

Columns 16-20: Number of frequencies for which coefficients are desired (NPER)

Columns 21-30: Digitizing rate (DDT) in seconds. Allow six decimal places. Experiments by Kerwin and Narita (5) show that added mass and damping are highly dependent on the digitizing rate.

Columns 31-40: Static restoring moment for pitch (ft-lb/radian) or static restoring force for heave (lb/ft)(CC). Allow six decimal places. These are the static restoring coefficients in pitch or heave.

Columns 41-50: Displacement in pounds (DISP). Allow six decimal places.

Columns 51-60: Length between perpendiculars in feet (HLEN). Allow six decimal places.

Columns 61-65: Number of points at beginning of digitized data that should be discarded (NSTRT). This number was determined when converting from analog to digital data. It is the number of points (one thousandth of a second) from the beginning of the input data to the point at which the magnet circuit parts (less than 24 points).

Card 2 Format (3I5)

Columns 1- 5: Sampling period constant (KDT). The results of varying the integer KDT are shown in Table I of Kerwin and Narita (5).

Columns 6-10: Exciting period constant (KP). Variations of the integer KP will vary the exciting period ($T = 4 \times KP \times DT$), and therefore, the frequency ($w = 2\pi/T$). Results of this variation for an idealized response are shown in Table 2 of Kerwin and Narita (5).

Columns 11-15: Convolution Interval constant (JMP). This integer permits change in the convolution interval from .001 sec. (JMP = 1) to .020 sec. (JMP = 20) to any other interval desired. The larger the interval the lower the computer time. The effect of convolution interval on the coefficients is shown in Table III of Gies and Hines (4).

Output

The printed output consists of eight columns.

Column 1: Sampling period in seconds (DT).

Column 2: Exciting period in seconds (T).

Column 3: Frequency in radians per second (OMEGA).

Column 4: Virtual mass coefficient (A).

Column 5: Damping coefficient (B).

Column 6: Non-dimensionalized frequency (OMEGA).

Column 7: Non-dimensionalized virtual mass coefficient (A).

Column 8: Non-dimensionalized damping coefficient (B).

Special Comments

1. This program will compute the virtual mass and damping in heave or virtual inertia and damping in pitch by simply changing the spring constant (CC) and the non-dimensionalizing cards (APRIME and BPRIME) located near the end of the program.

For heave:

```
APRIME = (BIGA*GRAV)/DISP
BPRIME = (BIGB*SQRTF(HLEN*GRAV))/DISP
```

For Pitch:

```
APRIME = (BIGA*GRAV)/(DISP*HLEN**2)
BPRIME = (BIGB*SQRTF(HLEN*GRAV))/(DISP*HLEN**2)
```

2. The total number of points of input data must be divisible by 24. Therefore, MT + NSTRT = 24 (number of digitized data cards). This number cannot be greater than 3000 with the present dimensions.

```
      DIMENSION FMT(12),NRES(3000),RESP(3000),C(2400),R(10000),Y(400),
     1  CSR(2400)
      DIMENSION NTMP (3000)
      COMMON NRES,C,R,Y,CSR
      EQUIVALENCE (NRES,RESP)
      PI=3.1415926
      TWOPI=6.2831853
      GRAV=32.176632
 7    CALL CLOCK(2)
      READ 100,NRUN,MT,MA,NPER,DDT,CC,DISP,HLEN,NSTRT
 100  FORMAT(4I5,4F10.6,I5)
      MTS=MT+NSTRT
      IF(NRUN)  99,99,16
 99   CALL EXIT
C     STEP RESPONSE-   READ IN AND NORMALIZE
 16   READ 900, (NTMP(N),N=1,MTS)
 900  FORMAT(24I3)
      DO 60    N=1,MT
      NST=N+NSTRT
 60   NRES(N)=NTMP(NST)
C     AVERAGING END OF RESPONSE
      NLOW=MT-MA+1
      SUM=0.0
      DO 8       N=NLOW,MT
      SUM=SUM+FLOATF(NRES(N))
 8    CONTINUE
      AVEL=SUM/FLOATF(MA)
C     FLOAT AND NORMALIZE RESPONSE
      RITA=NRES(1)
      PIAN=RITA-AVEL
      DO 500    N=1,MT
      RESP(N)=(AVEL-FLOATF(NRES(N)))/PIAN
  500 CONTINUE
      PRINT 102,NRUN,MT,MA,AVEL,DDT,CC,DISP,HLEN
 102  FORMAT(///7H1   RUNI5,4X,I5,36H POINTS IN RECORD   AVERAGE OF LAS
     1TI5,10H POINTS ISF6.1,20H    DIGITIZING RATE=F6.4,4H SEC/34H
     2MOMENT FOR ONE RADIAN PITCH=F10.6,24H FT-LBS    DISPLACEMENT=F10.6
     4,15H LBS   LENGTH=F10.6,3H FT///)
      PRINT 103
 103  FORMAT(64H   ************ DIMENSIONAL ************   ** NON-DIMENS
     1IONAL **//62H      DT       T      OMEGA      A        B      OMEGA
     2A       B)
C     COMPUTATION FOR ONE PERIOD STARTS HERE
      DO 15       NPR=1,NPER
      READ  104,KDT,KP,JMP
 104  FORMAT (3I5)
      DT=FLOATF(KDT)*DDT
      TE=4.0*FLOATF(KP)*DT
      OMEGA=TWOPI/TE
      OMN=OMEGA*SQRTF(HLEN/GRAV)
C     COSINE OF EXCITING MOMENT FOR QUARTER CYCLE
      D=TWOPI/(4.0*FLOATF(KP))
      DO 10       N=1,KP
      AN=N-1
      C(N)=COSF(AN*D)
  10  CONTINUE
```

```
C       COSINE TIMES SIMPSONS MULTIPLIERS
        CSR(1)=0.33333333
        DO 9        N=2,KP,2
        CSR(N)=1.3333333*C(N)
        CSR(N+1)=0.66666667*C(N+1)
 9      CONTINUE
C       FORM RAREFIED STEP RESPONSE CURVE
        JS=4*KP
        JT=(2*KP)/JMP+1
        LT=(MT-1)/KDT+1
        LM=(LT-1)/JS+1
        LEX=JS*LM
        LMAX=LEX-JS
        M=1
        DO 11       N=1,LT
        R(N)=RESP(M)
        M=M+KDT
 11     CONTINUE
C       FILL IN ZEROS TO NEXT COMPLETE PERIOD OF EXCITING MOMENT
        LOW=LT+1
        DO 12       N=LOW,LEX
        R(N)=0.0
 12     CONTINUE
C       REPEAT FIRST PERIOD WORTH OF STEP RESPONSE FOR LATER USE
        DO 13       N=1,JS
        NLEX=N+LEX
        R(NLEX)=R(N)
 13     CONTINUE
C       COMPUTE RESPONSE TO EXCITING MOMENT
        KS=KP+KP
        KQ=KS+KS
        KY=KS+2
        JUMP=0
        DO 6            I=1,JT
        Y(I)=0.0
        DO 1            N=1,KP
        NA=N+JUMP
        SUM=0.0
        DO 2            M=1,LM
        NAKS=NA+KS
        SUM=SUM+R(NA)-R(NAKS)
        NA=NA+KQ
 2      CONTINUE
        IF(N-1)  99,5,3
 3      NA=KY-N+JUMP
        DO 4        M=1,LM
        NAKS=NA+KS
        SUM= SUM-R(NA)+R(NAKS)
        NA=NA+KQ
 4      CONTINUE
 5      Y(I)=Y(I)+CSR(N)*SUM
 1      CONTINUE
        JUMP=JUMP+JMP
 6      CONTINUE
C       GET SINE AND COSINE HARMONICS OF RESPONSE
        KM=KS/JMP+1
```

```
      SUMC=0.5*(Y(1)-Y(KM))
      JK=KP/JMP
      SUMS=Y(JK+1)
      MAX=KP/JMP-1
      DO 14       J=1,MAX
      JW=J+1
      JY=KM-J
      JJMP=J*JMP
      SUMC=SUMC+C(JJMP+1)*(Y(JW)-Y(JY))
      JW=KP/JMP+1-J
      JX=KP/JMP+1+J
      SUMS=SUMS+C(JJMP+1)*(Y(JW)+Y(JX))
14    CONTINUE
C     COMPUTE VIRTUAL MASS AND DAMPING
      JKP=JK*KP
      DW=2.0*FLOATF(JKP)**1/PI
      A=(1.0+SUMS/DW)/CC
      B=SUMC/(DW*CC)
      ASQ=A**2+B**2
      BIGA=(CC-A/ASQ)/OMEGA**2
      BIGB=-B/(OMEGA*ASQ)
      BPRIME=(BIGB*SQRTF(HLEN*GRAV))/DISP
      APRIME=(BIGA*GRAV)/DISP
      PRINT 105,DT,TE,OMEGA,BIGA,BIGB,OMN,APRIME,BPRIME
105   FORMAT(8F8.3)
15    CONTINUE
      GO TO 7
      END(1,1,0,0,0,0,1,1,0,1,0,0,0,0,0)
```

APPENDIX D

TABLES OF DATA

This appendix contains tables of the data used in Figures VI - XLIII. Table VIII gives the values of virtual inertia and damping in pitch with the bow up initially. Table IX contains the values of virtual mass and damping in heave. The values of virtual inertia and damping in pitch with the stern up initially are given in Table X. The symbols used in this appendix are defined in Chapter IV.

Table VIII

VIRTUAL INERTIA AND DAMPING COEFFICIENTS IN PITCH

WITH BOW UP INITIALLY

(1) Froude Number 0.0; Depth 12.6 x Draft

w	A	B	W	A'	B'
4.134	6.044	2.057	1.674	.148	.020
4.909	5.923	5.032	1.988	-.145	.050
6.042	5.204	8.908	2.447	.128	.089
7.140	4.559	10.400	2.892	.112	.103
7.854	4.251	10.412	3.182	.104	.104
8.727	3.990	9.626	3.535	.098	.096
9.817	3.851	7.710	3.977	.095	.077
11.220	3.994	6.648	4.545	.098	.066
12.083	3.902	8.557	4.895	.096	.085
13.090	3.648	6.762	5.303	.090	.067

(2) Froude Number 0.10; Depth 12.6 x Draft

w	A	B	W	A'	B'
1.496	8.382	3.556	0.606	0.206	0.035
2.001	6.085	3.329	0.811	0.149	0.033
2.380	5.766	1.642	0.964	0.142	0.016

Table VII (continued)

(2) Froude Number 0.10; Depth 12.6 x Draft (continued)

w	A	B	W	A'	B'
2.992	6.608	1.191	1.212	0.162	0.012
3.491	6.945	3.443	1.414	0.171	0.034
4.134	6.449	7.339	1.674	0.158	0.073
4.909	5.577	10.007	1.988	0.137	0.100
6.042	4.846	10.417	2.447	0.119	0.104
7.140	4.486	10.609	2.892	0.110	0.106
7.854	4.289	10.308	3.182	0.105	0.103
8.727	4.139	9.254	3.535	0.102	0.092
9.817	4.163	8.165	3.977	0.102	0.081
11.220	3.905	8.348	4.545	0.096	0.083
12.083	3.956	4.727	4.895	0.097	0.047
13.090	4.284	8.208	5.303	0.105	0.082

(3) Froude Number 0.20; Depth 12.6 x Draft

w	A	B	W	A'	B'
1.496	0.758	-10.454	0.606	0.019	-0.104
2.001	8.511	-3.450	0.811	0.209	-0.034
2.380	8.757	4.353	0.964	0.215	0.043
2.992	6.538	12.648	1.212	0.161	0.126
3.491	4.816	14.116	1.414	0.118	0.140
4.134	4.077	11.985	1.674	0.100	0.119
4.909	3.870	11.188	1.988	0.095	0.111
6.042	3.880	8.650	2.447	0.095	0.086
7.140	4.091	9.383	2.892	0.100	0.093

Table VIII (continued)

(3) Froude Number 0.20; Depth 12.6 x Draft (continued)

w	A	B	W	A'	B'
7.854	4.037	9.842	3.182	0.099	0.098
8.727	3.999	9.515	3.535	0.098	0.095
9.817	4.147	10.076	3.977	0.102	0.100
11.220	3.876	10.315	4.545	0.095	0.103
12.083	3.766	10.475	4.895	0.102	0.104
13.090	3.803	13.396	5.303	0.093	0.133

(4) Froude Number 0.30; Depth 12.6 x Draft

w	A	B	W	A'	B'
1.496	5.467	20.249	0.606	0.134	0.201
2.001	3.084	24.213	0.811	0.076	0.241
2.380	1.152	25.182	0.964	0.028	0.251
2.992	-1.550	20.394	1.212	-0.038	0.203
3.491	-1.227	11.212	1.414	-0.030	0.112
4.134	1.360	4.632	1.674	0.033	0.046
4.909	2.679	6.017	1.988	0.066	0.060
6.042	3.260	5.034	2.447	0.080	0.050
7.140	3.770	7.346	2.892	0.093	0.073
7.854	3.766	8.747	3.182	0.092	0.087
8.727	3.749	9.287	3.535	0.092	0.092
9.817	3.935	10.911	3.977	0.097	0.109
11.220	3.506	12.189	4.545	0.086	0.121
12.083	3.549	12.215	4.895	0.095	0.122
13.090	3.343	16.909	5.303	0.082	0.168

Table VIII (continued)

(5) Froude Number 0.0; Depth 4.0 x Draft

w	A	B	W	A'	B'
4.134	5.272	5.416	1.647	0.129	0.054
4.909	4.753	6.538	1.988	0.117	0.065
6.042	4.487	8.459	2.447	0.110	0.084
7.140	4.149	10.351	2.892	0.102	0.103
7.854	3.949	10.871	3.182	0.097	0.108
8.727	3.789	10.782	3.535	0.093	0.107
9.817	3.779	10.129	3.977	0.093	0.101
11.220	3.910	13.433	4.545	0.096	0.134
12.083	3.643	14.621	4.895	0.089	0.145
13.090	3.716	12.685	5.303	0.091	0.126

(6) Froude Number 0.10;

w	A	B	W	A'	B'
1.496	2.455	-1.930	0.606	0.060	-0.019
2.001	5.790	-3.019	0.811	0.142	-0.030
2.380	7.033	-1.092	0.964	0.173	-0.011
2.992	7.314	4.260	1.212	0.180	0.042
3.491	6.651	7.937	1.414	0.163	0.079
4.134	5.561	10.499	1.674	0.137	0.104
4.909	4.718	10.375	1.988	0.116	0.103
6.042	4.520	9.692	2.447	0.111	0.096
7.140	4.306	10.550	2.892	0.106	0.105
7.854	4.135	10.545	3.182	0.102	0.105

Table VIII (continued)

(6) Froude Number 0.10;

w	A	B	W	A'	B'
8.727	3.989	9.714	3.535	0.098	0.097
9.817	3.997	8.042	3.977	0.098	0.080
11.220	4.009	9.223	4.545	0.098	0.092
12.083	3.896	7.206	4.895	0.096	0.072
13.090	4.213	6.489	5.303	0.103	0.065

(7) Froude Number 0.20; Depth 4.0 x Draft

w	A	B	W	A'	B'
4.134	4.180	10.391	1.674	0.103	0.103
4.909	3.673	7.837	1.988	0.090	0.078
6.042	3.920	6.646	2.447	0.096	0.066
7.140	3.849	8.470	2.892	0.095	0.084
7.854	3.710	9.126	3.182	0.091	0.091
8.727	3.594	9.103	3.535	0.088	0.091
9.817	3.677	8.673	3.977	0.090	0.086
11.220	3.519	14.329	4.545	0.086	0.143
12.083	3.313	10.868	4.895	0.081	0.108
13.090	3.959	10.099	5.303	0.097	0.100

(8) Froude Number 0.30; Depth 4.0 x Draft

w	A	B	W	A'	B'
4.134	4.286	3.017	1.674	0.105	0.030
4.909	3.396	5.293	1.988	0.083	0.053
6.042	3.035	2.849	2.447	0.075	0.028

Table VIII (continued)

(8) Froude Number 0.30; Depth 4.0 x Draft (continued)

w	A	B	W	A'	B'
7.140	3.021	4.673	2.892	0.074	0.046
7.854	2.865	5.622	3.182	0.070	0.056
8.727	2.711	6.097	3.535	0.067	0.061
9.817	2.673	6.539	3.977	0.066	0.065
11.220	2.439	9.967	4.545	0.060	0.099
12.083	2.316	8.672	4.895	0.057	0.086
13.090	2.460	10.313	5.303	0.060	0.103

(9) Froude Number 0.00; Depth 2.5 x Draft

w	A	B	W	A'	B'
4.134	6.105	9.527	1.674	0.150	0.095
4.909	5.482	10.311	1.988	0.135	0.103
6.042	4.850	11.635	2.447	0.119	0.116
7.140	4.354	12.166	2.892	0.107	0.121
7.854	4.102	11.888	3.182	0.101	0.118
8.727	3.876	10.862	3.535	0.095	0.108
9.817	3.736	8.512	3.977	0.092	0.085
11.220	3.935	4.829	4.545	0.097	0.048
12.083	4.198	7.273	4.895	0.103	0.072
13.090	3.751	10.415	5.303	0.092	0.104

Table VIII (continued)

(10) Froude Number 0.10; Depth 2.5 x Draft

w	A	B	W	A'	B'
1.496	7.435	-0.080	0.606	0.183	-0.001
2.001	8.169	2.578	0.811	0.201	0.026
2.380	7.902	5.542	0.964	0.194	0.055
2.992	6.790	10.384	1.212	0.167	0.103
3.491	5.662	13.075	1.414	0.139	0.130
4.134	4.464	13.557	1.674	0.110	0.135
4.909	3.832	11.541	1.988	0.094	0.115
6.042	3.915	10.311	2.447	0.096	0.103
7.140	3.809	11.054	2.892	0.094	0.110
7.854	3.686	11.100	3.182	0.091	0.110
8.727	3.571	10.478	3.535	0.088	0.104
9.817	3.557	8.936	3.977	0.087	0.089
11.220	3.731	9.303	4.545	0.092	0.093
12.083	3.571	10.070	4.895	0.088	0.100
13.090	3.559	7.098	5.303	0.087	0.071

(11) Froude Number 0.20; Depth 2.5 x Draft

w	A	B	W	A'	B'
4.134	2.412	12.260	1.674	0.059	0.122
4.909	2.380	7.774	1.988	0.058	0.077
6.042	3.194	7.192	2.447	0.078	0.072
7.140	3.281	9.442	2.892	0.081	0.094
7.854	3.225	10.300	3.182	0.079	0.102
8.727	3.186	10.656	3.535	0.078	0.106

Table VIII (continued)

(11) Froude Number 0.20; Depth 2.5 x Draft (continued)

w	A	B	W	A'	B'
9.817	3.298	10.777	3.977	0.081	0.107
11.220	3.385	16.555	4.545	0.083	0.165
12.083	3.061	15.979	4.895	0.075	0.159
13.090	3.361	13.167	5.303	0.083	0.131

(12) Froude Number 0.0; Depth 1.5 x Draft

w	A	B	W	A'	B'
4.134	6.397	15.271	1.674	0.157	0.152
4.909	5.540	15.464	1.988	0.136	0.154
6.042	4.858	15.555	2.447	0.119	0.155
7.140	4.434	15.282	2.892	0.109	0.152
7.854	4.238	14.702	3.182	0.104	0.146
8.727	4.086	13.503	3.535	0.100	0.134
9.817	4.061	11.494	3.977	0.100	0.114
11.220	4.276	11.804	4.545	0.105	0.117
12.083	4.077	10.259	4.895	0.100	0.140
13.090	3.832	10.886	5.303	0.094	0.108

(13) Froude Number 0.10; Depth 1.5 x Draft

w	A	B	W	A'	B'
1.496	25.581	5.601	0.606	0.628	0.056
2.001	13.479	12.373	0.811	0.331	0.123
2.380	8.693	11.523	0.964	0.213	0.115
2.992	6.345	7.678	1.212	0.156	0.076
3.491	5.980	7.722	1.414	0.147	0.077

Table VIII (Continued)

(13) Froude Number 0.10; Depth 1.5 x Draft (continued)

W	A	B	W	A'	B'
4.134	5.170	9.631	1.674	0.127	0.096
4.909	4.274	10.234	1.988	0.105	0.102
6.042	3.858	10.589	2.447	0.095	0.105
7.140	3.568	12.107	2.892	0.088	0.120
7.854	3.424	12.853	3.182	0.084	0.128
8.727	3.341	13.800	3.535	0.082	0.137
9.817	3.295	16.283	3.977	0.081	0.162
11.220	3.107	18.651	4.545	0.076	0.186
12.083	3.091	21.316	4.895	0.076	0.212
13.090	2.982	26.896	5.303	0.073	0.268

(14) Froude Number 0.20; Depth 1.5 x Draft

W	A	B	W	A'	B'
1.496	-16.359	46.158	0.606	-0.402	0.459
2.001	-16.074	34.368	0.811	-0.395	0.342
2.380	-13.062	21.825	0.964	-0.321	0.217
2.992	-6.887	8.805	1.212	-0.169	0.088
3.491	-3.296	7.007	1.414	-0.081	0.070
4.134	-0.893	7.020	1.674	-0.022	0.070
4.909	0.446	6.909	1.988	0.011	0.069
6.042	1.722	8.044	2.447	0.042	0.080
7.140	2.191	10.670	2.892	0.054	0.106
7.854	2.309	12.024	3.182	0.057	0.120
8.727	2.408	13.430	3.535	0.059	0.134

Table VIII (continued)

(14) Froude Number 0.20; Depth 1.5 x Draft (continued)

w	A	B	W	A'	B'
9.817	2.496	15.949	3.977	0.061	0.159
11.220	2.218	19.473	4.545	0.054	0.194
12.083	2.153	18.569	4.895	0.053	0.185
13.090	2.217	18.821	5.303	0.054	0.187

TABLE IX

VIRTUAL MASS AND DAMPING COEFFICIENTS IN HEAVE

(1) Froude Number 0.0; Depth 12.6 x Draft

w	D	E	W	D'	E'
1.496	-2.553	4.347	0.606	-1.748	1.206
2.001	-0.381	-0.760	0.811	-0.261	-0.211
2.380	1.584	-3.172	0.964	1.085	-0.880
2.992	3.918	-2.187	1.212	2.682	-0.607
3.491	4.541	0.885	1.414	3.109	0.245
4.134	4.286	5.028	1.674	2.934	1.394
4.909	3.608	8.215	1.988	2.470	2.278
6.042	2.831	8.467	2.447	1.938	2.348
7.140	2.694	7.586	2.892	1.844	2.104
7.854	2.632	7.510	3.182	1.802	2.083
8.727	2.548	7.198	3.535	1.744	1.996
9.817	2.495	6.278	3.977	1.708	1.741
11.220	2.523	5.627	4.545	1.727	1.560
12.083	2.474	5.055	4.895	1.694	1.402
13.090	2.558	3.279	5.303	1.751	0.909

(2) Froude Number 0.1; Depth 12.6 x Draft

w	D	E	W	D'	E'
1.496	11.570	7.409	0.606	7.921	2.055
2.001	3.531	6.303	0.811	2.417	1.748
2.380	2.332	-0.861	0.964	1.596	-0.239

Table IX (Continued)

(2) Froude Number 0.1; Depth 12.6 x Draft (continued)

W	D	E	W	D'	E'
3.570	5.399	0.885	1.446	3.696	0.245
4.134	4.652	5.293	1.674	3.185	1.468
4.488	4.066	7.232	1.818	2.784	2.006
4.909	3.384	7.783	1.988	2.317	2.158
5.236	2.999	7.413	2.121	2.053	2.056
5.610	2.773	6.521	2.273	1.898	1.808
6.042	2.698	5.833	2.447	1.847	1.618
6.545	2.656	5.736	2.651	1.818	1.591
7.140	2.573	5.955	2.892	1.761	1.651
7.854	2.455	6.103	3.182	1.680	1.692
8.727	2.335	5.908	3.535	1.598	1.639
9.817	2.272	5.140	3.977	1.555	1.425
11.220	2.313	5.544	4.545	1.583	1.538
12.083	2.223	5.053	4.895	1.522	1.401
13.090	2.374	4.963	5.303	1.625	1.376

(3) Froude Number 0.2; Depth 12.6 x Draft

W	D	E	W	D'	E'
1.496	1.208	6.803	0.606	0.827	1.887
2.001	2.325	5.557	0.811	1.592	1.541
2.380	3.016	5.364	0.964	2.065	1.487
2.992	3.596	6.647	1.212	2.462	1.843
3.491	3.616	8.343	1.414	2.475	2.314

Table IX (Continued)

(3) Froude Number 0.2; Depth 12.6 x Draft (continued)

w	D	E	W	D'	E'
4.134	3.306	10.031	1.674	2.263	2.782
4.909	2.764	10.747	1.988	1.893	2.980
6.042	2.522	8.596	2.447	1.727	2.384
7.140	2.648	8.027	2.892	1.813	2.226
7.854	2.634	8.038	3.182	1.803	2.229
8.727	2.584	7.621	3.535	1.769	2.113
9.817	2.566	6.258	3.977	1.757	1.736
11.220	2.751	4.789	4.545	1.883	1.328
12.083	2.546	4.142	4.895	1.743	1.149
13.090	2.851	3.877	5.303	1.952	1.075

(4) Froude Number 0.3; Depth 12.6 x Draft

w	D	E	W	D'	E'
1.496	4.659	7.064	0.606	3.189	1.959
2.001	2.006	6.164	0.811	1.373	1.710
2.380	1.788	3.778	0.964	1.224	1.048
2.992	2.700	2.695	1.212	1.848	0.747
3.491	2.929	4.421	1.414	2.005	1.226
4.134	2.471	6.246	1.674	1.691	1.732
4.909	2.047	5.298	1.988	1.402	1.469
6.042	2.309	4.837	2.447	1.581	1.341
7.140	2.311	6.241	2.892	1.582	1.731
7.854	2.270	6.902	3.182	1.554	1.914

Table IX (Continued)

(4) Froude Number 0.3; Depth 12.6 x Draft (continued)

W	D	E	W	D'	E'
8.727	2.228	7.482	3.535	1.525	2.075
9.817	2.228	7.907	3.977	1.526	2.193
11.220	2.332	9.446	4.545	1.597	2.620
12.083	2.342	10.977	4.895	1.603	3.044
13.090	2.412	12.993	5.303	1.651	3.603

(5) Froude Number 0.0; Depth 4.0 x Draft

W	D	E	W	D'	E'
4.134	3.333	13.912	1.674	2.282	3.858
4.909	2.110	12.481	1.988	1.445	3.461
6.042	2.440	7.496	2.447	1.670	2.079
7.140	2.681	8.172	2.892	1.836	2.266
7.854	2.655	8.485	3.182	1.817	2.353
8.727	2.595	8.213	3.535	1.776	2.278
9.817	2.567	6.887	3.977	1.757	1.910
11.220	2.757	4.472	4.545	1.888	1.240
12.083	2.914	5.771	4.895	1.995	1.600
13.090	2.729	5.405	5.303	1.868	1.499

(6) Froude Number 0.1; Depth 4.0 x Draft

W	D	E	W	D'	E'
1.496	7.553	0.840	0.606	5.171	0.233
2.001	6.746	3.748	0.811	4.619	1.040
2.380	6.006	5.885	0.964	4.112	1.632

Table IX (Continued)

(6) Froude Number 0.1; Depth 4.0 x Draft (continued)

W	D	E	W	D'	E'
2.992	4.833	8.935	1.212	3.309	2.478
3.491	3.944	10.593	1.414	2.700	2.938
4.134	3.056	10.711	1.674	2.092	2.970
4.909	2.534	9.070	1.988	1.735	2.515
6.042	2.616	7.416	2.447	1.791	2.057
7.140	2.611	7.789	2.892	1.787	2.160
7.854	2.539	7.870	3.182	1.738	2.183
8.727	2.452	7.486	3.535	1.679	2.076
9.817	2.397	6.218	3.977	1.641	1.724
11.220	2.512	3.833	4.545	1.720	1.063
12.083	2.675	3.964	4.895	1.831	1.099
13.090	2.629	5.004	5.303	1.800	1.388

(7) Froude Number 0.2; Depth 4.0 x Draft

W	D	E	W	D'	E'
4.134	2.962	12.307	1.674	2.028	3.413
4.909	2.534	10.809	1.988	1.735	2.998
6.042	2.610	8.971	2.447	1.787	2.488
7.140	2.671	9.043	2.892	1.829	2.508
7.854	2.638	9.089	3.182	1.806	2.521
8.727	2.590	8.720	3.535	1.773	2.418
9.817	2.582	7.538	3.977	1.767	2.091
11.220	2.749	5.868	4.545	1.882	1.627

Table IX (Continued)

(7) Froude Number 0.2; Depth 4.0 x Draft (continued)

W	D	E	W	D'	E'
12.083	2.853	6.211	4.895	1.953	1.723
13.090	2.884	5.608	5.303	1.975	1.555

(8) Froude Number 0.3; Depth 4.0 x Draft

W	D	E	W	D'	E'
4.134	1.666	11.325	1.674	1.140	3.141
4.909	2.095	11.143	1.988	1.434	3.090
6.042	2.359	11.513	2.447	1.615	3.193
7.140	2.463	11.856	2.892	1.686	3.288
7.854	2.495	11.991	3.182	1.708	3.326
8.727	2.523	11.914	3.535	1.727	3.304
9.817	2.586	11.364	3.977	1.770	3.152
11.220	2.787	10.551	4.545	1.908	2.926
12.083	2.957	10.977	4.895	2.024	3.044
13.090	3.105	12.403	5.303	2.126	3.440

(9) Froude Number 0.0; Depth 2.5 x Draft

W	D	E	W	D'	E'
4.134	3.024	12.418	1.674	2.070	3.444
4.909	2.683	10.211	1.988	1.837	2.832
6.042	2.770	9.214	2.447	1.896	2.555
7.140	2.714	9.626	2.892	1.858	2.670
7.854	2.638	9.692	3.182	1.806	2.688
8.727	2.556	9.352	3.535	1.750	2.593

Table IX (Continued)

(9) Froude Number 0.0; Depth 2.5 x Draft (continued)

W	D	E	W	D'	E'
9.817	2.507	8.245	3.977	1.716	2.286
11.220	2.601	6.014	4.545	1.781	1.668
12.083	2.771	5.423	4.895	1.897	1.504
13.090	2.845	6.908	5.303	1.948	1.916

(10) Froude Number 0.1; Depth 2.5 x Draft

W	D	E	W	D'	E'
1.496	20.971	-1.842	-0.606	14.357	-0.511
2.001	13.545	6.427	0.811	9.273	1.782
2.380	9.793	9.991	0.964	6.705	2.771
3.570	3.891	10.644	1.446	2.664	2.952
4.134	3.278	8.257	1.674	2.244	2.290
4.488	3.211	7.700	1.818	2.198	2.135
4.909	3.169	7.293	1.988	2.170	2.023
5.236	3.112	7.506	2.121	2.130	2.082
5.610	3.016	7.859	2.273	2.065	2.180
6.042	2.886	8.225	2.447	1.976	2.281
6.545	2.741	8.491	2.651	1.877	2.355
7.140	2.601	8.610	2.892	1.781	2.388
7.854	2.480	8.598	3.182	1.698	2.384
8.727	2.380	8.419	3.535	1.629	2.335
9.817	2.330	7.909	3.977	1.595	2.194
11.220	2.422	7.703	4.545	1.658	2.136

Table IX (Continued)

(10) Froude Number 0.1; Depth 2.5 x Draft (continued)

W	D	E	W	D'	E'
12.083	2.499	9.055	4.895	1.677	2.511
13.090	2.385	9.315	5.303	1.633	2.583

(11) Froude Number 0.2; Depth 2.5 x Draft

W	D	E	W	D'	E'
4.134	2.372	11.473	1.674	1.624	3.182
4.909	2.619	10.547	1.988	1.793	2.925
6.042	2.620	10.934	2.447	1.794	3.032
7.140	2.572	10.892	2.892	1.761	2.989
7.854	2.567	10.650	3.182	1.757	2.954
8.727	2.568	10.396	3.535	1.758	2.883
9.817	2.618	9.768	3.977	1.792	2.709
11.220	2.796	9.836	4.545	1.914	2.728
12.083	2.818	10.562	4.895	1.929	2.929
13.090	2.923	9.816	5.303	2.001	2.722

(12) Froude Number 0.3; Depth 2.5 x Draft

W	D	E	W	D'	E'
4.134	-0.863	18.709	1.674	-0.591	5.189
4.909	0.307	17.763	1.988	0.210	4.926
6.042	1.368	16.208	2.447	0.937	4.495
7.140	2.063	16.127	2.892	1.412	4.472
7.854	2.333	16.468	3.182	1.597	4.567
8.727	2.564	16.743	3.535	1.755	4.643

Table IX (Continued)

(12) Froude Number 0.3; Depth 2.5 x Draft (continued)

W	D	E	W	D'	E'
9.817	2.827	16.799	3.977	1.936	4.659
11.220	3.261	17.969	4.545	2.233	4.983
12.083	3.509	21.007	4.895	2.402	5.826
13.090	3.663	26.489	5.303	2.508	7.346

(13) Froude Number 0.0; Depth 1.5 x Draft

W	D	E	W	D'	E'
4.134	3.568	14.952	1.674	2.442	4.146
4.909	3.481	14.488	1.988	2.383	4.018
6.042	3.366	14.731	2.447	2.304	4.085
7.140	3.211	14.704	2.892	2.198	4.078
7.854	3.131	14.288	3.182	2.143	3.962
8.727	3.080	13.330	3.535	2.108	3.697
9.817	3.119	11.642	3.977	2.135	3.229
11.220	3.335	10.539	4.545	2.283	2.923
12.083	3.371	11.149	4.895	2.308	3.092
13.090	3.377	9.799	5.303	2.312	2.717

(14) Froude Number 0.1; Depth 1.5 x Draft

W	D	E	W	D'	E'
1.496	7.635	13.071	0.606	5.227	3.625
2.001	6.079	15.620	0.811	4.162	4.332
2.380	5.176	16.662	0.964	3.543	4.621
3.570	3.508	16.873	1.446	2.401	4.679

Table IX (Continued)

(14) Froude Number 0.1; Depth 1.5 x Draft (continued)

W	D	E	W	D'	E'
4.134	3.287	15.945	1.674	2.250	4.422
4.488	3.295	16.183	1.818	2.256	4.488
4.909	3.249	14.975	1.988	2.224	4.153
5.236	3.249	14.754	2.121	2.224	4.092
5.610	3.241	14.581	2.273	2.219	4.044
6.042	3.217	14.415	2.447	2.203	3.998
6.545	3.177	14.182	2.651	2.175	3.933
7.140	3.124	13.778	2.892	2.139	3.821
7.854	3.070	13.065	3.182	2.102	3.623
8.727	3.034	11.870	3.535	2.077	3.292
9.817	3.066	10.159	3.977	2.099	2.817
11.220	3.169	9.493	4.545	2.170	2.633
12.083	3.091	9.626	4.895	2.116	2.670
13.090	3.015	7.719	5.303	2.064	2.141

(15) Froude Number 0.2; Depth 1.5 x Draft

W	D	E	W	D'	E'
4.134	7.287	41.452	1.674	4.989	11.496
4.909	7.727	47.198	1.988	5.290	13.089
6.042	8.029	48.396	2.447	5.497	13.421
7.140	8.739	51.877	2.892	5.983	14.387
7.854	9.045	56.343	3.182	6.193	15.625
8.727	9.093	63.102	3.535	6.225	17.500
9.817	9.277	69.166	3.977	6.351	19.181

Table IX (Continued)

(15) Froude Number 0.2; Depth 1.5 x Draft (continued)

w	D	E	W	D'	E'
11.220	8.982	96.379	4.545	6.149	26.728
12.083	8.373	98.104	4.895	5.732	27.207
13.090	7.674	109.152	5.303	5.254	30.271

Table X

VIRTUAL INERTIA AND DAMPING COEFFICIENTS IN PITCH

WITH STERN UP INITIALLY

(1) Froude Number 0.0; Depth 2.5 x Draft

w	A	B	W	A'	B'
4.134	6.239	11.512	1.674	0.153	0.115
4.909	5.393	12.660	1.988	0.132	0.126
6.042	4.936	13.040	2.447	0.121	0.130
7.140	4.638	13.722	2.892	0.114	0.137
7.854	4.464	13.669	3.182	0.110	0.136
8.727	4.320	12.878	3.535	0.106	0.128
9.817	4.311	11.117	3.977	0.106	0.111
11.220	4.487	11.659	4.545	0.110	0.116
12.083	4.293	11.989	4.895	0.105	0.119
13.090	4.271	7.490	5.303	0.105	0.075

(2) Froude Number 0.10; Depth 2.5 x Draft

w	A	B	W	A'	B'
4.134	5.681	13.112	1.674	0.139	0.130
4.909	5.155	13.723	1.988	0.127	0.137
6.042	4.706	13.599	2.447	0.116	0.135
7.140	4.436	13.203	2.892	0.109	0.131
7.854	4.287	12.573	3.182	0.105	0.125
8.727	4.163	11.168	3.535	0.102	0.111
9.817	4.168	8.885	3.977	0.102	0.088

Table X (Continued)

(2) Froude Number 0.10; Depth 2.5 x Draft (continued)

W	A	B	W	A'	B'
11.220	4.142	8.564	4.545	0.102	0.085
12.083	4.021	5.396	4.895	0.099	0.054
13.090	4.366	2.909	5.303	0.107	0.029

(3) Froude Number 0.20; Depth 2.5 x Draft

W	A	B	W	A'	B'
4.134	4.805	11.995	1.674	0.118	0.119
4.909	4.280	11.695	1.988	0.105	0.116
6.042	4.207	10.357	2.447	0.103	0.103
7.140	4.116	10.630	2.892	0.101	0.106
7.854	3.993	10.381	3.182	0.098	0.103
8.727	3.887	9.276	3.535	0.095	0.092
9.817	3.953	7.508	3.977	0.097	0.075
11.220	3.800	9.409	4.545	0.093	0.094
12.083	3.634	5.535	4.895	0.089	0.055
13.090	4.036	2.929	5.303	0.099	0.029

(4) Froude Number 0.30; Depth 2.5 x Draft

W	A	B	W	A'	B'
4.134	-0.474	17.922	1.674	-0.012	0.178
4.909	1.141	17.490	1.988	0.028	0.174
6.042	2.139	14.980	2.447	0.053	0.149
7.140	3.048	13.605	2.892	0.075	0.135
7.854	3.353	13.301	3.182	0.082	0.132

Table X (Continued)

(4) Froude Number 0.30; Depth 2.5 x Draft (continued)

W	A	B	W	A'	B'
8.727	3.635	12.226	3.535	0.089	0.122
9.817	4.063	11.824	3.977	0.100	0.118
11.220	4.115	11.047	4.545	0.101	0.110
12.083	4.563	11.287	4.895	0.112	0.112
13.090	4.185	15.276	5.303	0.103	0.152

(5) Froude Number 0.0; Depth 1.5 x Draft

W	A	B	W	A'	B'
4.134	6.883	18.676	1.674	0.169	0.186
4.909	6.040	18.502	1.988	0.148	0.184
6.042	5.392	18.430	2.447	0.132	0.183
7.140	4.973	18.032	2.892	0.122	0.179
7.854	4.778	17.286	3.182	0.117	0.172
8.727	4.630	15.774	3.535	0.114	0.157
9.817	4.614	13.156	3.977	0.113	0.131
11.220	4.870	11.645	4.545	0.120	0.116
12.083	4.808	13.190	4.895	0.118	0.131
13.090	4.559	10.144	5.303	0.112	0.101

(6) Froude Number 0.10; Depth 1.5 x Draft

W	A	B	W	A'	B'
1.496	12.627	16.152	0.606	0.310	0.161
2.001	9.374	20.587	0.811	0.230	0.205
2.310	7.845	21.912	0.936	0.193	0.218

Table X. (Continued)

(6) Froude Number 0.10; Depth 1.5 x Draft (continued)

w	A	B	W	A'	B'
2.618	6.644	22.518	1.061	0.163	0.224
2.992	5.598	22.508	1.212	0.137	0.224
3.491	4.958	21.722	1.414	0.122	0.216
4.134	4.844	19.512	1.674	0.119	0.194
4.488	4.870	20.043	1.818	0.120	0.199
4.909	4.850	19.065	1.988	0.119	0.190
5.512	4.799	19.544	2.233	0.118	0.194
6.042	4.715	18.958	2.447	0.116	0.189
7.140	4.590	18.111	2.892	0.113	0.180
7.854	4.553	17.099	3.182	0.112	0.170
8.727	4.583	15.394	3.535	0.113	0.153
9.817	4.771	13.726	3.977	0.117	0.137
11.220	4.692	12.701	4.545	0.115	0.126
12.083	4.785	7.869	4.895	0.118	0.078
13.090	5.182	7.384	5.303	0.127	0.073

(7) Froude Number 0.20; Depth 1.5 x Draft

W	A	B	W	A'	B'
1.496	-12.599	53.476	0.606	-0.309	0.532
2.001	-11.603	43.198	0.811	-0.285	0.430
2.310	-9.567	36.008	0.936	-0.235	0.358
2.618	-7.401	29.487	1.061	-0.182	0.293
2.992	-4.917	23.794	1.212	-0.121	0.237
3.491	-2.029	21.075	1.414	-0.050	0.210

Table X. (Continued)

(7) Froude Number 0.20; Depth 1.5 x Draft (continued)

w	A	B	W	A'	B'
4.134	0.263	18.498	1.674	0.006	0.184
4.488	0.938	18.923	1.818	0.023	0.188
4.909	1.688	17.230	1.988	0.041	0.171
5.512	2.454	17.143	2.233	0.060	0.171
6.042	2.982	16.810	2.447	0.073	0.167
7.140	3.571	17.169	2.892	0.088	0.171
7.854	3.813	16.810	3.182	0.094	0.167
8.727	4.128	15.806	3.535	0.101	0.157
9.817	4.571	15.898	3.977	0.112	0.158
11.220	4.680	12.943	4.545	0.115	0.129
12.083	5.302	7.462	4.895	0.130	0.074
13.090	5.884	13.259	5.303	0.144	0.132